

# Numerical study of the impact of osteotomies and expander location in surgically assisted rapid palatal expansion for transverse maxillary deficiency

Tomas Verplanken

Student number: 01708012

Supervisors: Prof. dr. ir. Wim Van Paepegem, Renaat Coopman

Counsellor: Dr. Manuel Da Silva Pinheiro (Former postdoctoral researcher at UGent, now enrolled for MBA program in Portugal)

Master's dissertation submitted in order to obtain the academic degree of  
Master of Science in Electromechanical Engineering

Academic year 2021-2022

---

# Numerical study of the impact of osteotomies and expander location in surgically assisted rapid palatal expansion for transverse maxillary deficiency

Tomas Verplanken

Student number: 01708012

Supervisors: Prof. dr. ir. Wim Van Paepegem, Renaat Coopman

Counsellor: Dr. Manuel Da Silva Pinheiro (Former postdoctoral researcher at UGent, now enrolled for MBA program in Portugal)

Master's dissertation submitted in order to obtain the academic degree of  
Master of Science in Electromechanical Engineering

Academic year 2021-2022

---

# Preface

This master thesis is the result of eight months of hard work and was written as part of my graduation to obtain my degree in Mechanical Energy Engineering. The main reason I chose this subject is to broaden my engineering skills and try to immerse myself in a new topic. The idea of working together with doctors and surgeons always appealed to me, as a direct influence on people's life can be achieved.

The results of this research would not have been possible without the help of various people. I want to take a moment to explicitly show my gratitude towards them.

First of all, I would like to thank my promotor and supervisor, Prof. dr. ir. Wim Van Paepegem, for giving me the opportunity to perform topical research on a challenging subject. The support concerning the finite element modeling was of great help. Your flexibility in supervision and your valuable feedback during the last few months kept me motivated and allowed me to perform this research in the best way possible. I sincerely appreciate the confidence and interest you have shown in me and this research.

My sincere appreciation also goes out to Dr. Renaat Coopman, for the time you have made to provide me with suggestions concerning the clinical aspects of the research. You were involved in the project during the course of the year and always available to provide me with relevant advice. Without your help, I would not have been able to conduct this master's dissertation in such an accurate and clinically relevant way.

At last, I would also like to thank my parents for giving me the opportunity to obtain this degree. Furthermore, credit goes to my brothers and friends for their perpetual support and guidance during these past five years. It was always relieving to clear my mind during stressful periods. If I ever lost motivation or interest, you always kept me motivated to strive for excellence.

Tomas Verplanken

Ghent, May 26, 2022



# Permission of use on loan

“The author gives permission to make this master dissertation available for consultation and to copy parts of this master dissertation for personal use. In all cases of other use, the copyright terms have to be respected, in particular with regard to the obligation to state explicitly the source when quoting results from this master dissertation.”

Tomas Verplanken

26 May, 2022



# Remark on the master's dissertation and the oral presentation

“Deze masterproef vormt een onderdeel van een examen. Eventuele opmerkingen die door de beoordelingscommissie tijdens de mondelinge uiteenzetting van de masterproef werden geformuleerd, werden niet verwerkt in deze tekst.”

“This master's dissertation is part of an exam. Any comments formulated by the assessment committee during the oral presentation of the master's dissertation are not included in this text.”



# Numerical study of the impact of osteotomies and expander location in surgically assisted rapid palatal expansion for transverse maxillary deficiency

By Tomas Verplanken

Master's dissertation submitted in order to obtain the academic degree of Master of Science in Electromechanical Engineering

**Academic year:** 2021-2022

**Supervisors:** Prof. dr. ir. Wim Van Paepegem, Dr. Renaat Coopman

Faculty of Engineering and Architecture  
Ghent University

## **Abstract:**

Transverse maxillary deficiency (TMD) is a common deficiency with a prevalence of around 15%. It is characterized by a narrow maxilla, a high palatal vault, crowded maxillary teeth and a uni- or bilateral crossbite. The aetiology of the deficiency may involve developmental, congenital, traumatic or iatrogenic factors. The deficiency may contribute to the development of persistent mouth breathing, crowding of the maxillary teeth, aesthetic discrepancies, nose breathing problems and sleep apnoea syndrome. The treatment can vary depending on the amount of expansion, the sex and the age of the patient. For skeletally mature patients, the preferred treatment by maxillofacial surgeons is the surgically assisted rapid palatal expansion or SARPE procedure. The main rationale of the surgical assistance is to osteotomize the buttresses of the midface to reduce the resistance against transversal expansion. Once the surgery is performed, orthodontic forces are applied through the expander device. Multiple parameters exist in this procedure: the presence of certain surgical osteotomies, the type of expansion device and the positioning of the expander. This master thesis aims to gain insight in the biomechanical behavior of this SARPE procedure and to improve the predictability of the expansion profile when certain parameters are varied. The analyzed parameters are the palatal expander position, the presence of a (uni- and bilateral) pterygoid disjunction and the influence of an asymmetric lateral osteotomy. First, a 3D model was constructed from a CT image using several segmentation tools. Multiple models were then constructed, depending on the investigated parameter. A finite element analysis was then conducted and the displacement profile and stress distribution was analyzed. With the results obtained in this study, the predictability of the procedure can be increased and better clinical results can be achieved. The need for further research was demonstrated as well.

**Keywords:** SARPE, FEA, TMD, bone-borne expander, Maxillary expansion

# Numerical study of the impact of osteotomies in surgically assisted rapid palatal expansion

Tomas Verplanken

Supervisor(s): Prof. dr. ir. Wim Van Paepegem, Dr. Renaat Coopman  
Counsellor: Dr. Manuel Da silva Pinheiro

---

## Abstract

**Objectives:** This paper aims to gain insight in the biomechanical behavior of the SARPE procedure and aims to improve the predictability of the outcome when certain parameters are varied. The displacement profile and stress distribution of maxillofacial landmarks resulting from bone-borne transpalatal expanders with variations in surgical assistance are analyzed.

**Methods:** Two parameters are investigated: the influence of the pterygomaxillary disjunction (PMD) and the influence of the location of the lateral osteotomy. In total, four models were built: one model without any PMD, a uni - and bilateral PMD model and one model with an asymmetric positioned lateral osteotomy. Displacement profiles and Von Mises stresses were evaluated.

**Results:** With the presence of the PMD, posterior resistance against the transversal expansion is decreased. No significant changes in axial tipping were observed. Stress reductions of around 10% - 20% are found around the maxillofacial complex. The asymmetric lateral osteotomy model showed larger displacements at the side of the more superiorly positioned lateral osteotomy. Reduced stresses were observed at the body of the maxilla and the medial pterygoid plate (superiorly). Increased stresses were observed at the lateral and medial (inferiorly) pterygoid plate.

**Conclusion:** The presence of the PMD does not influence the tipping behavior significantly. Generally, the PMD reduces the stresses (10% - 20%). Larger stress reductions of up to 35% are found at the cranial Foramina. The more superior positioned lateral osteotomy tends to increase the displacement of the alveolar bone at that side, however also increasing the stresses at the lateral pterygoid plates. Based on these results, a PMD on that side is advised.

**Keywords:** Maxillary expansion, SARPE, Transverse maxillary deficiency, FEA, Bone-borne expander

---

## I. INTRODUCTION

Transverse maxillary deficiency (TMD) is a common deficiency characterized by a narrow maxilla, a high palatal vault, crowded maxillary teeth and a uni- or bilateral crossbite. The deficiency may contribute to the development of persistent mouth breathing, crowding of the maxillary teeth, nose breathing problems and sleep apnoea syndrome [1][2].

Maxillary expansion treatments have been used for over a century to correct transverse maxillary deficiencies. Three expansion treatments are mostly used today: rapid maxillary expansion (RME), slow maxillary expansion (SME) and surgically assisted rapid palatal expansion (SARPE).

There is an ossification and interdigitation process of the midpalatal suture, which varies greatly with age and sex of the patient. Mostly around the age of fifteen years, the midpalatal suture has matured, resulting in an increased resistance against transversal expansion [3]. This decreases the elasticity of the facial skeleton and the possibility of orthopaedic expansion of the bone base of the maxilla. When the midpalatal suture has matured, nonsurgical orthodontic treatment (RME or SME) would result in unpredictable expansion and a series of unwanted effects: lateral tipping of the teeth, alveolar bone bending, instability of the expansion among other complications [1] [4]. SARPE is required for skeletally mature patients. The optimal SARPE treatment modality is patient specific and depends on the personal experiences of the clinician, the maturation stage of the sutures and the magnitude of the required expansion [5].

In skeletally mature patients, surgery is required to temporarily interrupt the key resisting elements of the midfacial skeleton. In this way, the maxilla can be expanded in a more predictable manner with the use of lower forces [6]. The piriform aperture pillars (anterior support), the ossified midpalatal suture (median support), the zygomaticomaxillary (lateral support) and pterygomaxillary (posterior support) buttresses form the main resistances to the transversal displacement of the maxilla [7].

There is no consensus in literature on the optimal set of osteotomies, neither on the exact influence each osteotomy has on the expansion profile [8]. No FEA has yet been performed on the use of an asymmetric surgery, such as a one sided PMD or superoinferior variations of the lateral osteotomy. The aim of the present study was to evaluate the influence of surgical variations of the SARPE procedure on the expansion profile and stress distribution in the craniofacial complex. To evaluate these effects, a finite element analysis was conducted.

## II. MATERIALS AND METHODS

A 3D model was constructed starting from a CT scan of a skull. Segmentation of the CT scan was performed using MIMICS software (version 23.0; Materialise, Leuven, Belgium). The segmented anatomical structures were exported in 3-MATIC software (version 15.0; Materialise, Leuven, Belgium) in the STL format. Mesh errors resulting from low resolution of the CT scan and low contrast between different HU values were corrected and a high quality model was obtained. A cephalometric analysis was performed to obtain the correct maxillofacial land-

marks and the anatomical planes, which were required to define the different osteotomies. Locally at the maxilla, the sphenoid bone and the frontal part of the facial bones, a surface mesh with elements of 1 mm was chosen. The other parts of the cranium were meshed with elements of 4 mm in size. Using this surface mesh, a high quality volumetric mesh (C3D10 elements) was created, which resulted in a dense mesh consisting of over 2.3 million elements. Next, the material properties were assigned according to Lee and al. [9] (Table I). The thickness of the cortical shell of the maxilla was determined according to the study by Peterson [10]. All materials were assumed to be elastic, isotropic, linear and homogeneous.

A coordinate system is set up to refer all displacements. This coordinate system has an origin at the posterior nasal spine. The x-axis is defined along the midpalatal suture, the y-axis is along the transversal direction and the z-axis is along the superoinferior direction, with positive values for the anterior, lateral and superior direction respectively. Using this newly defined coordinate system, the displacements can be transformed from the general coordinate system to this local coordinate system.

TABLE I: Mechanical properties of the used materials

Material	Young's modulus [MPa]	Poisson's ratio [/]
Cortical bone	13 700	0.31
Trabecular bone	1 370	0.31
Enamel	80 000	0.26
Dentin	20 000	0.15

In all these simulations, a transpalatal distractor (TPD) was simulated. The TPD was modeled in ABAQUS by imposing several constraints to the model. Reference points were indicated on the alveolar ridge, and between these points an axial connector was constructed, allowing only a displacement along the direction of the wire between the two points. The start and end point of this transpalatal wire were then connected with beam elements to the alveolar ridge. The expander was activated 5 mm in the lateral direction (Y). As suggested by Gautam and al. [11], several nodes around the Foramen Magnum were completely fixed in all directions.

Multiple osteotomy variants and combinations are performed on the models. In Figure 2, the different possible osteotomy lines are demonstrated schematically. The lateral (red), vertical

(blue), median (yellow) and pterygoid (white) osteotomies can be performed on the model. Using this set of osteotomies, several models can be created, depending on the required analysis.

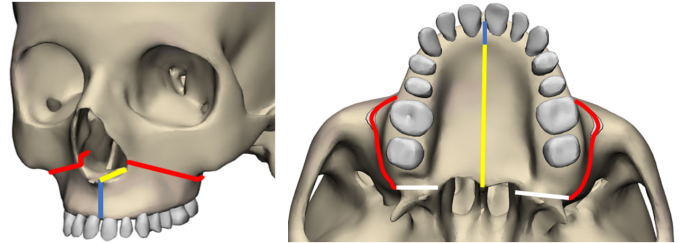


Fig. 2: Schematic representation of the osteotomy lines on the 3D finite element model. Lateral (red), vertical (blue), median (yellow) and pterygomaxillary (white)

The obtained FEA model was first validated by recreating finite element studies found in literature by Lee and al. [9] and Möhlenrich [12]. The model was then further verified by comparing the obtained results to the contemporary literature. The FEM behaves as literature indicates and hence, the model can be used to perform research with. The effect of two variables is analyzed: on the one hand, the influence of the pterygomaxillary disjunction (PMD), on the other hand the presence of a more superior located lateral osteotomy on one side is analyzed.

**Pterygoid disjunction models:** In total, three models are analyzed. There is a model without any pterygomaxillary disjunction, a model with a PMD performed unilaterally (left side) and a model with bilateral PMDs. On all models, the lateral, vertical and median osteotomies are performed as well. The palatal expander was modeled between the second premolars and an expansion of 5 mm was simulated.

**Superior lateral osteotomy models:** The location where the lateral osteotomy can be placed is bounded by several limitations. The osteotomy needs to be at least 5 mm superior of the apex of the incisor, to avoid damaging the teeth. Another requirement is that the osteotomy should be at least 5 mm inferior of the Infraorbital Foramen, since this is a weakened location on the skull and fracture patterns can originate from this Foramen. Taking these limitations into account, a model was created where the most inferior location was chosen on one side (left) and on the other side the most superior location (right). In Figure 3, both the symmetrical and asymmetrical lateral osteotomy

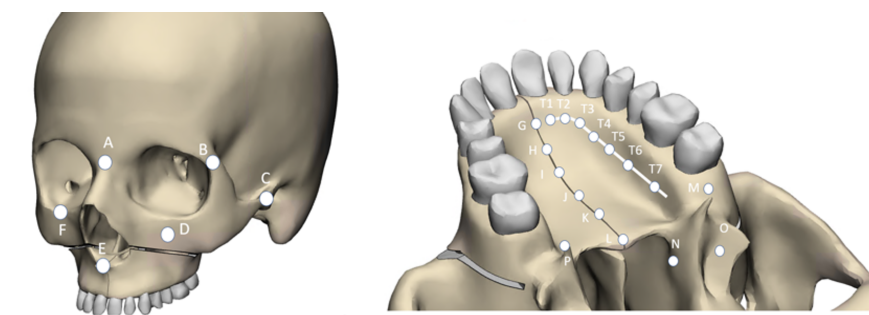


Fig. 1: Evaluated cephalometric landmarks

are illustrated. The palatal expander was modeled between the second premolars, and again an expansion of 5 mm was simulated.

Using these models, the influence of the pterygoid disjunction and the presence of asymmetries in the lateral osteotomies can be analyzed. Both the displacement and Von Mises stresses at several maxillofacial landmarks are evaluated. The analyzed maxillofacial landmarks are depicted in Figure 1.

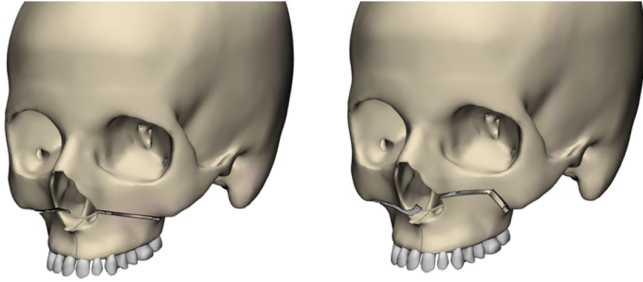


Fig. 3: Symmetric (left) and asymmetric (right) lateral osteotomy

### III. RESULTS & DISCUSSION

#### A. Pterygoid plate disjunction

The results measured at the alveolar bone are shown in Table II. Using this data, the total amount of symmetry can be obtained. On average, the expansion on the right side is 52.3%, 51.3% and 56.3% for respectively the symmetric, unilateral and bilateral PMD models. More pronounced differences for the unilateral pterygoid disjunction are present for the most posterior measurement point. By performing the PMD, posterior resistance against the expansion is removed, and more expansion is occurring on the disjuncted side. The effects for the unilateral PMD are small and may be clinically irrelevant.

Next, the influence of the pterygoid disjunction on the horizontal tipping behavior is measured. Small opening angles are measured in all models. The smallest opening angle is  $5.82^\circ$ , obtained when the PMD is performed bilaterally. The horizontal tipping is the largest when the PMD is only performed unilaterally, with an opening angle of  $6.71^\circ$ . The tipping in the frontal plane increases as the pterygoid plates are disjuncted, with values ranging from  $6.13^\circ$  for the model without PMD,  $6.68^\circ$  for the unilateral PMD and  $7.42^\circ$  for the bilateral PMD.

TABLE II: Displacements at the level of the alveolar bone - PMD models

Vector sum	Orientation	T1	T2	T3	T4	T5	T6	T7
No PMD [mm]	Left	3.32	3.22	3.01	2.82	2.62	2.03	1.44
	Right	3.62	3.49	3.27	3.12	2.81	2.23	1.65
Unilateral PMD [mm]	Left	3.42	3.31	3.09	2.89	2.67	2.07	1.15
	Right	3.56	3.42	3.21	3.06	2.75	2.19	1.62
Bilateral PMD [mm]	Left	3.27	3.13	2.86	2.67	2.47	1.92	1.39
	Right	4.00	3.89	3.73	3.47	3.12	2.60	1.89

Next to the displacement measurements, the stresses are also measured at several maxillofacial landmarks. The stress distribution is given in Figure 4. The model where the PMD is performed on one side has similar stresses as the analyzed PMD model on that side and similar stresses as the base model on the other side. In this way, the results can be omitted from the analysis. By performing the PMD, a different stress distribution is observed. The anteriorly positioned maxillofacial landmarks (maxillary body, infraorbital margin, frontonasal suture) all show reduced stresses, with reductions of around 10% to 20%. At the maxillary tuberosity a reduction of around 67% is observed, and an increase of around 47.5% at the medial pterygoid plate (inferiorly measured). The stresses at the cranial Foramina are shown in Table III. By performing the PMD, the stresses at the cranial Foramina are lowered, with reductions of up to 32% at the Foramen Optica.

TABLE III: Stresses measured at the cranial Foramina - PMD models

	No PMD [MPa]	Bilateral PMD [MPa]	Reduction [%]
Foramen Ovale	51.75	41.71	19.5
Foramen Lacerum	65.65	61.71	6.01
Foramen Optica	83.28	56.54	32.10

Since the total expansion is the same in all the models, the models can be compared to each other. In literature, the exact influence of the PMD remains unknown. Bays & Greco [13] reported a larger posterior expansion when the PMD was performed, whereas Han and al. [14] reported the opposite behavior. This indicates the uncertainty in literature concerning the exact influence of the PMD. Multiple variables such as sex, age, position of the expander, expander type and patient anatomy could influence the effect the PMD has on the expansion.

The model without PMD already shows a small asymmetry. According to Koudstaal [15], this means that there is already an imbalance present in the equilibrium of the resisting forces of the maxillary segments. Small deviations in the palatal expander position or in the lateral osteotomy, as well as the presence of soft tissues, such as muscles and ligaments, can affect the resistance on each side.

The main rationale in literature to perform the PMD is to lower the horizontal tipping. The obtained results show small differences in this tipping behavior, which may be clinically irrele-

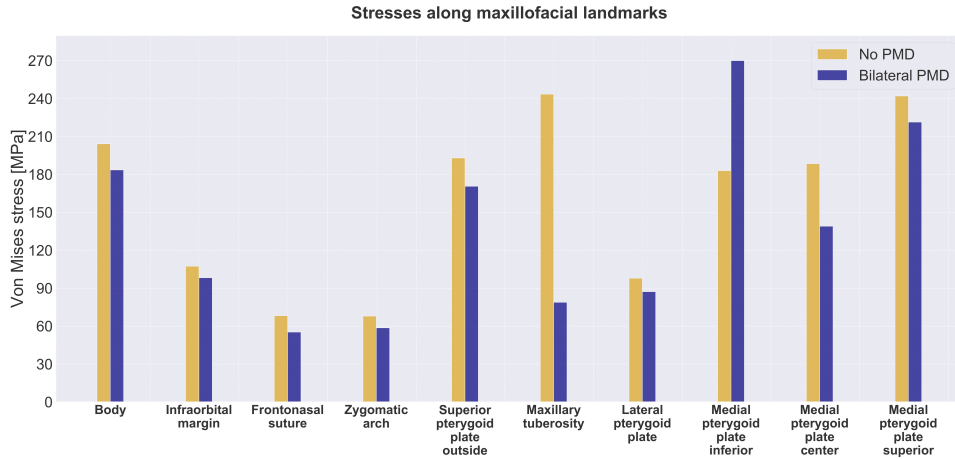


Fig. 4: Stress distribution in the maxillofacial complex - PMD models

vant. These findings are in accordance with Möhlenrich and al. [16], who reported a more parallel transverse expansion when PMD was performed, however with few statistical differences. A finite element study performed by Holberg and al. [17] showed that the pterygoid disjunction generally reduced stresses at most anatomic structures of the midface. This is confirmed by the simulations performed in this FEA. With reduced stresses, the procedure might lead to an increased stability. For the maxillofacial landmarks considered in the study, reductions of around 10% - 20% are observed by Holberg [17]. In the models obtained in this simulation, the PMD led to a decrease of stresses of around 15%, with exceptions at the maxillary tuberosity (67%) and the medial pterygoid plate, measured inferiorly (47%).

The study by Holberg [17] also showed significantly reduced stresses at the Foramina of the cranial base, with reductions of up to 75% at the Optic Foramen. When the stresses are reduced at the Foramina of the cranial base, the possibility of (mini)fractures is decreased and severe complications can be avoided. As can be seen from Table III, similar behavior is noticed in this model, albeit with smaller values: a reduction of around 32.1% is observed at the Foramen Optica in this model, whereas Holberg and al. [17] measured reductions up to 75%. Nevertheless, the same conclusion can be drawn: the pterygoid disjunction allows for lower stresses at the cranial Foramen, in this way reducing the risk of (mini)fractures at these Foramen. This results in an increased stability of the procedure.

With bone-borne expanders, the stresses at the palatum and alveolar bone remain similar. There is no influence on alveolar bone-related complications such as gingival recession and root resorption.

### B. Superior lateral osteotomy

The results measured at the alveolar bone are shown in Table IV. The total expansion is quite similar between the two models. However, due to the asymmetry in the lateral osteotomy, an unbalance is created in the amount of expansion on each side. The average relative amount of expansion on the right side is around 52 % for the base model, whereas it is around 60 % for the asymmetric lateral osteotomy model.

The horizontal tipping shows worse behavior in the asymmetrical model: an opening angle of  $7.3^\circ$  was measured, whereas with the symmetrical model an opening angle of  $5.85^\circ$  was observed. For the vertical tipping, a smaller opening angle of  $5.4^\circ$  was observed in the asymmetric model. The symmetric model has an opening angle of around  $6.1^\circ$ .

In Figure 5, the stresses at the several maxillofacial landmarks are reported. Large differences are observed between both models. A significant reduction of the stresses at the body of the maxilla is observed, with a reduction of 87%. Slightly higher stress values are observed at the Infraorbital margin. The zygomatic arch and the frontonasal suture show reduced stresses. The lateral pterygoid plates are shown in Figure 6. Together with the results depicted in Figure 5, it can be seen that the stresses at the pterygoid plates of the superiorly located osteotomy are generally higher than those observed at the inferior osteotomy, especially at the lateral pterygoid plates.

Only one study in literature describes the asymmetry between left and right maxillary segments in patients with a bone-borne distractor with PMD [18]. Some factors that could influence the asymmetric behavior are mentioned: differences in the re-

TABLE IV: Displacements at the level of the alveolar bone - Lateral osteotomy variation models

Vector sum	Orientation	T1	T2	T3	T4	T5	T6	T7
Symmetric lateral osteotomy [mm]	Left	3.32	3.22	3.012	2.82	2.615	2.03	1.43
	Right	3.62	3.49	3.27	3.12	2.81	2.23	1.65
Asymmetric lateral osteotomy [mm]	Left	2.75	2.68	2.51	2.34	2.18	1.72	1.25
	Right	4.18	4.02	3.78	3.60	3.23	2.59	1.94

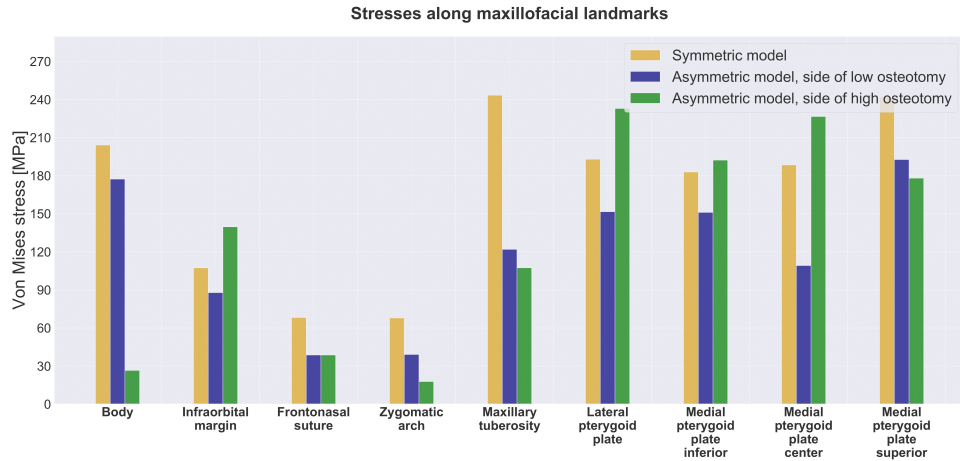


Fig. 5: Stress distribution in the maxillofacial complex - Lateral osteotomy variation models

sistance of the soft tissues and alveolar bone, the placement of distractor and the orientation of the distractor in the transversal plane. According to Huizinga and al. [18], transversal asymmetry may occur when the palatal expander is positioned obliquely in the frontal plane.

the pterygoid plates are avoided. The interaction of the pterygoid plate disjunction together with the superior located lateral osteotomy is outside of the scope of this research and requires further research.

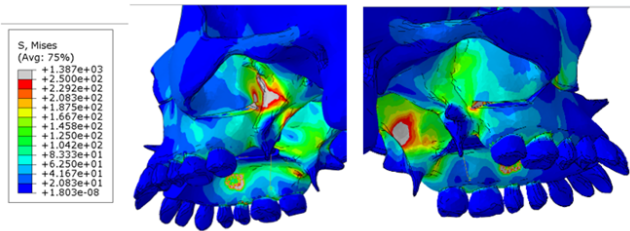


Fig. 6: Stresses at the lateral pterygoid plates, left (asymmetric) and right (symmetric) side of the model

When the lateral osteotomy is positioned more superiorly, the total expansion remains the same but a larger displacement was obtained at that side. As the maxilla is osteotomized at a more superior location, a larger part of the maxilla is osteotomized, resulting in a lowered resistance against the transversal expansion and increased displacements at that side.

According to Möhlenrich and al. [12], who investigated the influence of several osteotomies, the largest stress reduction is found when performing the lateral osteotomy. This indicates that the anterior piriform aperture pillars and the lateral zygomatic buttresses show the largest resistance against the transversal expansion. One could argue that variations in this lateral osteotomy could also lead to significant changes in the stress distribution. The results obtained in this study also confirm this.

Higher stress concentrations are observed at most of the pterygoid plates. A recommendation is made to also separate the pterygoid plates if it is opted to perform a more superiorly lateral osteotomy. In this way, the stresses at the pterygoid plates and the cranial Foramina are reduced, and possible fractures at

IV. CONCLUSIONS

Two possible factors that influence the expansion profile were analyzed. Following conclusions are drawn concerning the presence of a uni- or bilateral PMD:

1. By performing the pterygoid disjunction, (posterior) resistance against the transversal expansion is removed. For a one sided pterygoid disjunction, the transversal expansion at this side will increase. By performing the pterygoid disjunction bilaterally, the total amount of expansion is increased at the alveolar bone level. More resistance against the transversal expansion is removed and hence larger expansions are obtained for the same input. The amount of horizontal tipping was decreased by the disjunction of the pterygoid plates. These differences may be clinically irrelevant. This is in accordance with literature [16]. The vertical tipping was increased by the presence of the pterygoid disjunctions.
2. The PMD allows generally for stress reductions in the maxillofacial complex of around 10% to 20%, depending on the location of the measurement. At some anatomical landmarks, such as the medial pterygoid plate (inferiorly measured), the stresses are increased by the PMD. For any other measurement on the pterygoid plates, the stresses are reduced.
3. Holberg and al. [17] showed that the PMD allows for significantly reduced stresses at the Foramina of the cranial base, diminishing the possibility of fractures around these Foramina. Similar results as Holberg were found in this study, albeit with smaller values [17].

For the simulations regarding the variations in superoinferior location of the lateral osteotomy, following conclusions are drawn:

1. The superiorly located osteotomy allows for a larger displacement on that side, but the total transversal expansion remains the same. For the symmetric case, 52% of the transversal expansion was measured on the right alveolar bone side and around 60% was observed for the asymmetrical model. Lower vertical tipping was observed, but larger horizontal tipping.

2. The superoinferior placement of the lateral osteotomy has a significant influence on the stress distribution. Care should be taken for the pterygoid plates, as higher stress concentrations are observed at the lateral pterygoid plates. An additional PMD is suggested based on these results. This interaction however was not simulated and this still requires further research.

Several limitations were also encountered during the research: the absence of correct (viscoelastic) material properties, the time dependency (and stress relaxation) of the procedure and the inclusion of soft tissues can still significantly improve the quality of the simulations. The opportunity to expand on these limitations show the requirement for further research.

#### REFERENCES

- [1] Rafał Nowak, Alina Strzałkowska, and Ewa Zawiślak. "Treatment options and limitations in transverse maxillary deficiency". In: *Dental and Medical Problems* 52.4 (2015), 389–400. DOI: 10.17219/dmp/59388.
- [2] Suresh Menon, Ravi Manerikar, and Ramen Sinha. "Surgical Management of Transverse Maxillary Deficiency in Adults". In: *Journal of Maxillofacial and Oral Surgery* 9.3 (2010), 241–246. DOI: 10.1007/s12663-010-0034-7.
- [3] Fernanda Angelieri et al. "Midpalatal suture maturation: Classification method for individual assessment before rapid maxillary expansion". In: *American Journal of Orthodontics and Dentofacial Orthopedics* 144.5 (2013), 759–769. DOI: 10.1016/j.ajodo.2013.04.022.
- [4] Lokesh Suri and Parul Taneja. "Surgically assisted rapid palatal expansion: A literature review". In: *American Journal of Orthodontics and Dentofacial Orthopedics* 133.2 (2008), 290–302. DOI: 10.1016/j.ajodo.2007.01.021.
- [5] Anirudh Agarwal. "Maxillary expansion". In: *International Journal of Clinical Pediatric Dentistry* 3.3 (2010), 139–146. DOI: 10.5005/jp-journals-10005-1069.
- [6] Marcela Cristina Andrucio and Mirian Aiko Matsumoto. "Transverse maxillary deficiency: Treatment alternatives in face of early skeletal maturation". In: *Dental Press Journal of Orthodontics* 25.1 (2020), 70–79. DOI: 10.1590/2177-6709.25.1.070-079.bbo.
- [7] Vivek Shetty et al. "Biomechanical rationale for surgical-orthodontic expansion of the adult maxilla". In: *Journal of Oral and Maxillofacial Surgery* 52.7 (1994), 742–749. DOI: 10.1016/0278-2391(94)90492-8.
- [8] Aldin Kapetanović et al. "Efficacy of miniscrew-assisted rapid palatal expansion (Marpe) in late adolescents and adults: A systematic review and meta-analysis". In: *European Journal of Orthodontics* 43.3 (2021), 313–323. DOI: 10.1093/ejo/cjab005.
- [9] Seong Cheon Lee et al. "Effect of bone-borne rapid maxillary expanders with and without surgical assistance on the craniofacial structures using finite element analysis". In: *American Journal of Orthodontics and Dentofacial Orthopedics* 145.5 (2014), 638–648. DOI: 10.1016/j.ajodo.2013.12.029.
- [10] Jill Peterson, Qian Wang, and Paul C. Dechow. "Material properties of the dentate maxilla". In: *The Anatomical Record Part A: Discoveries in Molecular, Cellular, and Evolutionary Biology* 288A.9 (2006), 962–972. DOI: 10.1002/ar.a.20358.
- [11] Pawan Gautam, Ashima Valiathan, and Raviraj Adhikari. "Stress and displacement patterns in the craniofacial skeleton with rapid maxillary expansion: A finite element method study". In: *American Journal of Orthodontics and Dentofacial Orthopedics* 132.1 (2007). DOI: 10.1016/j.ajodo.2006.09.044.
- [12] S.C. Möhlhenrich et al. "Simulation of three surgical techniques combined with two different bone-borne forces for surgically assisted rapid palatal expansion of the maxillofacial complex: A finite element analysis". In: *International Journal of Oral and Maxillofacial Surgery* 46.10 (2017), 1306–1314. DOI: 10.1016/j.ijom.2017.05.015.
- [13] Robert A. Bays and Joan M. Greco. "Surgically assisted rapid palatal expansion: An outpatient technique with long-term stability". In: *Journal of Oral and Maxillofacial Surgery* 50.2 (1992), 110–113. DOI: 10.1016/0278-2391(92)90352-z.
- [14] Un Ae Han, Yoonji Kim, and Je Uk Park. "Three-dimensional finite element analysis of stress distribution and displacement of the maxilla following surgically assisted rapid maxillary expansion". In: *Journal of Cranio-Maxillofacial Surgery* 37.3 (2009), 145–154. DOI: 10.1016/j.jcms.2008.10.002.
- [15] Maarten J. Koudstaal et al. "Relapse and stability of surgically assisted rapid maxillary expansion: An anatomic biomechanical study". In: *Journal of Oral and Maxillofacial Surgery* 67.1 (2009), 10–14. DOI: 10.1016/j.joms.2007.11.026.
- [16] S.C. Möhlhenrich et al. "Immediate dental and skeletal influence of distractor position on surgically assisted rapid palatal expansion with or without pterygomaxillary disjunction". In: *International Journal of Oral and Maxillofacial Surgery* 50.5 (2021), 649–656. DOI: 10.1016/j.ijom.2020.10.003.
- [17] Christof Holberg, Stefanie Steinhäuser, and Ingrid Rudzki. "Surgically assisted rapid maxillary expansion: Midfacial and cranial stress distribution". In: *American Journal of Orthodontics and Dentofacial Orthopedics* 132.6 (2007), 776–782. DOI: 10.1016/j.ajodo.2005.12.036.
- [18] Martin P. Huizinga et al. "Bone-borne surgically assisted rapid maxillary expansion: A retrospective three-dimensional evaluation of the asymmetry in expansion". In: *Journal of Cranio-Maxillofacial Surgery* 46.8 (2018), 1329–1335. DOI: 10.1016/j.jcms.2018.05.021.



# Contents

**Preface**

**Permission of use on loan**

**Remark on the master's dissertation and the oral presentation**

<b>1</b>	<b>Introduction</b>	<b>1</b>
1.1	Background . . . . .	1
1.2	Motivation and objectives . . . . .	4
1.3	Structure of the thesis . . . . .	5
<b>2</b>	<b>Literature review</b>	<b>7</b>
2.1	Anatomy . . . . .	7
2.1.1	General anatomical considerations . . . . .	7
2.1.2	Facial bones and sutures . . . . .	9
2.1.3	Sphenoid bone . . . . .	10
2.1.4	Palatum . . . . .	11
2.1.5	Maxillofacial buttresses . . . . .	11
2.1.6	Dentoalveolar complex . . . . .	12
2.1.7	Bone . . . . .	13
2.2	The midpalatal suture . . . . .	15
2.3	Transverse maxillary deficiency . . . . .	16
2.3.1	Diagnosis . . . . .	16
2.3.2	Symptoms . . . . .	17
2.3.3	Treatment . . . . .	17
2.4	SARPE . . . . .	18
2.4.1	Overview of the procedure . . . . .	19
2.4.1.1	Diagnosis and presurgical orthodontic treatment . . . . .	19
2.4.1.2	Surgical procedure . . . . .	20
2.4.1.3	Post-orthodontic treatment . . . . .	21

---

2.4.2	Expander types . . . . .	23
2.4.2.1	Tooth-borne . . . . .	23
2.4.2.2	Bone-borne . . . . .	23
2.4.3	Complications . . . . .	25
2.4.3.1	Tipping . . . . .	25
2.4.3.2	Relapse . . . . .	27
<b>3</b>	<b>Materials and methods</b>	<b>31</b>
3.1	Imaging . . . . .	32
3.2	Segmentation . . . . .	32
3.3	3D Cephalometric analysis . . . . .	37
3.4	Osteotomies . . . . .	39
3.4.1	Nasal septum disjunction . . . . .	39
3.4.2	Midpalatal osteotomy . . . . .	39
3.4.3	Lateral osteotomy . . . . .	40
3.4.4	Pterygoid plate disjunction . . . . .	41
3.5	Expander device . . . . .	41
3.6	Finite element modeling . . . . .	42
3.6.1	Material properties . . . . .	42
3.6.2	Interaction . . . . .	44
3.6.3	Boundary and loading conditions . . . . .	45
3.6.4	Finite element meshing and sensitivity analysis . . . . .	46
3.6.5	Validation of the finite element model . . . . .	47
<b>4</b>	<b>Variations in the palatal expansion device location</b>	<b>52</b>
4.1	Models . . . . .	52
4.2	Results and discussion . . . . .	54
4.2.1	Results displacements . . . . .	58
4.2.2	Discussion displacements . . . . .	64
4.2.3	Results stresses . . . . .	68
4.2.4	Discussion stresses . . . . .	69
4.3	Conclusions palatal expander location . . . . .	72
<b>5</b>	<b>Variations in the surgical technique</b>	<b>75</b>
5.1	Influence of the pterygoid plate disjunction . . . . .	77
5.1.1	Models pterygoid disjunction . . . . .	77
5.1.2	Results displacement . . . . .	78
5.1.3	Discussion displacement . . . . .	82
5.1.4	Results stresses . . . . .	85
5.1.5	Discussion stresses . . . . .	86

---

5.2	Influence of the lateral osteotomy site . . . . .	88
5.2.1	Models influence lateral osteotomy . . . . .	88
5.2.2	Results displacement . . . . .	89
5.2.3	Discussion displacement . . . . .	91
5.2.4	Results stresses . . . . .	92
5.2.5	Discussion stresses . . . . .	93
5.3	Conclusions . . . . .	94
<b>6</b>	<b>General conclusion and future work</b>	<b>97</b>



# List of Figures

1.1	Transverse maxillary deficiency: frontal (left) and occlusal (right) view . .	1
1.2	Facial bones and sutures: coronal view . . . . .	2
1.3	RPE expander . . . . .	3
1.4	SARPE treatment: surgical cuts are indicated in red, regions of large resistance indicated in blue, expansion direction indicated in black . . . .	4
1.5	Workflow thesis . . . . .	5
2.1	Anatomical reference planes . . . . .	8
2.2	Facial bones and sutures: coronal view . . . . .	9
2.3	Bones of the skull: sagittal view . . . . .	10
2.4	Sphenoid bone . . . . .	10
2.5	Occlusal view skull . . . . .	11
2.6	Indication of the buttresses found in the skull, frontal (A) and sagittal (B) view . . . . .	12
2.7	Anatomy of the tooth . . . . .	12
2.8	Material property determination of the maxilla, according to Peterson, grouped in five sets: the alveolar process (red) , maxillary body (orange), posterior region (green), zygomatic process (blue) and the palatal process (gray) . . . . .	14
2.9	Increasing interdigitation of the midpalatal suture . . . . .	15
2.10	Fusion stages of the midpalatal suture . . . . .	15
2.11	Sarpe treatment with osteotomy lines indicated in red . . . . .	18
2.12	Initial (black) and post-treatment (red) superpositions of cephalometric tracings . . . . .	19
2.13	Possible osteotomies indicated in red . . . . .	22
2.14	Example of a tooth-borne Hyrax expander (left) and a bone-borne transpalatal distractor (right) . . . . .	24
2.15	Equivalent force system in the coronal (left) and occlusal (right) plane . .	25

---

2.16	Influence of the surgical procedure and TPD placement on expansion profile . . . . .	26
2.17	Expansion at different instants . . . . .	29
2.18	Skeletal and dental relapse . . . . .	29
3.1	Workflow master thesis . . . . .	31
3.2	Interface MIMICS software . . . . .	33
3.3	Segmentation process MIMICS . . . . .	35
3.4	Basic model 3-MATIC . . . . .	36
3.5	Cephalometric landmarks and anatomical planes . . . . .	38
3.6	Nasal septum disjunction: frontal view 3D model (left) and axial section view (right), osteotomy indicated in red . . . . .	39
3.7	Midsagittal osteotomy: inferior view 3D model (left) and sagittal section view, osteotomy indicated in red (right) . . . . .	40
3.8	Lateral osteotomy: frontal view 3D model (left) and axial section view (right) . . . . .	40
3.9	Pterygoid plate disjunction: 3D model inferior (left) and oblique view (right) . . . . .	41
3.10	3D models of the scanned (left) and the designed (right) palatal expander . . . . .	41
3.11	Sectioning of the maxilla: Body and frontal processes (yellow), zygomatic processes (green), alveolar region (blue), posterior part (not in figure) . . . . .	43
3.12	Axial connector and MPC beam connections indicated in purple . . . . .	44
3.13	Inferior view of the encastre boundary condition imposed on selected nodes around the Foramen Magnum . . . . .	45
3.14	Surface and volumetric mesh of the model . . . . .	46
3.15	Comparison between the study performed by Möhlhenrich (left) and this study (right): model with only sagittal osteotomy (top) and both sagittal and lateral osteotomies (bottom); Stresses are depicted: blue equals 0 MPa, red equals 100 MPa . . . . .	48
3.16	Comparison between the study performed by Nowak and al (left) and this study (right); model with both sagittal and lateral osteotomies; Von misses stresses are depicted for both frontal view (top) and inferior view (bottom): blue equals 0 MPa (top and bottom), red equals 10 MPa (top) and 25 MPa (bottom) . . . . .	49
4.1	Symmetric lateral osteotomy . . . . .	53
4.2	Four different positions of the palatal expander . . . . .	53
4.3	Graphical result of the expansion: undeformed (left), deformation scale factor 1 (middle) and deformation scale factor 3 (right) . . . . .	54

---

4.4	Overlay plots, where the undeformed model is given in the wireframe, the deformed model in solid green: frontal (left), sagittal (middle) and occlusal (right) view . . . . .	54
4.5	Contour plots Von Mises stress (MPa) . . . . .	55
4.6	Contour plots displacement (mm) . . . . .	56
4.7	Local coordinate system . . . . .	56
4.8	Evaluated landmarks of the maxillofacial complex . . . . .	57
4.9	Displacement at the suture: point A is located around Foramen Incisivum, F at the posterior nasal spine - Palatal expander models . . . . .	58
4.10	Displacement at the alveolar bone - Palatal expander models . . . . .	59
4.11	Displacement (vector sum) at maxillofacial landmarks - Palatal expander models . . . . .	63
4.12	Displacement at the alveolar bone: symmetric and asymmetric premolar 2 models . . . . .	63
4.13	Possible anteroposterior movements. (I) The semicircle represents the left and right part of the palatum. The rectangle represents the articulation of the bones posteriorly. Point A is the most anterior point of the mid-palatal suture. (II) Expansion profile assuming the center of the rotation is somewhere on the midline. (III) Expansion profile assuming the centers of rotation are positioned around point B and C . . . . .	65
4.14	Stress distribution maxillofacial complex - Palatal expander models . . . .	68
4.15	Stress relaxation test: strain as input, time dependency of the stress as output . . . . .	70
5.1	Pterygoid disjunction models: oblique view, the same for all three models (top), no PMD (left), unilateral PMD (middle) and bilateral PMD (right) models. PMD indicated in yellow . . . . .	77
5.2	Displacement at the suture: point A is located around Foramen Incisivum, F at the posterior nasal spine - PMD models . . . . .	78
5.3	Symmetry of the expansion measured at the alveolar bone - PMD models	80
5.4	Stress distribution in the maxillofacial complex - PMD models . . . . .	85
5.5	Symmetric (top) and asymmetric (bottom) lateral osteotomies . . . . .	88
5.6	Comparison displacement alveolar bone - Lateral osteotomy variation models . . . . .	90
5.7	Stress distribution maxillofacial complex - Lateral asymmetric osteotomy	92
5.8	Stresses at the lateral pterygoid plates, left (superior lateral osteotomy) and right (inferior lateral osteotomy) side of the model . . . . .	93



# List of Tables

2.1	Common anatomical directions . . . . .	8
2.2	Bone composition (mass %) . . . . .	13
2.3	Material properties cortical bone of the maxilla . . . . .	14
2.4	Comparison relapse rates . . . . .	27
3.1	HU of common materials and tissues . . . . .	33
3.2	Cephalometric landmarks . . . . .	37
3.3	Anatomical planes . . . . .	38
3.4	Material properties . . . . .	43
4.1	Horizontal tipping - Palatal expander models . . . . .	61
4.2	Vertical tipping - Palatal expander models . . . . .	62
4.3	Material properties cortical bone . . . . .	69
5.1	Anterior displacements alveolar bone - PMD models . . . . .	79
5.2	Transversal displacements alveolar bone - PMD models . . . . .	79
5.3	Superior displacements alveolar bone - PMD models . . . . .	79
5.4	Horizontal tipping - PMD models . . . . .	81
5.5	Vertical tipping - PMD models . . . . .	81
5.6	Stresses measured at the cranial Foramina - PMD models . . . . .	86
5.7	Anterior displacements alveolar bone - Lateral osteotomy variation models	89
5.8	Transversal displacements alveolar bone - Lateral osteotomy variation models . . . . .	89
5.9	Superior displacements alveolar bone - Lateral osteotomy variation models	90



# Acronyms

The list is ordered according to the occurrence in the dissertation.

TMD	Transverse maxillary deficiency
RPE	Rapid palatal expansion
SARPE	Surgically assisted rapid palatal expansion
NSD	Neurosensory disturbances
FEA	Finite element analysis
CT	Computed tomography
3D	Three dimensional
MIMICS	Materialise Interactive Medical Image Control System
BC	Boundary conditions
PA	Posteroanterior
MPS	Midpalatal suture
MTDI	Maxillomandibular transverse differential index
CR	Center of resistance
CBCT	Cone Beam Computed Tomography
DICOM	Digital Imaging and Communications in Medicine
HU	Hounsfield units
STL	Standard Tessellation Language

UZ	Universitair ziekenhuis
MPC	Multi point connector
TPD	Transpalatal distractor
VM	Von Mises
PNS	Posterior Nasal Spine
For. Inc.	Foramen Incisivum
CI	Central Incisor
ANS	Anterior Nasal Spine
PM	Premolar
M	Molar
FEA	Finite Element Analysis
FEM	Finite Element Model
PMD	Pterygomaxillary disjunction



# Chapter 1 | Introduction

## 1.1 Background

Transverse maxillary deficiency (TMD) is a common malocclusion with an estimated prevalence of around 8%-22% [1] [2]. The transversal deficiency is mostly characterized by a narrow upper jaw, a posterior crossbite (uni- or bilateral), crowding of the maxillary teeth, a deep and narrow palate and large dark spaces in the buccal corridor [3]. A frontal and occlusal view of the deficiency is depicted in Figure 1.1, where the crowding of the teeth can be seen on the frontal view and the deep and narrow palatum on the occlusal view [4]. The transverse deficiency can not be healed with time and growth of the face. The earlier the diagnosis is made, the easier it is to treat the deficiency. When left untreated, the deficiency can lead to aesthetic discrepancies, nose breathing problems and sleep apnoea syndrome [1]. A crossbite and an asymmetry of the facial skeleton can develop as well [5]. Excessive tooth wear can occur, as well as problems to the temporomandibular joints [6].



**Figure 1.1:** Transverse maxillary deficiency: frontal (left) and occlusal (right) view [4]

The skull consists out of 28 separate bones, divided in the cranium, the facial skeleton and the mandible. The upper jaw, or maxilla, forms the majority of the facial skeleton, as can be seen in Figure 1.2. Between two adjacent bones, a suture is present. A suture is a connective tissue that connects the surfaces of adjacent bone parts and acts as a joint between them [7]. Sutures have characteristic morphological changes during growth of the patient. Sutures ossify and this ossification/maturation process leads to fusion of the adjacent bones.

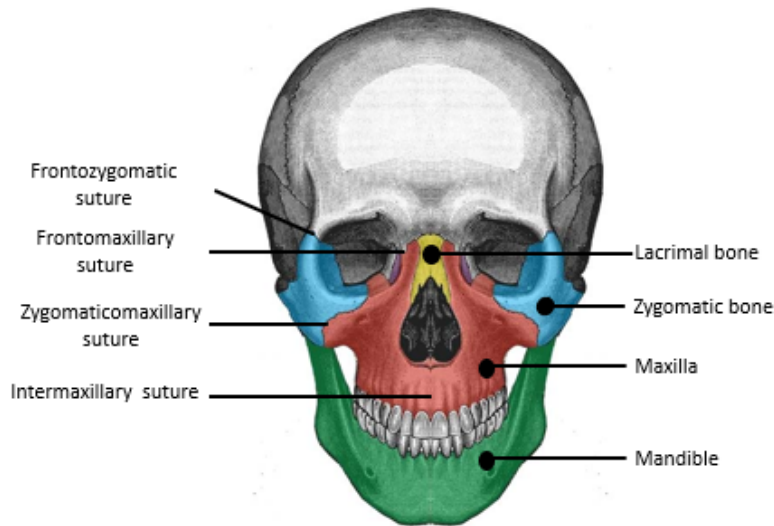


**Figure 1.2:** Facial bones and sutures: coronal view [8]

The transverse maxillary deficiency indicates that the maxilla is too narrow in the transversal direction. To correct this narrow maxilla, several treatment modalities can be proposed. The choice of the treatment modality depends on multiple factors, such as age, sex, the required amount of expansion and the maturation stage of the circummaxillary sutures [3]. For children up to fifteen years, the sutures are not yet completely ossified. If this is the case, rapid palatal expansion (RPE) has become the routine orthodontic procedure to treat TMD. The main object of RPE is to correct maxillary arch narrowness and widen the upper jaw. It involves the use of an expander appliance that is fixed to the upper teeth. In Figure 1.3, an example of such an expander appliance is shown. This expander is permanently fixed for 6-12 months. In the first two to three weeks, a screw will be adjusted to widen the upper jaw [9]. The appliance imposes forces on the maxilla and gradually opens the maxillary sutures, as these are not yet completely ossified [10]. Many studies have shown its efficiency in expanding the maxilla.



**Figure 1.3:** RPE expander [9]

For adults, the circummaxillary sutures ossify completely. Due to this ossification process, a purely orthodontic treatment like RPE is unsuccessful. Larger forces are required to perform the expansions, which can lead to excessive tipping of the teeth and a higher instability of the procedure [3]. For (young) adults, a more invasive surgical approach is required. The surgically assisted rapid palatal expansion (SARPE) procedure has become the main treatment modality for adult patients with maxillary transverse deficiency. This treatment consists of a surgical procedure and an expander device. Surgery is required to temporarily interrupt the main resisting elements of the facial skeleton. In literature, the piriform aperture pillars (anterior support), the ossified midpalatal suture (median support), the zygomaticomaxillary (lateral support) and pterygomaxillary (posterior support) buttresses form the main resistances to the transversal displacement of the maxilla [11]. These regions which show increased resistance against the expansion are indicated with blue arrows on Figure 1.4.

By performing surgical cuts (osteotomies), the regions which show high resistance against the expansion are disconnected from the rest of the facial skeleton. By this disjunction, there is a lower resistance against the transversal expansion, in this way lowering the required expansion forces and increasing the stability and predictability of the procedure. Once the surgery has been performed, the treatment is analogue to the RPE treatment. The expander device imposes the required forces and transmits them to either the teeth or the palatal bone [12]. The maxilla is widened by these forces and the transversal deficiency is corrected. The surgical procedure, as well as the expander device is depicted in Figure 1.4 [13].

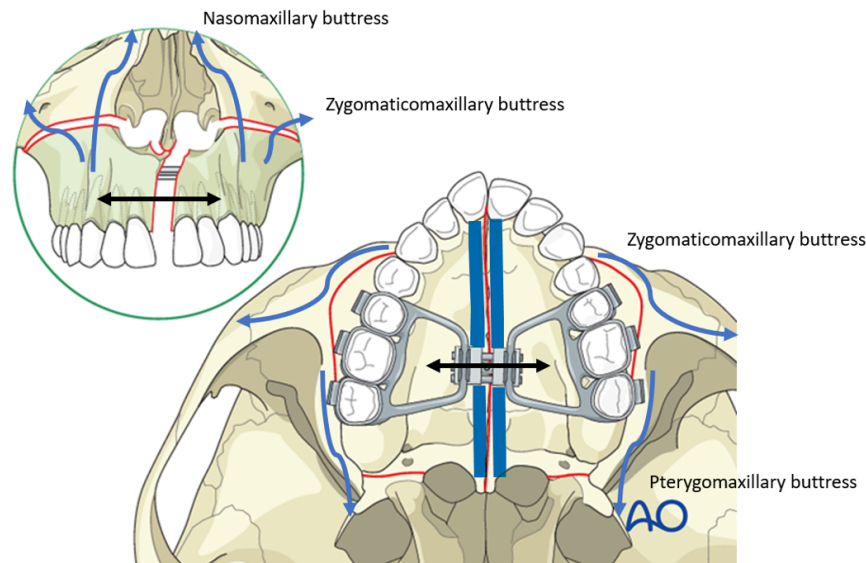


**Figure 1.4:** SARPE treatment: surgical cuts are indicated in red, regions of large resistance indicated in blue, expansion direction indicated in black [13]

Important to note is that there is no consensus in literature concerning the optimal treatment modality. Especially the type of expander device and the amount, types and optimal locations of osteotomies remain a point of discussion in literature [12]. Depending on which trade offs are made, a different surgical procedure is preferred. Due to the mechanical complexity of the stomatognathic system, the ethical issues concerning in vivo research and the inability to examine the mechanical properties of the human skeleton in vivo, it is very difficult to gain more insight in the biomechanical behavior of the maxillofacial complex and its structures. To deepen the knowledge on these subjects, the use of finite element analysis has been embraced by the medical world. In this way, the SARPE procedure can be evaluated using a reconstruction of the skull and finite element analyses [14] [15].

## 1.2 Motivation and objectives

There is a lack of consensus in literature concerning the stability, optimal surgical procedure, expander type and the expansion profile of the SARPE procedure. The main objective of this master thesis is to gain a better understanding of two influencing factors: on the one hand, surgical variations are analyzed, where the influence of the pterygoid plate disjunction and the presence of an asymmetric lateral osteotomy is analyzed. On the other hand the influence of different palatal expander placements is measured. Using the obtained results, the predictability, performance and clinical outcome of the SARPE procedure can be improved.

### 1.3 Structure of the thesis

The dissertation is divided in six chapters. In the first chapter, an introduction is given. In chapter 2, a literature review is conducted concerning the anatomy and biomechanics of the maxilla, the transverse maxillary deficiency, the SARPE procedure and the complications. In chapter 3, the development of the finite element model is described, starting from a CT-scan up to the meshed 3D model of the cranium and teeth. The CT data is segmented using MIMICS (Materialise, Leuven, Belgium). The cranium is reconstructed and osteotomies are performed. The material properties are determined and the boundary conditions are set up in ABAQUS. In chapter 4, a finite element study will be conducted where the palatal expander position is varied. In chapter 5, the presence of a uni- or bilateral pterygoid plate disjunction and the influence of an asymmetrically superiorly positioned lateral osteotomy is analyzed. In chapter 6, the general conclusions and future work are reported. The general workflow, followed to obtain the finite element model, can be seen on Figure 1.5.

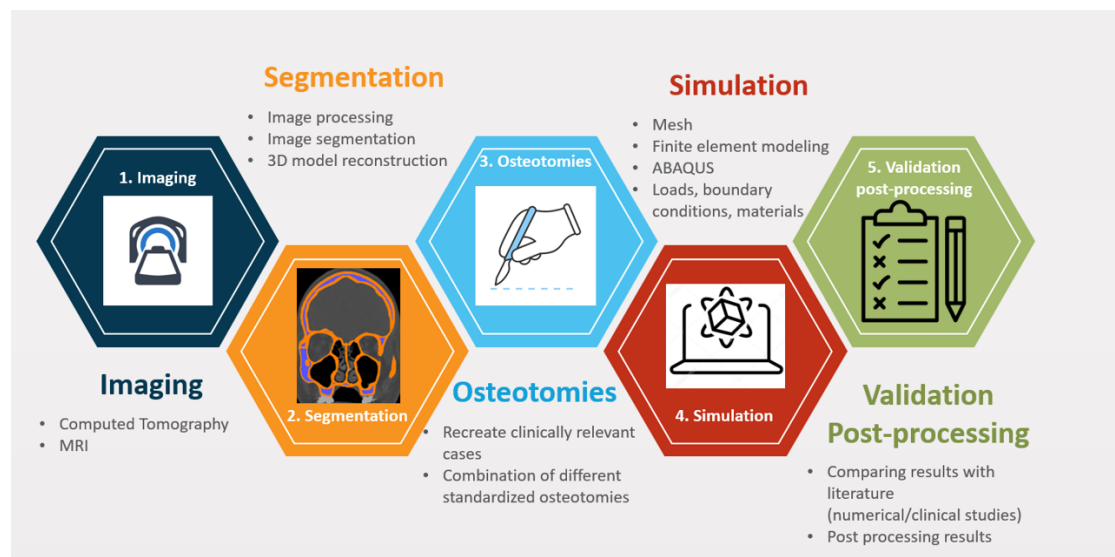


Figure 1.5: Workflow thesis



# Chapter 2 | Literature review

## 2.1 Anatomy

In this section, a general introduction to the anatomical concepts and the relevant anatomical regions is described. The regions of interest for this dissertation are the facial bones, the palatum and the dentoalveolar complex. A short overview of the bone anatomy will be described as well.

### 2.1.1 General anatomical considerations

When dealing with anatomical descriptions, it is necessary to mention the conventions concerning localization with respect to the anatomical planes. The conventions and concepts further used in this dissertation are referenced to three reference planes which can be seen in Figure 2.1. These reference planes include [16]:

1. **The sagittal plane (profile view):** divides the body into sinister (left) and dexter (right) sides.
2. **The coronal plane (frontal view):** divides the body into dorsal (back) and ventral (front) portions.
3. **The transverse (axial) plane:** divides the body into superior (towards head) and inferior (towards tail) portions.

Using these three body planes, an anatomical motion in the X-Y-Z coordinate system can be described and CT images can be analyzed. Orientations are defined according to directions relative to the body axis. Some of the most used anatomical directions are listed in Table 2.1 [17].

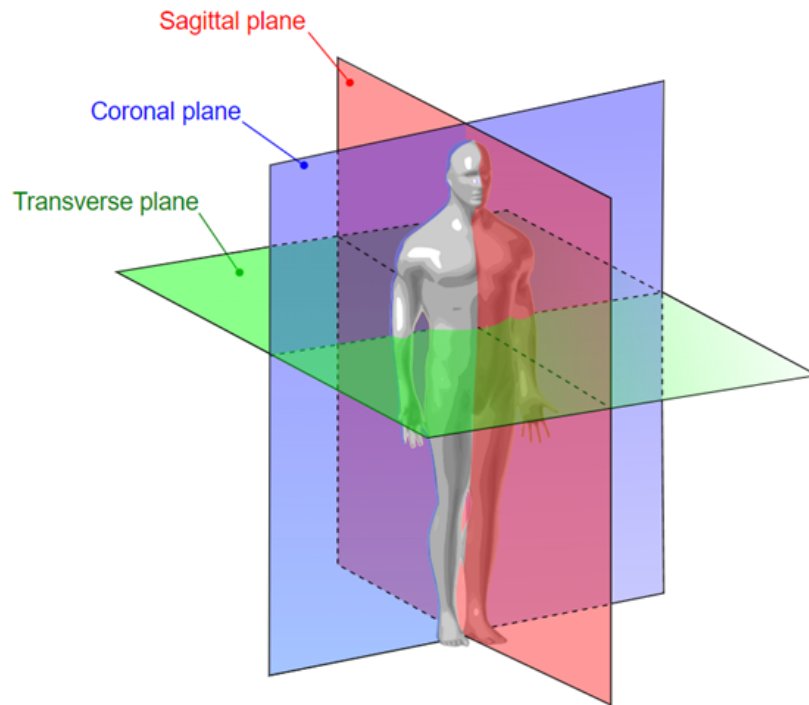


**Figure 2.1:** Anatomical reference planes [16]

**Table 2.1:** Common anatomical directions [17]

Anatomical direction	Definition
Anterior	In front of, front
Posterior	After, behind, towards the rear
Superior	Above, over
Inferior	Below, under
Lateral	Toward the side, away from the midline
Medial	Towards the midline
Bilateral	Involving both sides of the body
Unilateral	Involving one side of the body

### 2.1.2 Facial bones and sutures

The skull is the bony skeleton of the head and is the most complex bony structure in the body. It consists of 28 separate bones, consisting of the cranium, the facial skeleton and the mandible [18]. The facial skeleton or viscerocranium supports the soft tissues of the face. The maxilla forms the majority of the viscerocranium. The maxilla is a paired bone, separated by the intermaxillary suture and consists out of five parts: the zygomatic, frontal, palatine and alveolar processes, and the body [19]. The face contains other bones as well. The zygomatic bone contributes to the structure of the eye orbits, as well as the ability to articulate. It is also an attachment point for the masseter muscle which is a primary muscle involved in mastication. The lacrimal bones form part of the medial wall of the orbit. The mandible is essential for mastication and the only mobile bone of the face [18]. The facial bones are depicted in Figure 2.2 and Figure 2.3 [8].

Next to the bones, the skull also contains several sutures. A suture is a connective tissue that connects the surfaces of adjacent bone parts and acts as a joint between them [7]. The major sutures addressed in this research are the circummaxillary sutures (intermaxillary, zygomaticomaxillary and the frontomaxillary), as indicated in Figure 2.2 [20].

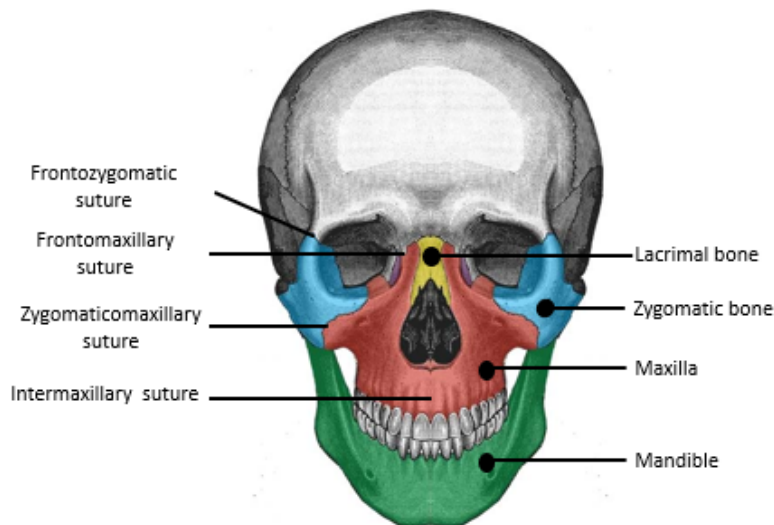


**Figure 2.2:** Facial bones and sutures: coronal view [8]

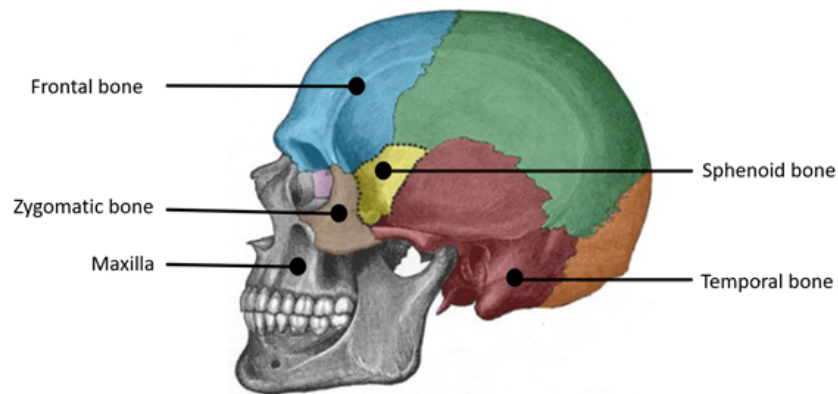


**Figure 2.3:** Bones of the skull: sagittal view [8]

### 2.1.3 Sphenoid bone

The sphenoid bone is an unpaired bone and consists of a body, paired greater wings, paired lesser wings and two pterygoid processes. These pterygoid processes will prove to be of importance for the SARPE procedure, as they are often osteotomized during the procedure. The sphenoid bone has a structural function, since multiple muscles involved in mastication attach to the bone [21]. The pterygoid processes descend inferiorly from the point of junction between the sphenoid body and the greater wing. The pterygoid plates consist of two parts: the medial and lateral pterygoid plate [22].

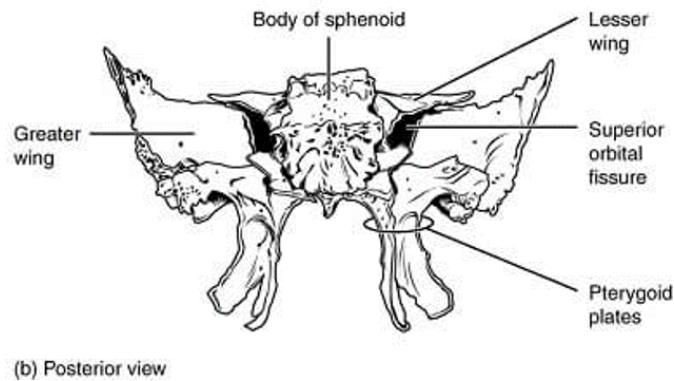


**Figure 2.4:** sphenoid bone [21]

### 2.1.4 Palatum

The palatum forms a division between the nasal and oral cavities. It consists of a hard palate (maxillary process) located anteriorly, and a soft palate (palatine bone) which is located posteriorly [8]. The midpalatal suture extends from the Foramen Incisivum to the posterior aspect of the palate [23]. An inferior view of the skull can be seen in Figure 2.5 [19], where the sphenoid bone also can be observed.

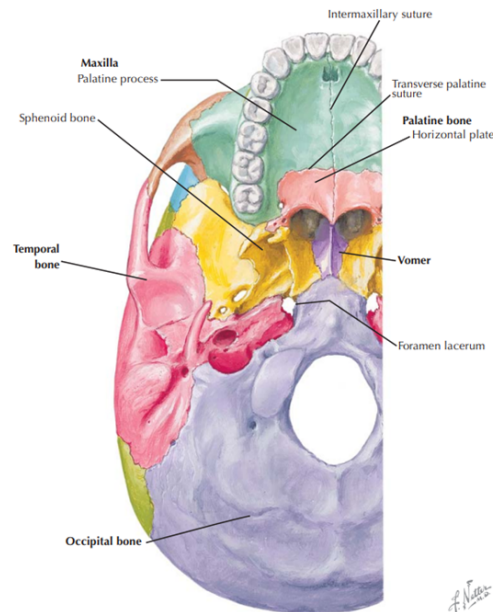


**Figure 2.5:** Occlusal view skull [19]

### 2.1.5 Maxillofacial buttresses

The midface can be conceptualized as a lattice-like system of buttresses. The buttresses develop as a skeletal adaptation due to the masticatory forces. According to the theory of Wolff, there is osseous reinforcement along the lines of maximal internal stress as the skull matures. These reinforcements manifest externally as a thickening of the shell of the cortical bone. As the masticatory forces are transmitted into the craniofacial complex, the bone withstanding the maximal internal stress will reinforce and the buttresses will form [11]. The strongest midfacial buttresses are vertically oriented, due to the large mastication loads in this direction. The horizontal buttresses reinforce the vertical ones. The three major maxillary buttresses involved in the SARPE procedure are the nasomaxillary, zygomaticomaxillary and pterygomaxillary buttresses, depicted in Figure 2.6 [24] [25].

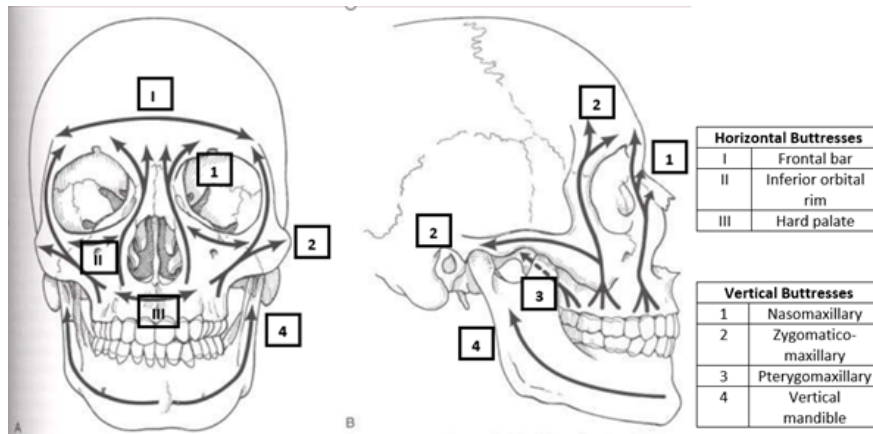


**Figure 2.6:** Indication of the buttresses found in the skull, frontal (A) and sagittal (B) view [25]

### 2.1.6 Dentoalveolar complex

All teeth have the same general structure. The visible part of the tooth is called the crown, whereas the roots are embedded in the bone. The tooth itself consists of different layers: the outer layer is called the enamel and it is the hardest tissue of the body. The middle layer consists of dentine which is softer than enamel and has a similar composition as bone. The most inner layer is called the pulp [26]. The teeth are implanted in depressions within the alveolar bone and are surrounded by the periodontium. This periodontium consists of the periodontal ligament, cementum on the root surface and gingiva. The periodontium provides support for the teeth, it transmits masticatory forces and it provides a biological seal for the teeth [26] [27].

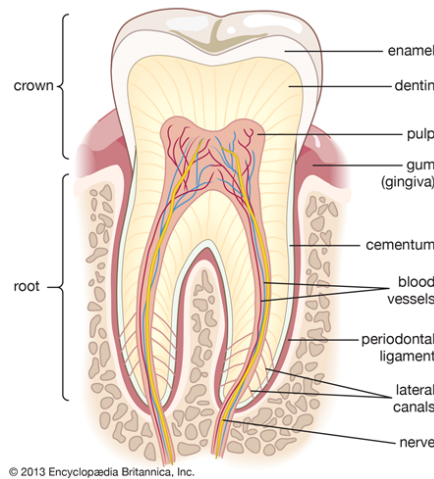


**Figure 2.7:** Anatomy of the tooth [26]

### 2.1.7 Bone

Bone is composed of three major components: an inorganic phase, an organic phase and water. The inorganic phase is mainly made of calcium hydroxyapatite ( $\text{Ca}_{10}(\text{PO}_4)_6(\text{OH})_2$ ), organized in mineral plates in between the collagen fibers. The organic phase is mostly collagen type 1 which provides the tensile strength of the bone [28]. This combination of different materials makes bone a non-homogeneous, composite and anisotropic material. All bones have an exterior layer called the cortical or compact bone. The cortical bone forms a solid osseous shell around the bone. It consists of dense and parallel, concentric, lamellar units, called the osteons. In the interior, there is a network of intersecting plates called the trabecular bone. In general there is a lower density, less homogeneity and a lesser degree of parallel orientation. The surface to volume ratio in cortical bone is much lower than in trabecular bone. Cortical bone is generally stiffer and able to resist higher ultimate stresses, however it is also more brittle than trabecular bone. The biomechanical behavior of cortical bone is rather uniform, whereas the properties of the trabecular bone vary depending on the apparent density. The composition of both bone types can be found in Table 2.2 [29] [30] [31].

**Table 2.2:** Bone composition (mass%) [30]

	Inorganic	Organic	Water
Cortical bone	59.9	28.1	12
Trabecular bone	65	25	10

Each bone in the body has a unique microstructure and composition, depending on the different loading conditions of each bone. When a different loading is applied, the bone can have two structural responses: altering the structural density or increasing the degree of structural orientation i.e. anisotropy. These dynamic responses to different loading conditions are possible due to bone remodeling, where on the one hand bone tissue is removed by osteoclastic resorption and new bone is formed by osteoblasts. With ageing, the balance of bone resorption and formation becomes negative. This is called osteoporosis [31].

Since each bone has a unique microstructure and mechanical properties, it is important to implement the correct mechanical properties of the bones found in the midface. In a study by Peterson and al. [32], different sites on the maxilla were located and the density, thickness and the elastic moduli of the cortical bone were determined. The location sites can be found in Figure 2.8 and the material properties can be found in Table 2.3. The cortical bone in the alveolar region tends to be thicker, less dense and less stiff whereas the cortical bone from the body of the maxillae is thinner, denser and

stiffer. The palatal cortical bone is similar to the cortical bone from the alveolar region. The locations where higher loads are occurring due to mastication will result in denser and stiffer cortical bone, according to Wolff's law. The anisotropy of the maxilla is small and can be neglected. Not much is known in terms of the mechanical properties of the trabecular bone of the maxilla [32].

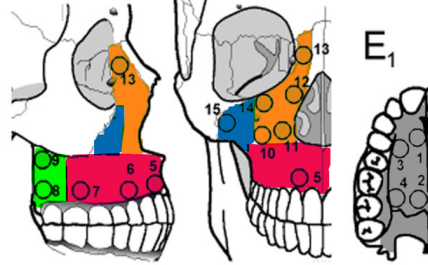


**Figure 2.8:** Material property determination on the maxilla, according to Peterson [32], grouped in five sets: the alveolar process (red), maxillary body (orange), posterior region (green), zygomatic process (blue) and the palatal process (gray)

**Table 2.3:** Material properties cortical bone of the maxilla [32]

Site	Density [mg/cm <sup>3</sup> ]		Thickness [mm]		E1 [GPa]		E2 [GPa]		E3[GPa]		Anisotropy	
	Mean	SD	Mean	SD	Mean	SD	SD	Mean	Mean	SD	Mean	SD
1	1.65	0.17	1.7	0.5	8.3	1.9	11.3	2.7	14.1	2.9	0.81	0.11
2	1.75	0.14	1.8	0.9	8.9	1.9	11.9	2.3	16.5	4.0	0.74	0.11
3	1.75	0.18	2.3	1.1	10.3	2.0	13.6	2.1	17.3	3.4	0.80	0.10
4	1.70	0.16	2.0	1.0	8.9	2.9	10.9	2.7	15.6	3.7	0.70	0.09
5	1.65	0.15	2.2	1.3	10.0	3.3	11.0	2.7	14.3	3.8	0.78	0.09
6	1.64	0.19	2.4	1.6	7.2	1.5	8.7	2.3	12.2	1.9	0.72	0.17
7	1.72	0.20	2.1	0.9	9.8	2.4	11.3	3.0	16.0	4.3	0.72	0.13
8	1.61	0.14	1.2	0.6	6.9	1.1	8.8	1.0	10.5	1.3	0.85	0.07
9	1.77	0.16	1.0	0.3	9.8	2.3	11.7	1.4	15.6	2.8	0.77	0.11
10	1.75	0.16	1.2	0.5	7.6	2.3	10.7	3.3	14.2	4.2	0.77	0.12
11	1.69	0.15	1.7	0.7	9.0	1.9	11.2	2.2	16.4	3.6	0.69	0.08
12	1.82	0.12	1.5	0.4	10.0	1.7	13.5	1.6	17.6	3.4	0.78	0.10
13	1.83	0.17	1.4	0.3	9.9	3.0	12.8	2.8	17.0	3.3	0.75	0.08
14	1.81	0.11	1.5	0.6	9.4	1.6	13.3	2.1	17.8	2.3	0.75	0.11
15	1.90	0.12	1.1	0.3	9.2	1.5	14.0	1.7	18.7	3.4	0.77	0.15
Grand mean	1.75	0.16	1.9	0.9	9.1	2.3	11.7	2.7	15.6	3.7	0.76	0.11
ANOVA	F	F	P	F	F	P	F	P	F	P	F	P

## 2.2 The midpalatal suture

The midpalatal suture is an end-to-end type of suture with characteristic morphological changes during growth. On the one hand there is an increased interdigitation of the suture, as can be seen in Figure 2.9. Melsen and al. [33] described a three-stage maturation process. The first stage is during the infantile period, where the suture is broad and Y-shaped. The vomerine bone is lodged in a groove between the two maxillary bones. In the juvenile period, bony spicules begin to form, resulting in a "wavy" appearance. In a final stage, the spicules become increasingly interdigitated, resulting in a "closed" appearance [33]. There is also an ossification process, where the number of bone spicules increases with increasing maturation. This ossification process and the increased interdigitation will result in the fusion of the maxillary halves. This fusion process progresses from posterior to anterior position [34].

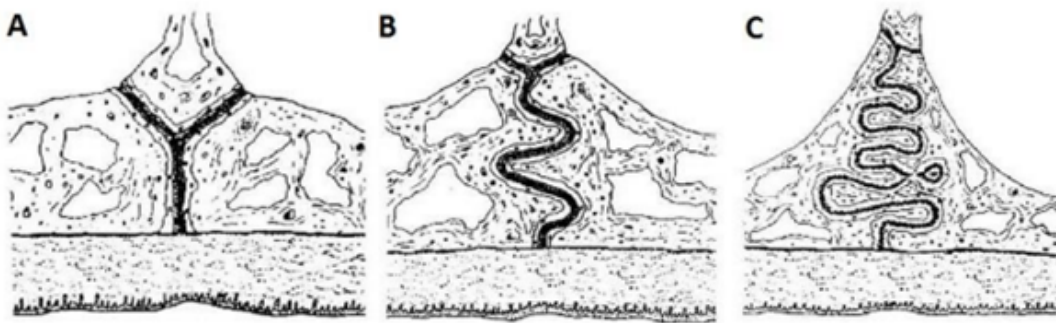


**Figure 2.9:** Increasing interdigitation of the midpalatal suture [33]

In Figure 2.10 one can find the different maturation stages of the suture. At stage E, there is complete fusion with the maxillary bones [35].

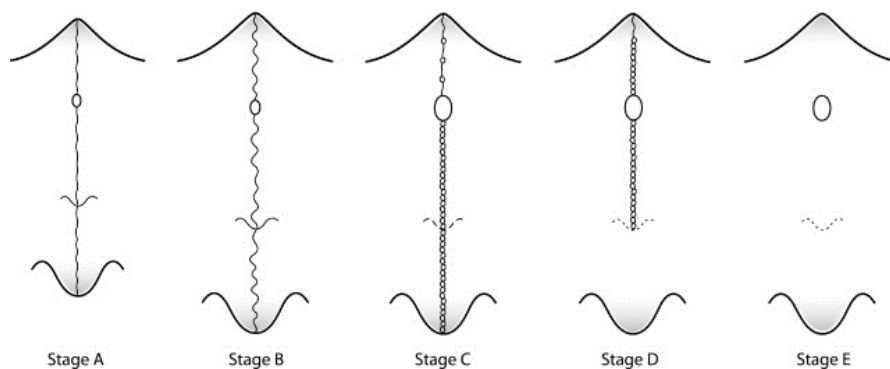


**Figure 2.10:** Fusion stages of the midpalatal suture [35]

The fusion process in the midpalatal suture varies greatly with age and sex, as reported by multiple studies [34] [36]. The time of fusion can range from early childhood to the third decade of life [37]. There are even cases where the suture of patients up to 71 years old had not completed the maturation process [34]. According to Samra and Hadad, the most important parameter in determining the palatal suture maturation stage is the density of the suture, which can be obtained from CT images [20].

The maturation of the midpalatal suture will be of great importance to determine the optimal treatment for transverse deficiency of the maxilla, as will be discussed in following sections.

## 2.3 Transverse maxillary deficiency

Transverse deficiency, or maxillary hypoplasia, is a detrimental problem to facial growth and to the integrity of the dentoalveolar structures [38]. The aetiology of this deficiency may involve developmental, congenital, traumatic or iatrogenic factors [39]. Others report the causes to be due to abnormal habits, dys and parafunctions such as thumb sucking and mouth breathing habits, muscle disorders and congenital syndromes (Apert, Cruzone, Marfan etc.) [1]. The estimated prevalence is approximately 8-22% of the population [1] [2].

### 2.3.1 Diagnosis

The diagnosis of TMD can often be difficult, since there are minimal soft tissue changes and it is easily masked by other skeletal or dental discrepancies. The main clinical indications of the condition are, among others: a unilateral or bilateral posterior crossbite, a narrow palate and high palatal vault, para nasal hollowing, a narrow nasal base, dark buccal corridors and a disproportion between the width of the upper and lower dental arches [1] [23] [38] [40].

The diagnosis is based on a standardised PA cephalogram. The cephalogram is used to help with the treatment planning and diagnosis. It is used to assess the aetiology of the malocclusion and to determine whether the malocclusion is dental, skeletal, or a combination of both.

### 2.3.2 Symptoms

The maxillary deficiency can lead to several problems. First, it may contribute to the development of persistent mouth breathing, as well as the hypotension of the orbicularis oris muscle, involved in mimical movements [1]. Furthermore, the lowered tongue position can affect the shape of the upper dental arch, which can lead to crowding of the teeth. When left untreated, it can lead to aesthetic discrepancies, nose breathing problems and sleep apnoea syndrome [1]. A crossbite and skeletal facial asymmetries could develop as well [5].

### 2.3.3 Treatment

Several treatment procedures exist, which can be categorized in either surgical and non-surgical procedures. As long as the maxillary bones have not yet been fused, the transverse maxillary deficiency can be treated with an orthodontic expansion using a rapid palatal expander (RPE). Different appliances can be used as a source of pressure forces to widen the palate. The appliance is used to progressively open the palatum 0.5 to 1 mm per day [1]. With advancing maturation stage of the midpalatal suture, the degree of unwanted effects such as lateral tipping of the teeth, alveolar bone bending, instability of the implant, periodontal defects such as gingival recession, instability and thinning of the cortical plate is increased [1] [36]. The optimal timing for RPE is considered below the age of 15 [41]. Since the exact timing of the midpalatal suture maturation varies greatly among individuals, age or sex can not be used as a determining factor [42].

A second option to treat TMD is using surgical procedures. Two different options exist. There is a fully surgical treatment option, using the segmental Le Fort 1 osteotomies. These osteotomies will release the maxilla from adjacent bones and in this way, the transverse relationship can be corrected [38]. Using this technique, the vertical and sagittal maxillary dimensions can also be corrected. An expensive, second surgical procedure can also be prevented [36]. However, this segmentation of the maxilla using a Le Fort I osteotomy is linked to inaccuracy and instability, especially concerning the transversal displacements [36]. Other studies however detected less relapse with a Le Fort I osteotomy compared to alternative procedures (over a two year period) [43].

A less invasive and more stable treatment option is a partial maxillary osteotomy with the support of expander appliances. This is called a surgically assisted rapid palatal expansion or SARPE [38]. For the treatment of TMD, mostly the SARPE procedure is preferred over the segmental Le Fort I procedure, due to the lower invasiveness of the technique. The SARPE procedure will be the main focus of this master thesis, and hence will be discussed in following section in more detail.

## 2.4 SARPE

Surgically assisted rapid palatal expansion (SARPE) is a combined orthodontic and surgical procedure to treat transverse deficiency of the maxilla [12]. The treatment requires a coordinated approach involving the orthodontist and the maxillofacial surgeon. The procedure consists of several osteotomies to reduce the resistance to transverse expansion, as well as the use of an expander device to apply the required forces for the expansion. The goal of the SARPE procedure is a transverse expansion obtained entirely by bone formation, with no dental or periodontal damage and in the absence of dental or osseous relapse [40]. In Figure 2.11, the end result of the SARPE procedure is shown.

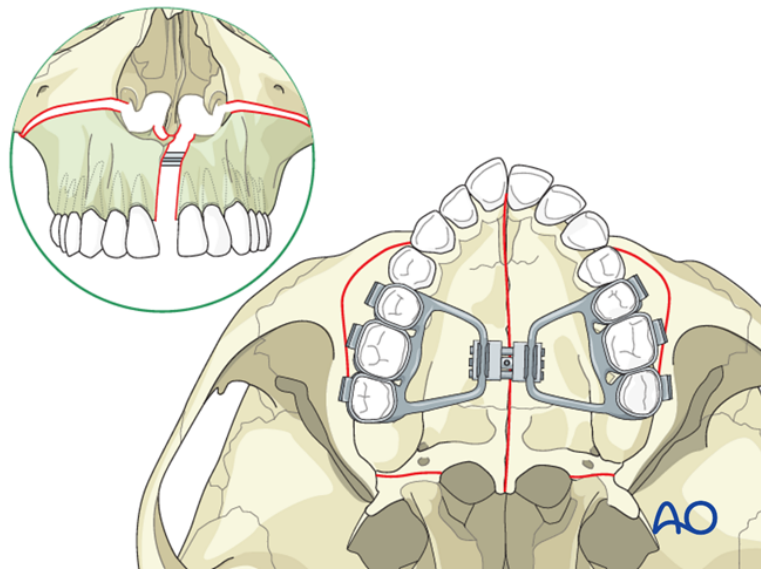


**Figure 2.11:** SARPE treatment with osteotomy lines indicated in red [13]

The factors that govern the choice for a surgical procedure include the type of deficiency (dental, skeletal or both), the skeletal maturation of the midpalatal suture, the magnitude of the discrepancy as well as the status of the periodontal tissue [40]. As a guide to determine the optimal treatment choice, a maxillomandibular transverse differential index (MTDI) is used. The MTDI is the difference between the expected and actual maxillomandibular width. If this value exceeds 5 mm in skeletally mature patients, the SARPE procedure is recommended [40].

Since the SARPE procedure contains a lot of variables, a lot of options exist in the treatment modality. In contemporary literature there is no conclusiveness regarding the optimal treatment [40]. The clinicians must decide the optimal treatment procedure on a patient specific basis and based on their own experiences. The end result of the pro-

cedure can be seen in Figure 2.12, where the initial and post treatment cephalometric analyses are shown [44].

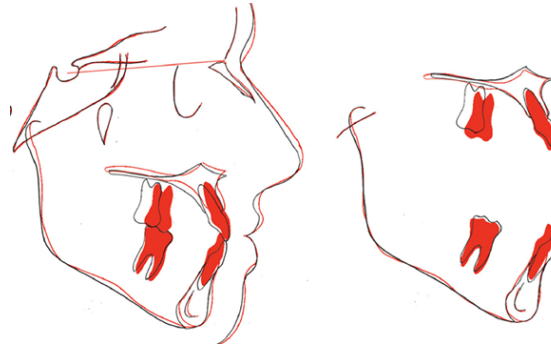


**Figure 2.12:** Initial (black) and post-treatment(red) superpositions of cephalometric tracings [44]

The SARPE procedure is a type of distraction osteogenesis. A distraction osteogenesis describes the growth of new bone created by gradually separating two bony surfaces using an osteotomy [45]. Initially, a fibrous callus develops at the initial osteotomy site, which gradually ossifies. As the fracture is mobilized using an orthodontic expander, this ossification process can not complete and a fibrous union results. By further expanding the bone, it can be gradually elongated. The distraction osteogenesis results in new strong bone, formed in a controlled manner. The bone also has a higher resistance to relapse [45].

### 2.4.1 Overview of the procedure

The procedure consists of a presurgical orthodontic treatment, the surgical procedure itself and the post-orthodontic treatment.

#### 2.4.1.1 Diagnosis and presurgical orthodontic treatment

The treatment planning consists of a clinical and radiographic examination of the maxillary arch form [46]. This procedure contains a multitude of steps. First, the diagnosis should be made by the orthodontist. The facial proportions and symmetry are analyzed. Some important measurements include the anteroposterior position of the maxilla, the symmetry of the face and the facial midline. In a following step, the cephalometry is performed, where the proportions of the facial skeleton are compared to the norm. After this a Plaster of Paris model of the maxilla and mandible are taken and the centric occlusion of the patient is recorded. This allows to analyze the occlusion as well as the shape of the dental arches. After this, a 3D-virtual planning of the surgery can be performed [47].

The goal of the presurgical orthodontic therapy is in the first place to align and level the occlusion. The maxillary and mandibular arches are coordinated and dental compensations are eliminated in preparation for the surgical correction. The roots of adjacent teeth are also diverged, which is required for the surgery. The surgeon should be aware of the arch space management during the presurgical orthodontic phase, which requires cooperation with the orthodontist [48].

#### 2.4.1.2 Surgical procedure

Surgery is required in skeletally adult patients to allow the transverse expansion of the maxilla, as was discussed before. By temporarily interrupting the key resisting elements of the mid-facial skeleton, the palatum can be expanded more easily with lower expander forces. The surgical procedure seeks to minimize the invasiveness of the procedure and increases the predictability of the outcome [11].

The choice of the osteotomies will prove to be important for the clinical outcome and will determine whether a predominantly orthopedic (skeletal) or orthodontic (dental) expansion will occur. According to the literature, once the circummaxillary sutures are completely ossified, the nasomaxillary, zygomaticomaxillary and pterygomaxillary buttresses form the main resistances to the transversal displacement of the maxilla [11].

The ossified midpalatal suture is a principal source of resistance to the expansion in the median region, due to the fusion process as was discussed before [36] [49]. The midpalatal osteotomy is hence essential before maxillary expansion can occur [11]. In practice, the maxillary halves are pried open. The zygomaticomaxillary buttress is considered to be the predominant buttress in the midface and hence also is a primary osteotomy site [11]. It provides resistance in the lateral regions of the midface [36] [49]. The piriform aperture pillars are the main area of resistance in the anterior region. In the posterior region, the pterygoid plates are the main source of resistance [36] [49].

There are several osteotomies which can be performed: a paramedian palatal osteotomy (one of both indicated in the figure), a buccal osteotomy from the piriform rim to the maxillopterygoid junction, a vertical osteotomy and a pterygoid plate disjunction. These osteotomies are depicted in Figure 2.13, where the osteotomy line is indicated in red [12].

The pterygomaxillary disjunction (PMD) remains a controversial osteotomy in literature, as more complications arise when the PMD is performed. Without the pterygoid disjunction the fused pterygoid processes will tend to splay outward. In this way the forces are transmitted to deeper anatomical regions such as the body and greater wings

of the sphenoid bone, which needs to be avoided. According to Shetty and al. [11], the pterygoid disjunction also influences the expansion shape: without the osteotomy, the expansion will be V-shaped, whereas a more parallel and uniform expansion is obtained when the pterygoid plates are osteotomized [11] [50]. Possible complications when performing the pterygoid disjunction are: trauma of the palatine artery or the cranial nerve, injury of the pterygoid plexus and an increased duration of the procedure [36] [49]. Variations on the surgical technique have been recommended based on the patient's age, missing teeth, presence of or tendency towards an anterior open bite and the requirement for a secondary Le Fort osteotomy.

Ultimately, the choice as to which osteotomies are performed depends on the required expansion profile, as well as on the surgeon's preference. There is a certain trade off the clinician needs to take into account: maximizing the mobility of the maxilla on the one hand and reducing the invasiveness of the procedure on the other hand.

#### **2.4.1.3 Post-orthodontic treatment**

After the surgery is performed, a latency period of seven days is instructed by the maxillofacial surgeon. After this period, the patient is instructed to activate the expander screw by 0.25 mm to 0.33 mm twice a day. It is advised to not distract with higher rates than 0.33 mm, since it could be detrimental to the patient's health and treatment outcome. During the active distraction phase, the process will provide incremental traction on the bony callus (fibrous bridge between bony parts), resulting in osteogenesis. Patients are monitored twice a week until the planned expansion is reached, two to three weeks post surgery. Once the planned expansion is reached, the distractor is left in place for several weeks. The rigid fixation by the distractor allows bone remodeling and maturation of the newly formed bone [45].

The length of the stabilisation period following the SARPE seems to influence the long-term transverse stability. Mostly, skeletal retention has been recommended for six to twelve months post SARPE. There is significantly less relapse reported if a six month retention period is used when compared to a three month period [46]. Relapse can be defined as the gradual recurrence of the abnormality for which the distraction was performed [51]. [52] [53].

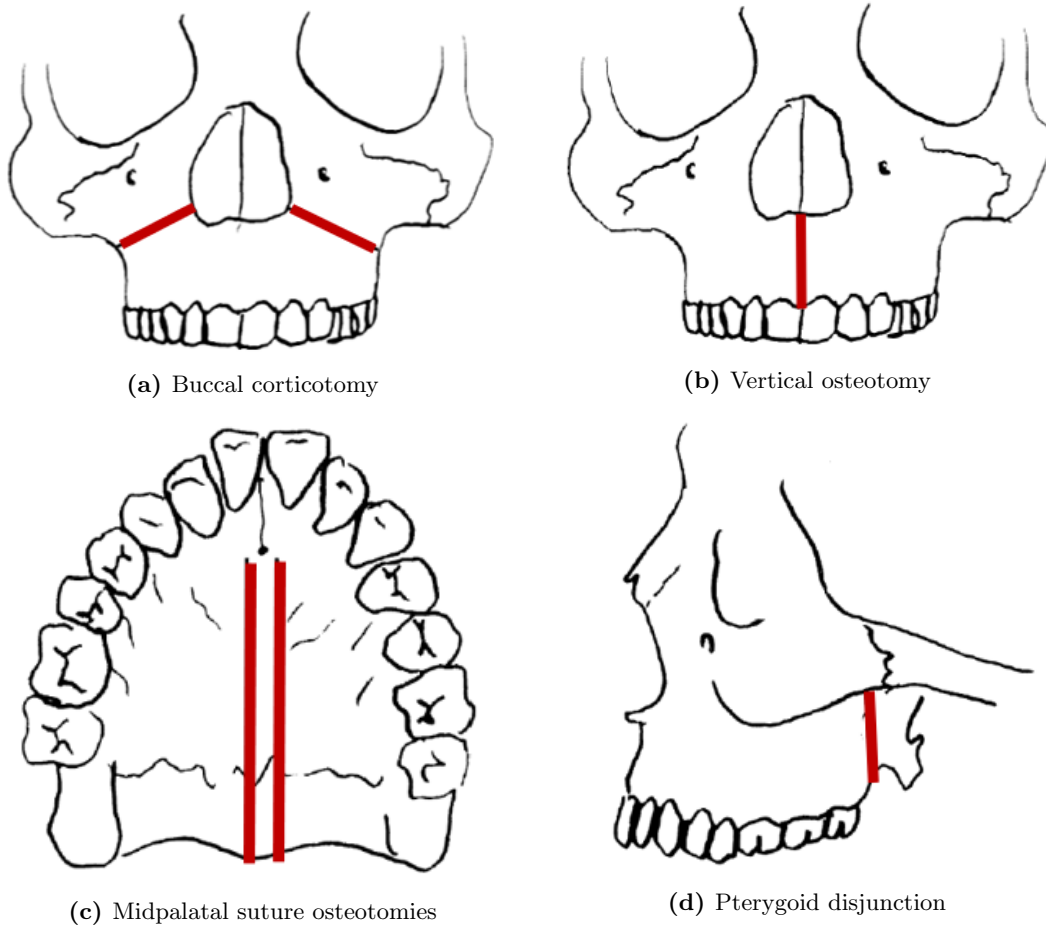


**Figure 2.13:** Possible osteotomies indicated in red [12]

## 2.4.2 Expander types

To perform the transversal expansion, a palatal expansion device is required. There is a large variety of expansion devices. These can be categorized in two major groups: the tooth-borne and the bone-borne appliances.

### 2.4.2.1 Tooth-borne

In tooth borne appliances, the expander itself is cemented to the teeth for anchorage [40]. The mechanical stresses are transferred to the roots and periodontal ligament of the teeth. In this way less force is transferred directly to the maxillary bone. There is a variety of different tooth borne expanders. As an example a Hyrax tooth borne device can be seen in Figure 2.14 [54].

An advantage of the tooth-borne expander is that it can be placed and removed without local anesthesia. The placement is less time consuming and Hyrax expanders are generally less expensive than bone-borne alternatives [55].

However, due to the force transfer to the periodontal ligaments, several adverse effects to the teeth and surrounding tissues occur, including among others, buccal tooth tipping, reduced buccal bone thickness, root resorption, bone fenestration and buccal gingival recessions [56] [57]. Bone resorption is the most common complication in tooth-borne appliances. Due to the application of the mechanical stresses to the teeth, the bone movement is not prevented during the retention period and the skeletal relapse can not be prevented, resulting in increased relapse rates according to some authors [40]. In patients with extremely narrow maxillae, a Hyrax device can not be placed due to its size [55].

### 2.4.2.2 Bone-borne

The bone-borne distractor is directly placed onto the palatum during the surgical procedure. It decreases the complications caused by the expansion protocol, such as tooth inclination and root resorption. An example of a bone borne distractor can be found in Figure 2.14 [58]. The use of the bone-borne device leads to an increase of predictability of the expansion. The undesirable effects on the teeth and periodontal ligament can be avoided. The force transmission to the alveolar bone is greater in bone-anchored than in tooth-anchored devices [58]. From the orthodontist's point of view, the bone-borne device is also preferred, since it is possible to initiate tooth leveling while skeletal expansion is still ongoing [59].

Some of the benefits of the bone-borne appliances include greater skeletal expansion of the maxilla and facial bones, reduced burden and adverse effects on the anchorage teeth and improved stability of the expansion [56]. However, a more recent study by Kunz et al. revealed the buccal tipping of the teeth, despite the absence of direct force transmission to the teeth. This could be induced by the moving bone segments [59]. The most common complication with the bone-borne device is appliance-related, followed by bone resorption [51]. There is also an increased risk due to the invasiveness of the procedure and an increased risk of wound infections [56].



**Figure 2.14:** Example of a tooth-borne Hyrax expander (left) [54] and a bone-borne transpalatal distractor (right) [58]

According to several studies, both appliances provide good long-term stability. A more recent study by Kunz et al. [59] suggests that both type of expanders serve their own purpose: the tooth borne expander should be expected to result in a more parallel pattern of expansion, with the largest transversal expansion at the premolars. The transpalatal distractor on the other hand should be selected whenever a more V-shaped pattern is required, with a more anterior opening [59].

### 2.4.3 Complications

A long-term follow-up study by Smeets and al. [60] revealed that one year after surgery, complications were found in 52.25 % of patients. The most prevalent complications are neurosensory disturbances or NSD (27.03%) and postoperative pain (13.51 %). There is an increase in dental complications and NSD with increasing age [60]. Other complications are, among others: intraoperative or postoperative bleeding, tooth discoloration, appliance loosening or breaking, asymmetric expansion, relapse and tipping [23] [61].

#### 2.4.3.1 Tipping

Tipping is the undesired rotational component of the expansion. To describe the movement of the craniofacial bones, one needs to determine the equivalent force system at the center of resistance [62]. The center of resistance (CR) is equivalent to the concept of the mass center of a free body. It is a conceptual, fixed point for which, when a force has its line of action passing through the CR, the body will present a pure translational movement. When the force is not passing through the CR, it will lead to a translational and rotational component. This rotational component will result in a rotation around the center of rotation, depending on the force moment [63]. The centers of resistance and rotation of the dentomaxillary complex are known in both the sagittal and axial planes and are shown in Figure 2.15, together with the applied force [62]. The center of rotation is depicted as a black dot with the letter R and the center of resistance is given by the open circle with a cross [62].

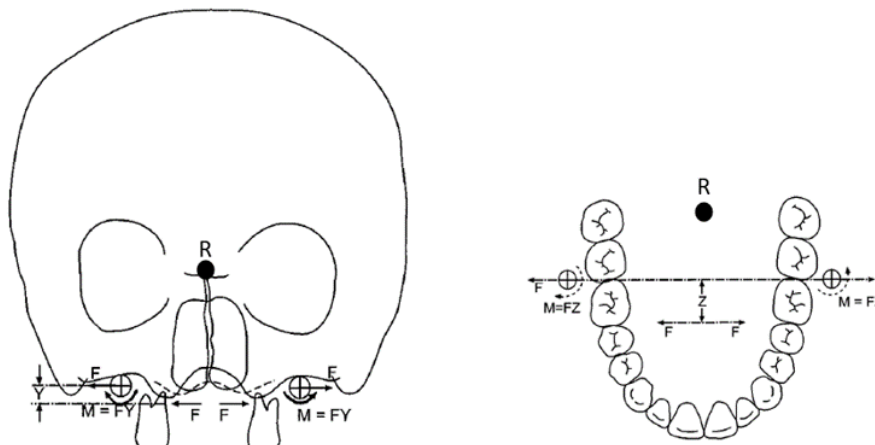


**Figure 2.15:** Equivalent force system in the coronal (left) and occlusal (right) plane [62]

As can be clearly seen, the line of action of the expansion forces do not pass through the centers of resistance. Due to this, the motion of the skeletal expansion will be both translational and rotational. The rotational part is undesired and is called tipping. In the coronal plane, this will result in a pyramidal shaped expansion and in the occlusal plane, it will lead to a non parallel V-shaped expansion profile [62].

Improvements to this tipping behavior can be obtained by placing the appliance more posteriorly. Another option is by increasing the rigidity of the appliance. A final option is to perform the pterygoid plate osteotomy. The influence of the pterygomaxillary disjunction on the center of resistance can be seen in Figure 2.16. Due to the disjunction, the CR's will move more anteriorly and the moment's arm is reduced. This shows that the pattern of maxillary expansion can be modified to certain patients needs by selective positioning of the transpalatal distractor and presence of the pterygoid disjunction. A more anterior positioning of the TPD will lead to increasingly more V-shaped distraction, and a more posterior positioning will lead to a more parallel expansion profile of the maxilla [64].

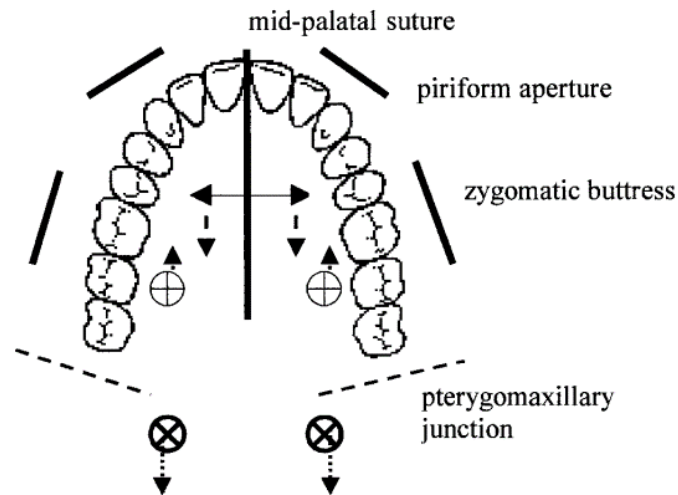


**Figure 2.16:** Influence of the surgical procedure and TPD placement on expansion profile [64]

When the forces are applied to the teeth, the teeth will also show this tipping behavior. In the premolar and molar teeth, there is a significant amount of buccal tipping after SARPE [65]. However, this dental tipping will mostly relapse, as will be mentioned in following section.

### 2.4.3.2 Relapse

Relapse can be defined as the gradual recurrence of the abnormality for which the distraction was performed [51]. In literature, there is a large variability in the reported stability of the SARPE procedure. Some of these relapse figures are reported in Table 2.4, together with other relevant information which could influence the relapse rates, such as the expander type, the surgical procedure as well as the age and sex of the patients.

**Table 2.4:** Comparison relapse rates

Author	Expansion device	Surgical procedure	Retention period	Age	Sex	Relapse rate	
						Inter canine	Inter molar
Marchetti et al (2009) [43]	Tooth borne (Spider)	Buccal, vertical, pterygoid disjunction	3 months	23.5 y	M/F	28 % (2.5 mm)	36 % (3 mm)
Byloff and Mossaz (2004) [66]	Tooth borne (Hyrax)	Buccal, vertical, pterygoid disjunction	3 months	[18;41]	M/F	20 % (1.05 mm)	33 % (2.9 mm)
Anttila et al. (2004) [67]	Tooth borne (Hyrax)	Buccal	6 months	/	/	10 % (0.4 mm)	18% (1.3 mm)
Berger et al. (1998) [68]	Tooth borne (Hyrax)	Le Fort I osteotomies	3 months	[13;35]	M/F	23 % (1,12 mm)	17 % (1,01 mm)
Bays and Greco (1992) [69]	Unknown	Buccal, vertical	Unknown	[15;40]	M/F	8 % (0.39 mm)	7 % (0.45 mm)

This variability can partly be explained by the difference in measuring points and the timing differences of the measurements [52]. The retention period, as well as the amount of required expansion, the surgical procedure and the expansion device could also partially explain the difference in relapse numbers [43]. Using the data provided in Table 2.4, a 25-30 % overexpansion of the transverse distance is proposed [43]. A more pragmatic way is to overexpand the lingual cusps of the upper posterior teeth until they are in contact with the buccal cusps of the lower posterior teeth [70].

In Figure 2.17, the amount of expansion with a Hyrax expander is shown. On this figure, one can see the expansion at different measurement moments. T2-T1 depicts the amount of expansion, T3-T2 shows the relapse during the retention period and T4-T3 is the post orthodontic relapse. From this figure, it can be clearly seen that the post retention relapse is the most significant. The largest amount of relapse is also recorded at the first molars, as they were used as anchorage for the tooth borne expander in this study [66].

It can be concluded from multiple studies that the skeletal expansion is quite stable [51] [52]. During expansion the skeletal maxillary width shows significant changes whereas the post SARPE changes can be considered negligible.

As opposed to the skeletal stability, the dental movement can not be considered as stable. The first molar and premolar show significant buccal tipping immediately after the SARPE procedure [70]. The dental movement shows a lot of relapse with a large variability. The dental relapse variability can be attributed to a multitude of factors, such as the device type, surgical technique and timing of the measurements [52].

The dental relapse can also be seen in Figure 2.18. In this figure, the blue line represents the expansion at the first molar, the red line shows the skeletal percentage of the expansion. The green line shows the maxillary skeletal expansion at the jugula and the magenta line shows the expansion across the nasal cavity. As can be seen from this figure, at first, only 47% of the expansion is skeletal. Around three weeks after the SARPE procedure, the amount of relative skeletal expansion increases up to 68%. This increase is due to the relapse of the dental movement. In this way the relative contribution of the skeletal expansion increases.

The dental relapse behavior can be influenced during the retention period. Here the potential overexpansion is corrected, as well as the correct occlusal relationship is ensured [52]. It remains important to note that a variety of aspects, including the location and magnitude of the maxillary transverse deficiency, the pre-surgical orthodontic expansion, the stabilization period length, the different maxillary osteotomies, the expander type, the age and the sex of the patient may influence the long-term stability of the procedure. Due to these multiple influencing factors, up to this day a large amount of uncertainty remains among clinicians regarding the optimal treatment of the transverse maxillary deficiency [46].

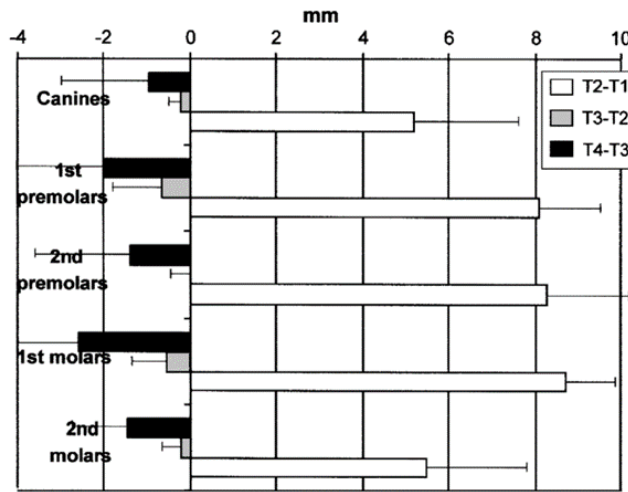


Figure 2.17: Expansion at different time instants and measuring points [66]

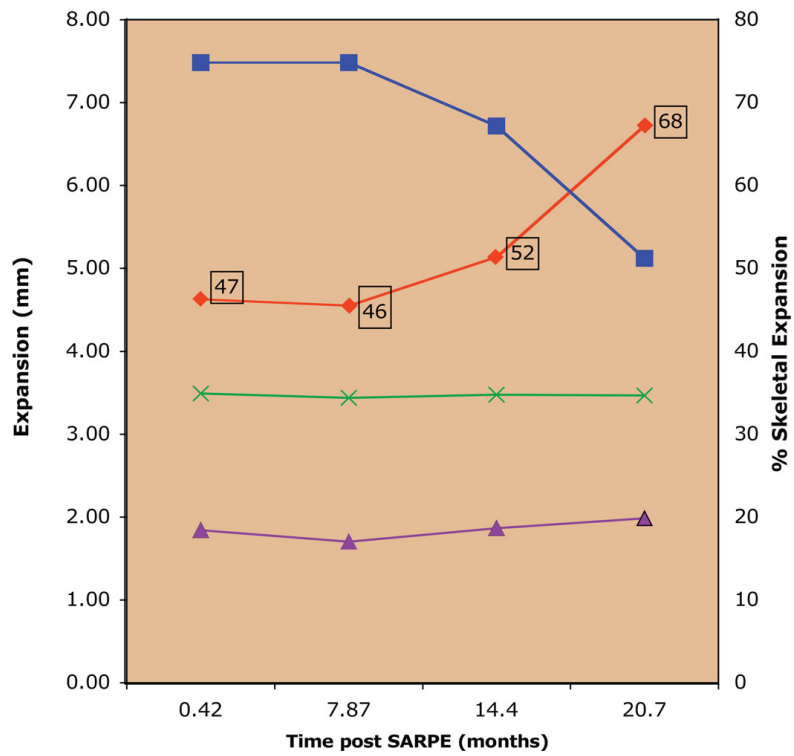


Figure 2.18: Skeletal and dental relapse [52]



# Chapter 3 | Materials and methods

The objective of this part of the study is to create a geometrically accurate model of the human cranium and teeth. The development of a finite element model of the skull requires five steps. First, medical images are taken showing the exact anatomy. This can be done using multiple medical imaging technologies, such as (CB)CT, MRI... A rough 3D model of the individual bones and tissues can be obtained by segmentation of these images. The third step is to perform the required osteotomies and to further process the rough model to obtain a realistic 3D surface. Clinically relevant cases are recreated, combining different osteotomies. A fourth step is to mesh and import the 3D model in the finite element software, where the required finite element analysis can be performed using ABAQUS. A final step is to validate the results with the help of clinical and numerical studies found in literature. The results are post-processed and conclusions are formulated. In following sections, the process and the different steps are explained in more detail. The workflow is also depicted in Figure 3.1.

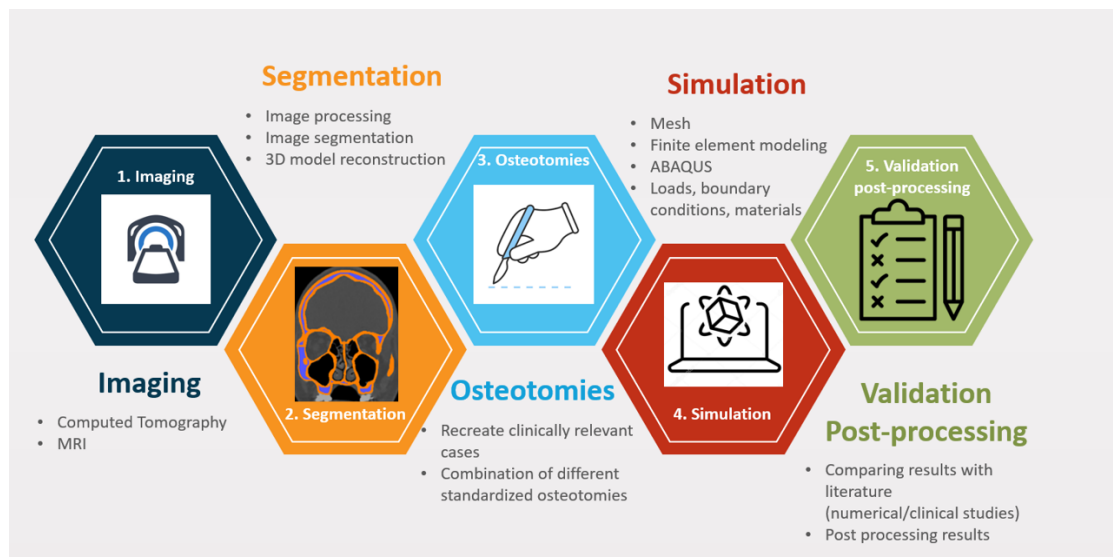


Figure 3.1: Workflow master thesis

### 3.1 Imaging

There are several imaging technologies, such as (CB)CT, MRI and CTA, among others. In this research CT images were used. CT (computed tomography) uses a thin fan-shaped beam of X-rays to obtain structural and functional information of different tissues of the body. These X-rays strike multiple rows of detectors, and these are rotated continuously as the patient moves through the scanner. The CT image is reconstructed based on the X-ray absorption profile characteristic of specific tissues and bones. Denser tissues, such as bone, appear white on a CT scan, whereas soft tissues will appear gray and air black [71].

CT scans are widely used in the medical imaging world, due to the possibility of excellent images. However, the patient is exposed to ionizing radiation. More recently, Cone Beam Computed Tomography or CBCT is rising in popularity. In this technique, a cone beam is used, which strikes a rectangular flat panel detector. The patient does not need to be moved during this procedure. Without any rotation, a 2D image is obtained, and when the scanner is rotated once over the patient a complete 3D dataset can be obtained. Some of the advantages are: reduced radiation dose, possibility of a high spatial resolution, reduced time to take the scan, reduction of metal artifacts and better accessibility [72].

The output of the (CB)CT scan is an array of sequentially numbered files. This is mostly stored in the DICOM (Digital Imaging and Communications in Medicine) format, which can be further processed using specific software.

This project is in cooperation with the UZ-Ghent hospital. An anonymized CT-scan of a patient, who required the SARPE procedure, was provided by the hospital of Ghent.

### 3.2 Segmentation

Image segmentation is the process of partitioning a digital image into multiple segments. A label is assigned to each pixel in the image. The pixels with a same label share certain characteristics. Image segmentation is mostly used to locate objects and boundaries in images. From this, a set of contours can be extracted and a 3D reconstruction can be obtained [73]. To perform this segmentation, Materialise MIMICS (Materialise, Leuven, Belgium) was used. MIMICS is an image processing software for 3D design of anatomical structures and the design of implants, developed by Materialise. The interface of the used software is shown in Figure 3.2.

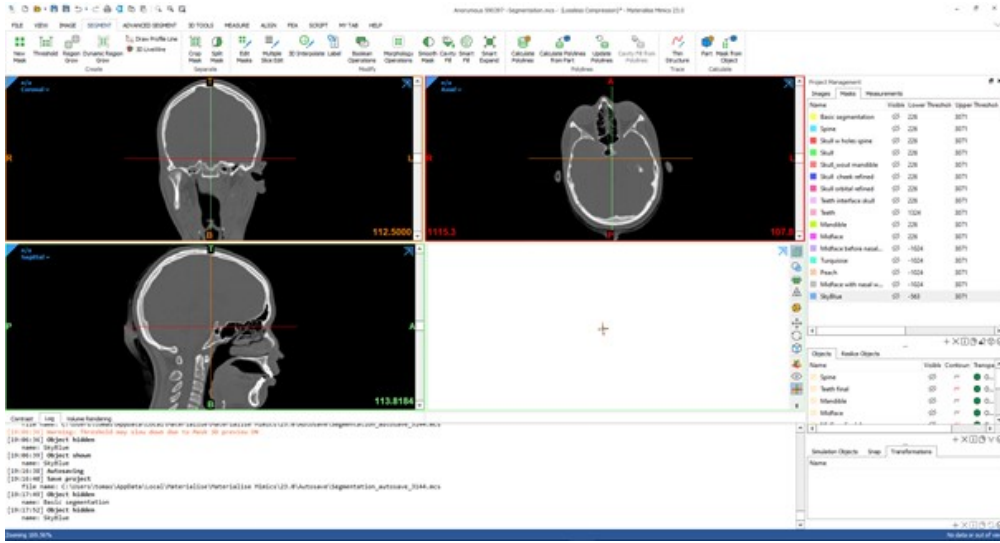


Figure 3.2: Interface MIMICS software

Due to the complexity of automated medical image segmentation, a semi-automatic, intensity based segmentation of the cranium was performed. The basic idea of intensity based segmentation is that voxels within a region of interest have similar radiodensity values. The Hounsfield scale can be used as a quantitative scale for describing the radiodensity of a voxel [73]. Based on the difference in Hounsfield unit (HU)-values, different anatomical sections are either included or excluded from the model. In Table 3.1, the HU values of several tissues of the body are shown [74].

Table 3.1: HU of common materials and tissues

Tissue / material	Hounsfield units
Air	-1024
Water	0
Fat	-100
Trabecular bone	[200 - 1400]
Cortical bone	[1400 - 2000]
Metal implants	3071
Enamel tooth	3071

For this research subject, a separate segmentation of the cranium and the teeth is required. DICOM data from the CT images were uploaded into Materialise MIMICS (version 23.0) in order to start the segmentation process.

A first step is to differentiate the bone from the rest of the soft tissues. This can be done by using an intensity-based segmentation technique called thresholding. Using this thresholding technique, a certain range of Hounsfield units (HU) is selected. For bone (trabecular and cortical), a range between 226 HU and 3071 HU is selected. The result of this operation can be seen in Figure 3.3.a, where the bone structures are separated from the soft tissues. Another segmentation tool often used is the region-growing tool. This extracts the region of interest by selecting a certain seed point and in this way can separate spatially disconnected regions.

Since only the cranium and the maxillary teeth are of importance for this research, the spine and the mandible are segmented out. This is done using the split mask tool, where the spine and mandible on the one hand, the cranium on the other are selected. The tool will split the combined mask in two separate masks, and only the cranium is kept (Figure 3.3.b).

Due to the low resolution of the CT-scan, there are several places where very thin bones are not picked up by the thresholding range. This results in several holes in the model. First, a profile line was analyzed to have a better insight in the HU-values around these holes. This profile line shows the HU-values along the profile line on a chosen slice. In this way, the threshold values were adapted to better capture the image. However, due to the resolution of the images, the orbitals, cheeks and vomer all required a lot of manual editing (Figure 3.3.c), using mostly the 3D-Livewire tool to set the boundaries of the segmentation.

The teeth are segmented separately. Since the enamel of the teeth has very high and distinctive HU values, the teeth can be separated using the threshold tool. Using a threshold range of 1324 HU - 3071 HU and a region-growing operation, the teeth can be separated from the maxillary bones. The patient in this case has braces which also have very high HU-values. Due to this, the thresholding technique can not be used to separate the braces from the teeth. Manual editing of the teeth is required to obtain a geometric correct model for the teeth. To separate the teeth from each other, further manual editing was required. The end result can be seen in Figure 3.3.d.

After the segmentation, the 3D models were exported into 3-MATIC (Materialise, Leuven, Belgium) for further processing of the model. Small errors and details were removed from the model and a smoothing operation was performed (three iterations with a smoothing factor of 0.50). The obtained model can be seen in Figure 3.4.

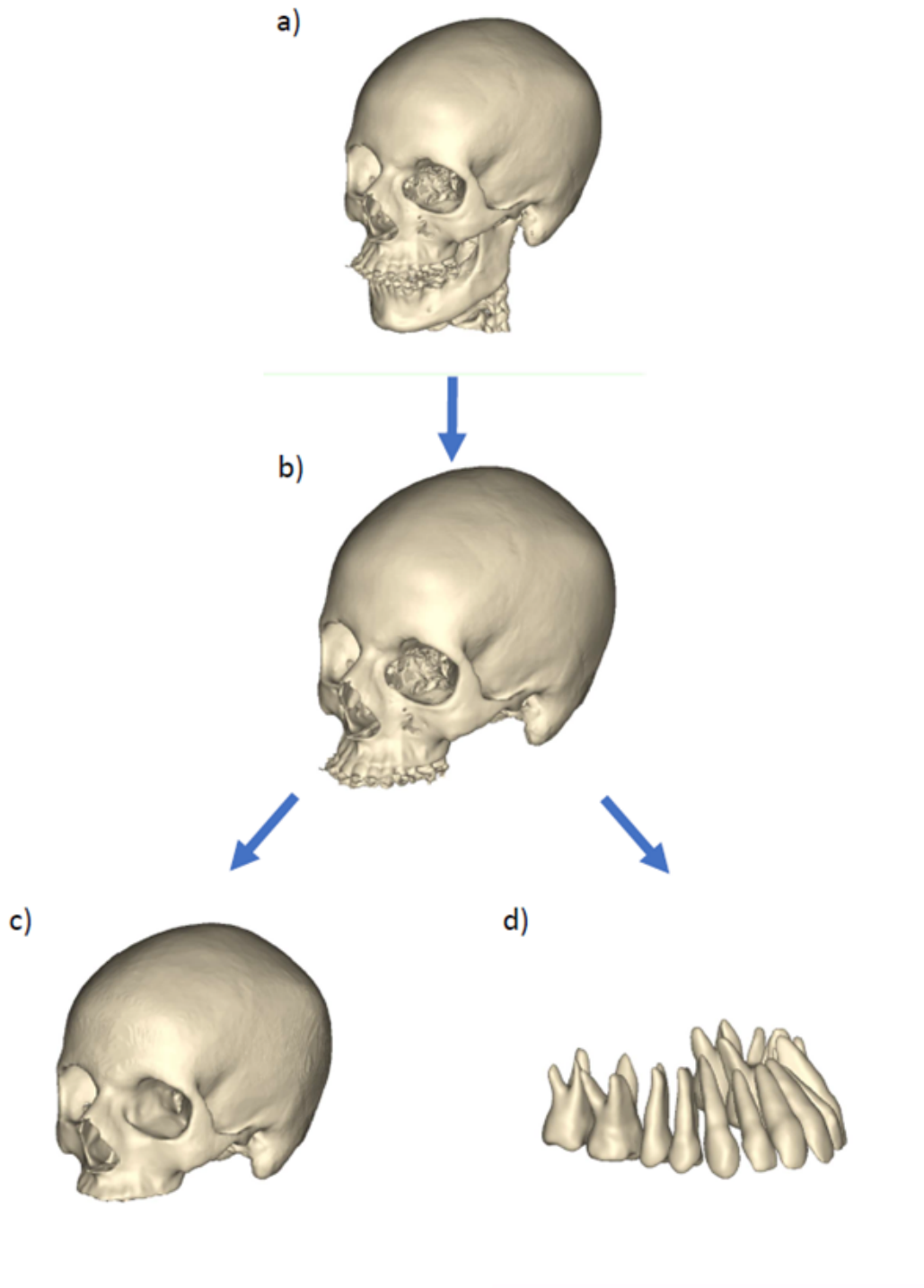


**Figure 3.3:** Segmentation process MIMICS



**Figure 3.4:** Basic model 3-MATIC

### 3.3 3D Cephalometric analysis

After this, basic cephalometric landmarks as well as the anatomical planes were defined. Using these planes, the different surgical osteotomies can be defined in 3-MATIC (Materialise, Leuven, Belgium). 3D cephalometric analyses are used for the diagnosis of deformities and the planning and long-term evaluation of craniofacial surgery. An overview of the 3D cephalometric landmarks can be seen in Table 3.2, where the definitions of the landmarks are according to Swennen [75]. Some of these landmarks will also be used to interpret the results of the simulations.

**Table 3.2:** Cephalometric landmarks

<b>Cephalometric landmark</b>	<b>Definition of the landmark</b>
Nasion (Na)	Midpoint of the frontonasal suture
Porion (Po)	Most superior point of the external acoustic meatus
Orbitale (Or)	Most inferior point of the infraorbital rim
Anterior Nasal Spine (ANS)	Most anterior midpoint of the anterior nasal spine of the maxilla
Posterior Nasal Spine (PNS)	Most posterior midpoint of the posterior nasal spine of the palatine bone
Upper Incisor (UI)	Most mesial point of the tip of the crown of the upper central incisor
Lower Incisor (LI)	Most mesial point of the tip of the crown of the lower central incisor
Frontozygomatic point (Fz)	Most medial and anterior point of the frontozygomatic suture
Zygion (Zy)	Most lateral point of the outline of the bony zygomatic arch
Basion (Ba)	Most anterior point of the Foramen Magnum

Using these cephalometric landmarks, anatomical planes are defined. These planes will form an anatomical reference system and will be useful for describing the osteotomies in a standardized and reproducible manner. The different anatomical planes can be seen in Figure 3.5 and an overview of the planes and their definition can be seen in Table 3.3. The definitions of the planes are according to Kuo and Cho [76] [77].

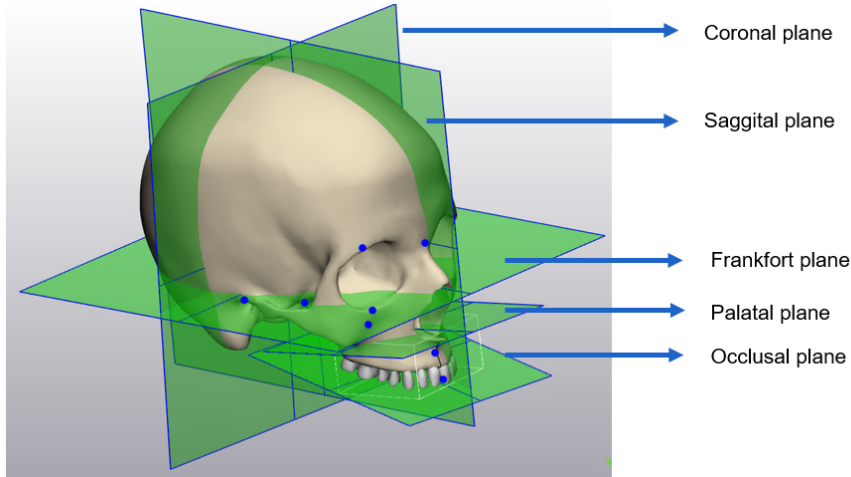


**Figure 3.5:** Cephalometric landmarks and anatomical planes

**Table 3.3:** Anatomical planes

Anatomical plane	Definition of the plane
Frankfort plane (FH)	The plane formed by the bilateral Orbitale and the midpoint of the bilateral Porion
Midsagittal plane (MSP)	The plane perpendicular to the FH plane and passing through the Nasion and Basion
Occlusal plane	Formed by the bisection of the MxO and MdO planes (consisting both of three dental points)
Coronal plane	A plane perpendicular to the midsagittal and Frankfort plane

### 3.4 Osteotomies

Since the SARPE procedure consists out of a surgical treatment, the osteotomies also need to be performed on the 3D model. The osteotomy sites, thickness and exact location were obtained in cooperation with a maxillofacial surgeon from UZ-Ghent. In this way a more realistic recreation of the surgical procedure is obtained and more accurate results can be achieved. In total, four osteotomies can be executed on the model. The goal of the osteotomies is to weaken the facial buttresses and lower the skull's resistance to the transverse expansion.

#### 3.4.1 Nasal septum disjunction

The nasal septum disjunction is performed onto all models. The complete vomer is released from the nasal floor and the palatum. In this way, septal deviation can be avoided. The osteotomy was defined along a translated Frankfort plane, to get as close as possible to the nasal floor. A 3D view and section view of the osteotomy is shown in Figure 3.6.

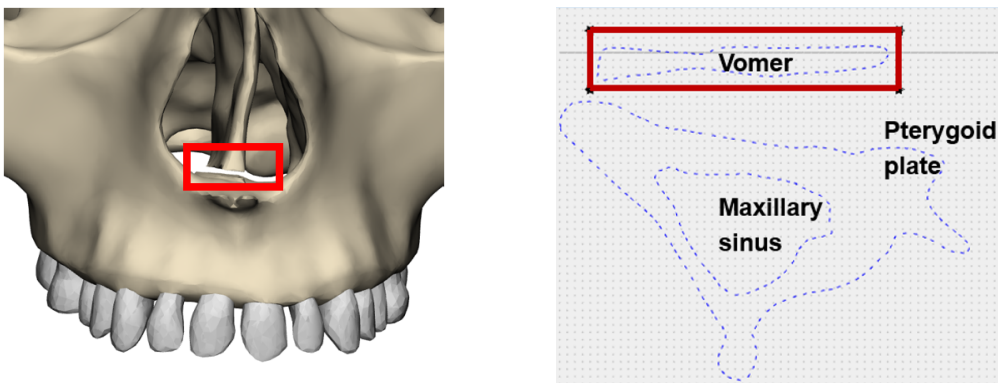


**Figure 3.6:** Nasal septum disjunction: frontal view 3D model (left) and axial section view (right), osteotomy indicated in red

#### 3.4.2 Midpalatal osteotomy

The midpalatal osteotomy is defined using the midsagittal plane. The osteotomy is 0.5 mm thick and cuts through the palatum along the midpalatal suture. The cut is extended superiorly until the nasal floor is reached. This osteotomy is required to allow for the transversal expansion and hence it is also performed on all models. The 3D and section view can be seen in Figure 3.7.

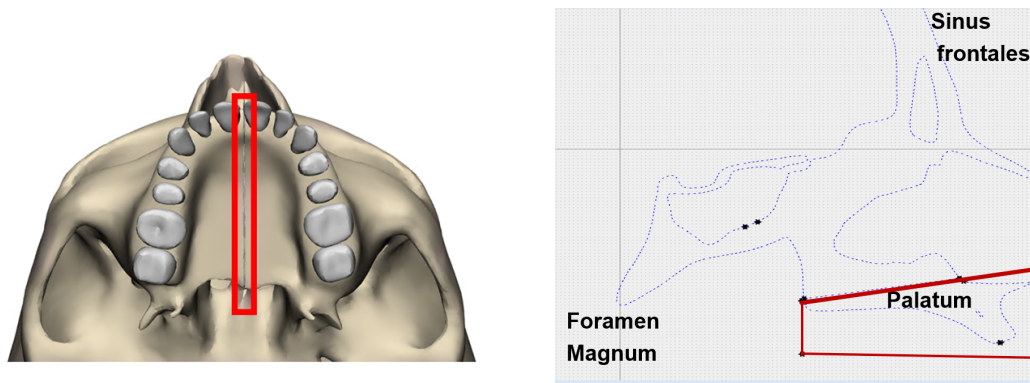


**Figure 3.7:** Midsagittal osteotomy: inferior view 3D model (left) and sagittal section view, osteotomy indicated in red (right)

### 3.4.3 Lateral osteotomy

The locations where the lateral osteotomy can be placed are bounded by several limitations. The osteotomy needs to be at least 5 mm superior of the apex of the incisor, to avoid damaging the teeth. Another requirement is that the osteotomy should be at least 5 mm inferior of the Infraorbital Foramen, since this is a weakened location on the skull and fracture patterns can originate from this Foramen. The goal of the osteotomy is to cut through the cortical shell of the maxilla. In this way the zygomaticmaxillary buttress and piriform pillars are released. The osteotomy starts at the medial nasal wall, cuts through the body of the maxilla and runs posteriorly until the second molar is reached. In Chapter 5, variations of this osteotomy are described in more detail. A possible osteotomy, complying to the prescribed requirements, is shown in figure 3.8.

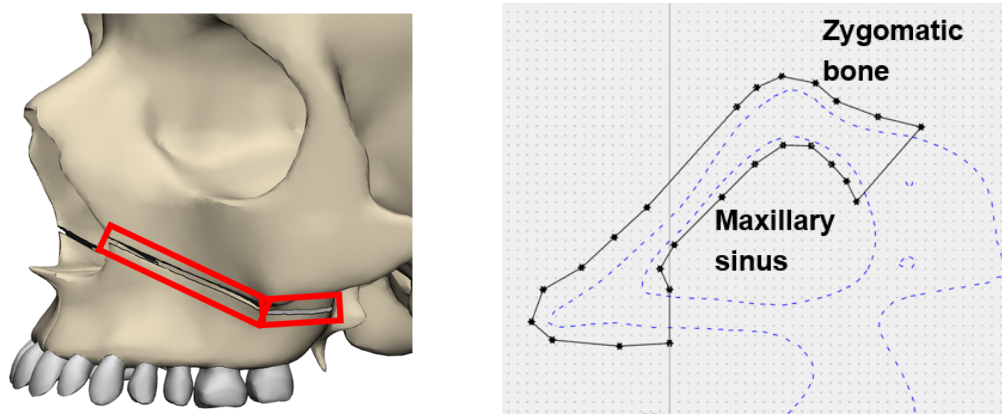


**Figure 3.8:** Lateral osteotomy: frontal view 3D model (left) and axial section view (right)

### 3.4.4 Pterygoid plate disjunction

The last osteotomy is the pterygoid plate disjunction. The osteotomy is defined once the lateral osteotomy is performed, where perpendicular to this osteotomy the pterygoid plates are released. The bilateral pterygoid plate disjunction can be seen in Figure 3.9, indicated in red. In these figures, the midpalatal and lateral osteotomies are also performed.

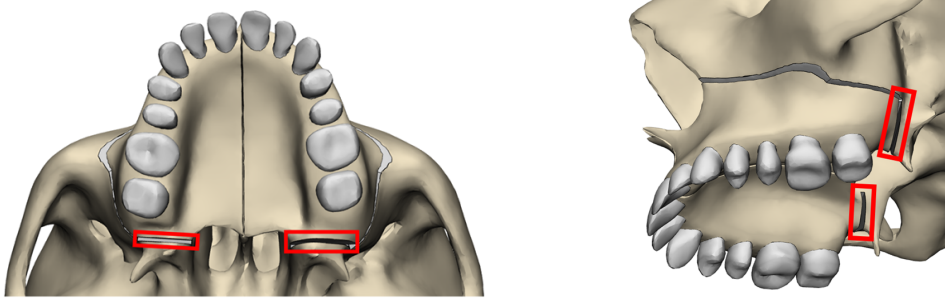


**Figure 3.9:** Pterygoid plate disjunction: 3D model inferior (left) and oblique view (right)

Once these osteotomies are performed, a volumetric mesh of the model can be obtained. This volumetric mesh was exported into ABAQUS (DASSAULT SYSTEMES, Velizy-Villacoublay, France) for the finite element analysis.

## 3.5 Expander device

In this dissertation, a transpalatal distractor was chosen as the expansion device. A real transpalatal expander was scanned and the STL file was obtained. Due to the optical reflections of the metallic surface, the optical sensor was not able to generate an accurate 3D-model. Therefore, a transpalatal expander was designed using the dimensions of the real device, together with drawings of the UNI-smile distractor. Both models are depicted in Figure 3.10.

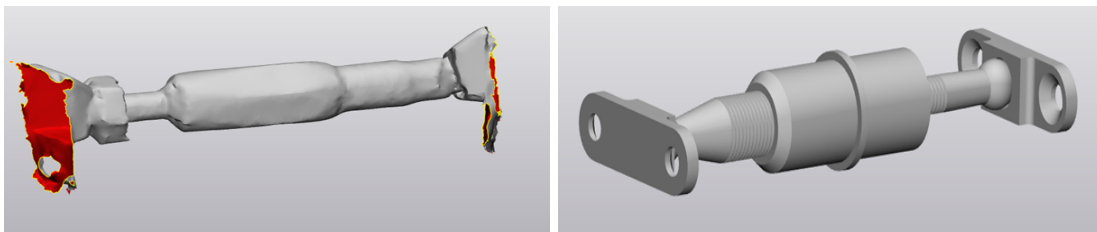


**Figure 3.10:** 3D models of the scanned (left) and the designed (right) palatal expander

## 3.6 Finite element modeling

In this section, the finite element modeling will be discussed. The material properties, boundary conditions, loading conditions, volumetric meshing and a verification with literature will be described in more detail.

### 3.6.1 Material properties

When a high quality CT-scan is available, material properties can be assigned to the volumetric mesh with HU-thresholding techniques. A CT scan can be calibrated and since each tissue has distinctive radio-absorptive properties, the cortical and trabecular bone can be differentiated using the correct threshold value. A limiting factor is the availability and correctness of empirical relations for certain anatomical regions. Each anatomical structure has unique properties, due to the unique anatomy and function of the bone. Other influencing factors are, among others, how the bone is loaded and the age of the patient. For the maxilla there seem to be no empirical relations between the HU-value and the elastic modulus in literature as of now, and hence this thresholding technique could not be used.

An experimental study by Peterson [32] investigated the cortical shell thickness and the material properties in several regions of the maxilla. Using this data, also found in the literature review of this dissertation (Figure 2.8 and Table 2.3), accurate material properties could be assigned to the model. As to reduce the complexity of the model, different regions with comparable material properties are grouped together. This leads to the segmentation of the maxilla in four separate groups, with distinctive thickness and material properties of the cortical shell: the alveolar process and the palatum, the body and frontal process, the zygomatic process and the posteriorly located part of the maxilla. This sectioning of the maxilla was performed in MIMICS. To make sure there is a smooth transition between consecutive maxillary segments, a Boolean operation was performed as well. The different segments are depicted in Figure 3.11.

For each maxillary segment, the trabecular and cortical bone sections need to be determined. Using the average thickness of a group of the cortical shell, found in the study by Peterson [32], the properties of the cortical bone were assigned to these groups separately. Using Boolean operations, the trabecular bone sections can also easily be obtained. The material properties of the different bone types can be found in Table 3.4.

For the material assignment of the teeth, both the enamel and dentin was modeled. With tooth borne appliances, the need for extra material properties concerning the dentoalveolar region need to be added to the model to obtain more accurate results. The material properties used for the simulations can be found in Table 3.4.

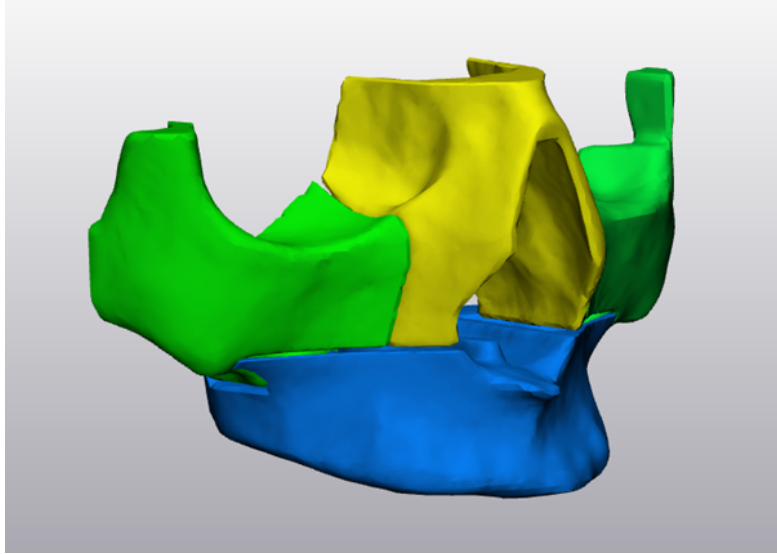


**Figure 3.11:** Sectioning of the maxilla: Body and frontal processes (yellow), zygomatic processes (green), alveolar region (blue), posterior part (not in figure)

Using the materials tool in MIMICS, a material can be assigned to the volumetric mesh using several options. For this case, the 'assign material by mask' option is required. Now, a material can be assigned to the volumetric mesh, based on the different created masks. Since the different parts of the maxilla were separated and the cortical and trabecular bone were separated in separate masks, we can simply apply the correct material properties to the subparts of the model. In this way, an accurate material assignment was obtained. The material properties for the different bone types can be found in Table 3.4.

**Table 3.4:** Material properties

Material	Young's modulus [MPa]	Poisson's ratio
Cortical bone	13 700	0.31
Trabecular bone	1 370	0.31
Enamel	80 000	0.26
Dentin	20 000	0.15

The material properties values were obtained from several finite element analyses [78] [79] [80] and an experimental study by Zhang and al., who determined the mechanical properties of the teeth [81]. All materials were assumed to be isotropic, linear, elastic and homogeneous.

### 3.6.2 Interaction

The expansion of the transpalatal distractor was modeled by imposing several constraints and connectors to the model in ABAQUS. First, several reference points were indicated on the alveolar ridge on both sides of the palatum. Between these points, the distance was divided into four equal segments. Between the second and third reference point, an axial connector in ABAQUS was constructed. This axial connector allows only a displacement in the direction of the wire between the two points. This can be seen in Figure 3.12. The two points of the axial connector still need to be attached to the alveolar ridge. This connection can be obtained using the MPC-connector type in ABAQUS. For this, the first attachment point is chosen as the master point. Several nodes on the surface of the alveolar ridge are then selected as slave nodes, representing the attachment of the abutment plate of the transpalatal distractor on the alveolar ridge. For the element type of the MPC-constraint, a BEAM-element was chosen in ABAQUS. The beam element provides a rigid connection between the master and slave nodes. This model tries to mimic the transpalatal expander device, without increasing the computational cost significantly. The beam connections can be seen in Figure 3.12.

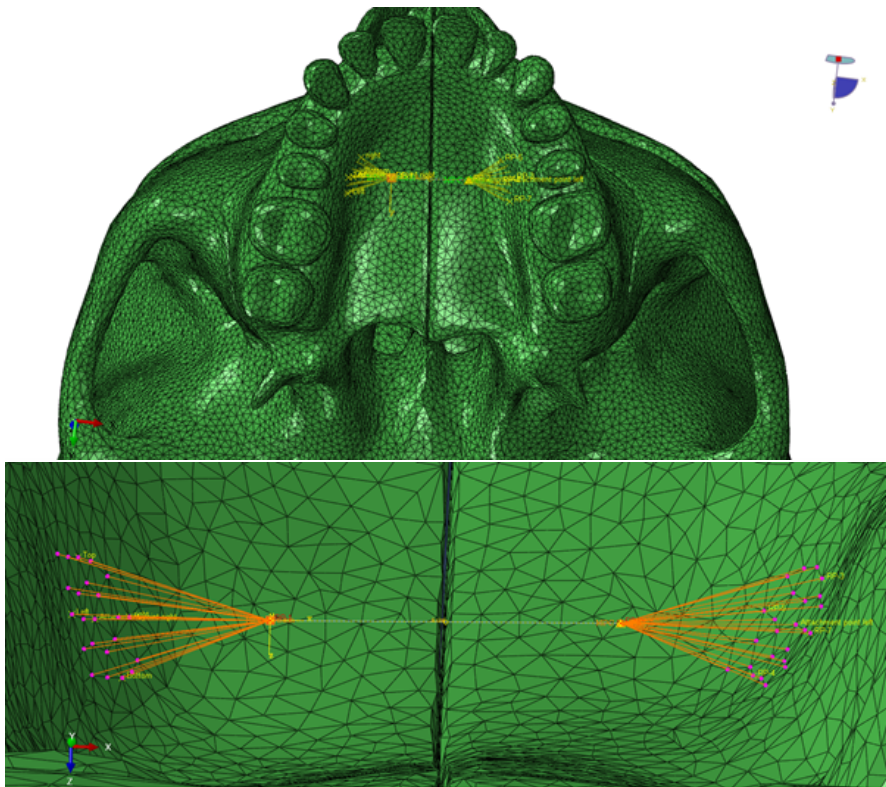


**Figure 3.12:** Axial connector and MPC beam connections indicated in purple

### 3.6.3 Boundary and loading conditions

As suggested by Gautam and al. [82], several nodes around the Foramen Magnum were completely fixed in all directions, using the encastre boundary condition. The boundary condition can be seen on Figure 3.13. Furthermore, an axial displacement of the axial connector was imposed. This displacement can be chosen in function of different goals: a realistic simulation can be obtained, simulating 5 to 6 mm. However, in literature mostly an expansion of 1 mm is modeled.

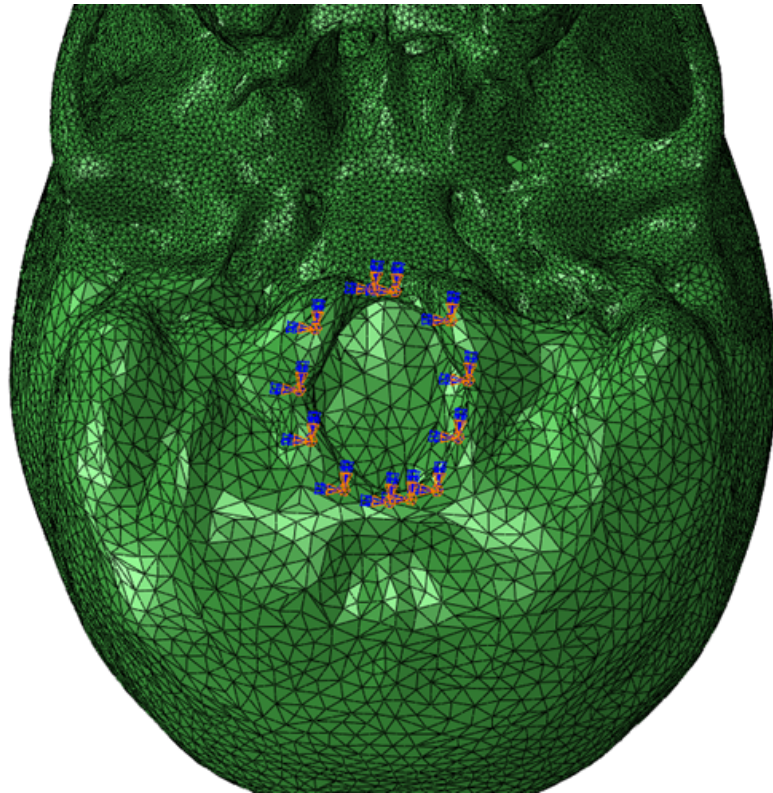


**Figure 3.13:** Inferior view of the encastre boundary condition imposed on selected nodes around the Foramen Magnum

### 3.6.4 Finite element meshing and sensitivity analysis

For the surface mesh, C3D10 elements are chosen. The C3D10 element is a general purpose quadratic tetrahedral element. Linear tetrahedrals have stiff formulations and exhibit phenomenae such as volumetric and shear locking. Quadratic tetrahedral elements, such as C3D10, minimize these problems. They offer good convergence rate with a minimum of shear or volumetric locking. This type of element is attractive because of the existence of fully automatic tetrahedral meshers. Since the geometry of the skull is highly irregular, such an automatic meshing is required [83].

In finite element analysis, the mesh density can have an influence on the solution. A finer mesh will result in more accurate results, however increasing the computing time significantly. To have a good trade off between the computing time and the obtained accuracy, a mesh sensitivity analysis is performed. In this sensitivity analysis, the same loading and boundary conditions are imposed on the model, with an increasingly fine mesh. From this mesh sensitivity analysis, a trade off between accuracy and calculation time was chosen. A mesh of globally 4 mm elements and locally, at the maxilla and adjacent bones, 1 mm elements was generated. This results in a mesh consisting of 2.1 million elements and 3.3 million nodes, which requires a calculation time of around six to seven hours for each simulation. An example of such a mesh can be seen in Figure 3.14.

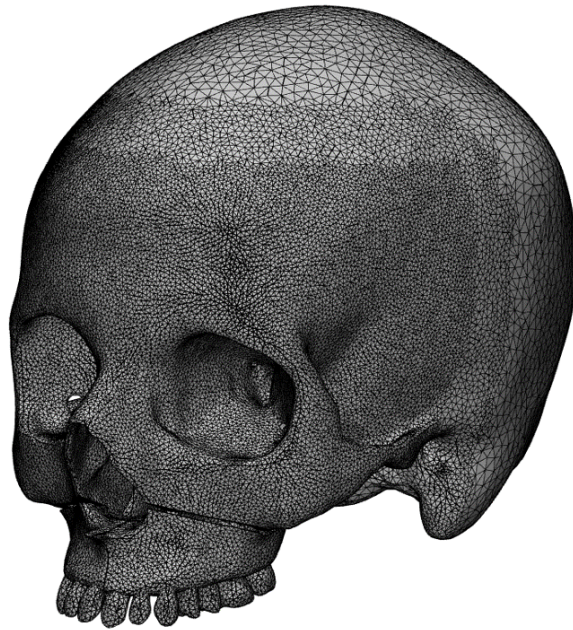


**Figure 3.14:** Surface and volumetric mesh of the model

### 3.6.5 Validation of the finite element model

In literature, few finite element analyses have been performed on the topic. Mostly the differences between bone-borne and tooth-borne appliances are being analyzed using the FEM. The model constructed in this chapter will be compared and verified to two other finite element studies.

A first study to verify the model is a study by Möhlhenrich and al., performed in 2017 [84]. In this study, three different surgical techniques, together with two types of bone-borne appliances are compared to each other. In this study, the cortical and trabecular bone were segmented as separate parts with different values for the Young's modulus and Poisson coefficient. These material properties were adapted for this simulation to compare the results. An expansion of 1 mm was chosen. For this study, two cases are compared: one with only the midpalatal osteotomy, and one with the lateral and midpalatal osteotomy. The graphic results are depicted in Figure 3.15 [84].

In both simulations, the depicted Von Mises stresses have a range from 0 MPa to 100 MPa (blue to red). As can be seen, both simulations show the highest stress regions around the same anatomical region. However, there are some differences found between the studies. A first difference is the fact that in the sagittal model, the forces are more spread out over the skull in the model, described in this section. Also a slightly higher maximal stress concentration is found around the zygomaticomaxillary suture. For the model where the lateral osteotomy is included as well (bottom), a better resemblance is found between the two studies. Still, the stress concentration shows slightly higher values (10 % locally) and the stresses are more spread out. At the end of this section, multiple reasons are formulated as to where the differences between the models could originate from.

A second study to verify the model is a study by Nowak and al., executed in 2021[79]. In this study, tooth- and bone-borne appliances are compared to each other, and the stress distributions and displacement patterns are measured. The material properties were adapted to make a correct comparison. The mesh in this study contained over 1.8 million elements, with an edge length of 1-2 mm. The device was placed at the second premolar and an expansion of 0.5 mm was simulated. From this study, the model with both the lateral and sagittal osteotomies will be recreated and compared. This comparison can be seen on Figure 3.16 [79].

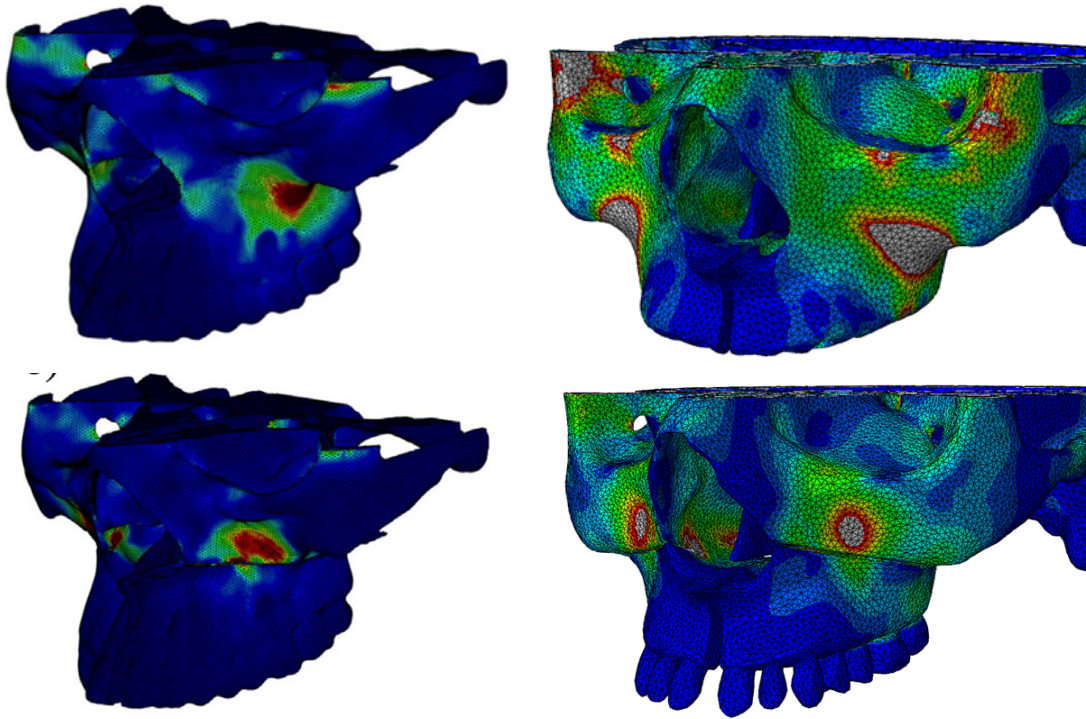


**Figure 3.15:** Comparison between the study performed by Möhlhenrich (left) and this study (right): model with only sagittal osteotomy (top) and both sagittal and lateral osteotomies (bottom); Stresses are depicted: blue equals 0 MPa, red equals 100 MPa

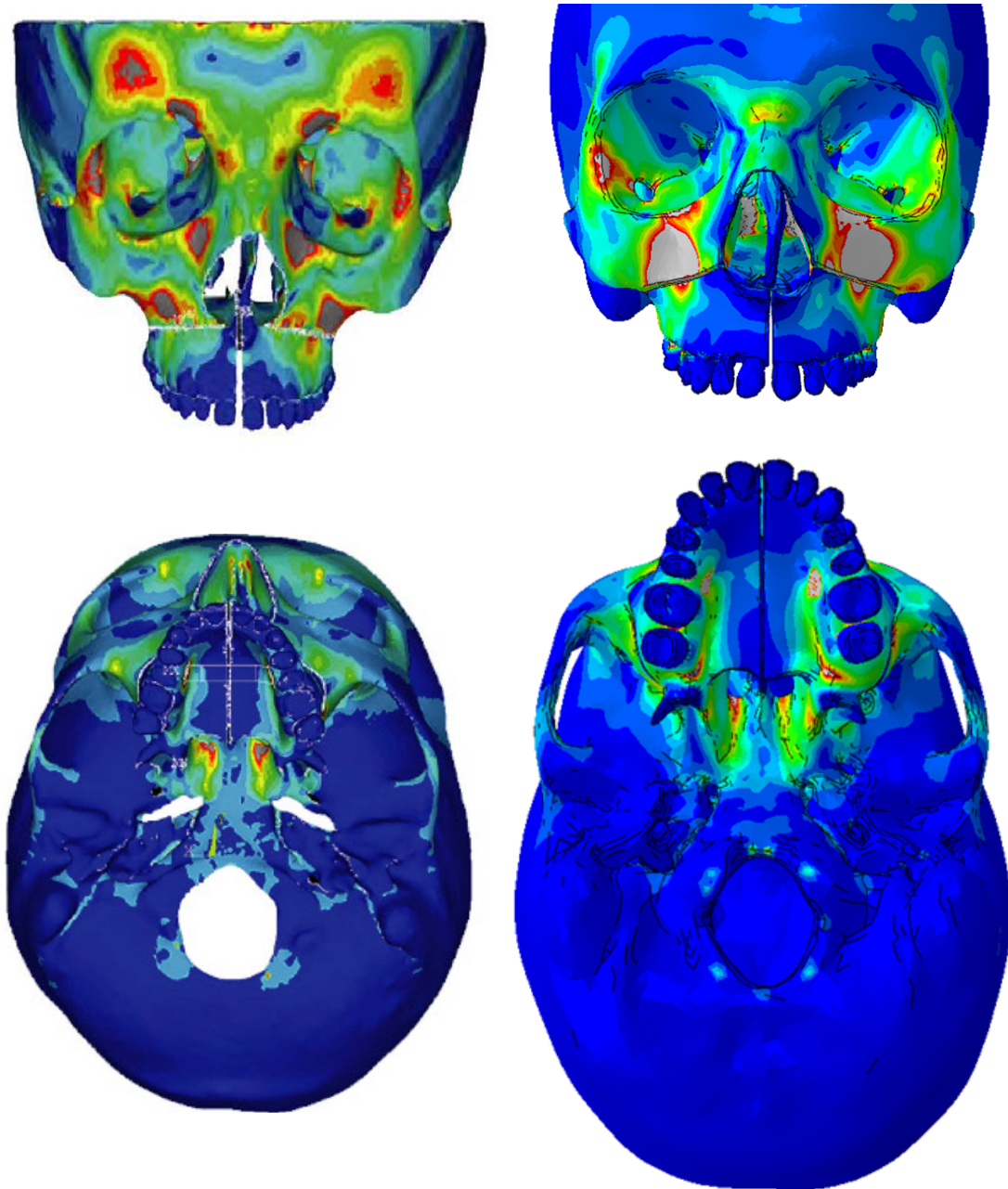


**Figure 3.16:** Comparison between the study performed by Nowak and al (left) and this study (right); model with both sagittal and lateral osteotomies; Von misses stresses are depicted for both frontal view (top) and inferior view (bottom): blue equals 0 MPa (top and bottom), red equals 10 MPa (top) and 25 MPa (bottom)

As can be seen, both models show similar stress distributions at the maxilla. The same order of magnitude is present in both cases. The highest stress concentrations are at the same regions for both models, as can be seen in both the frontal and inferior views. However, in this comparison there are also some differences. The model by Nowak shows a high stress concentration above the orbitals, which is not present in the model of this study. No possible explanation was given in literature for these high stress concentrations around this region. A possible explanation could be due to the material assignment procedure, however this was not discussed in great detail in the study by Nowak, and hence the exact reason for this difference remains unclear. These high stresses above the orbitals are not found in any other finite element study, and hence this could also be an inaccuracy or error in the model of Nowak [79] [80] [84].

Possible reasons for the differences between the results are enumerated in following list:

1. **Anatomy:** Unique anatomical properties and shapes of certain bones can result in other stress distributions. The model used in the study by Möhlhenrich has a longer (longitudal) maxilla, which could influence the results.
2. **Material assignment:** The distribution of the cortical and trabecular bone can have a significant influence on the results, since the elastic modulus of both materials also are significantly different (factor 10). Since in both studies the assignment of the material properties is not discussed in great detail, it is difficult to estimate the influence of the material assignment on the results.
3. **Osteotomies:** The definitions of the osteotomies are not discussed in great detail as well in these studies. Differences in the osteotomy definition can also result in slightly different results. It was not clearly stated how far posteriorly the lateral osteotomy runs, or how the osteotomies were constructed.
4. **Symmetry:** The initial (a)symmetry of the skull can also have an influence on the results of the models. The model used by Möhlhenrich has a (visually) much more symmetrical skull when compared to the model obtained in this study.

It remains important to note that none of these models in literature, nor this model has been verified using clinical or experimental data. No information is known about the forces these expanders impose on the teeth or alveolar ridge, or about the stress distribution in the maxillofacial complex. Using conventional sensors, these forces can not be measured accurately at this small scale, and hence only a comparative validation of this finite element model can be made. Based on the comparison between both studies, the model created in this section was deemed to be accurate and correct.



# Chapter 4 | Variations in the palatal expansion device location

In this chapter, a first set of simulations is performed where the expansion profile is analyzed in function of the location of the transpalatal distractor (TPD). A series of symmetric expansions will be performed where the expander is installed at four different locations: both at the first and second premolar and at the first and second molar. Next to these four symmetrical simulations, another simulation is performed where the expansion device is installed with a small inferior deviation of 2 mm with respect to the symmetric case. The (a)symmetric placement of the device in the frontal plane is the most clinically relevant, since maxillofacial surgeons can not accurately position the expander device in this plane. A narrow and high palatal vault can make it difficult to align the device correctly. For all these cases, both the displacement and stress distribution will be measured and analyzed. Using these measurements, the goal is twofold: on the one hand the influence of the TPD placement on the expansion profile is determined, on the other hand the influence of small (inferior) deviations of the TPD on one side is analyzed.

Since this is the first analysis, the complete post-processing of the results, as well as all the steps to get to these results is reported. In further simulations, a similar workflow is followed, but only the relevant results are reported.

## 4.1 Models

For these simulations, the nasal septum disjunction, the midpalatal and the lateral osteotomies are performed. The lateral osteotomy is symmetric with respect to the midsagittal plane. The osteotomy was defined using a duplicate of the Frankfort plane, which was then translated inferiorly and rotated around the lateral axis for 20 degrees. The intersection of this plane and the skull, as well as the osteotomy line can be seen

## CHAPTER 4. VARIATIONS IN THE PALATAL EXPANSION DEVICE LOCATION

on Figure 4.1. The different models obtained for this part of the study are summarized in Figure 4.2. The TPD is always positioned symmetrically between the premolars and molars. For the asymmetric model, the TPD is positioned at the second premolar and an inferior deviation of 2 mm is introduced. For all simulations, a transverse displacement of 5 mm is imposed on the model.

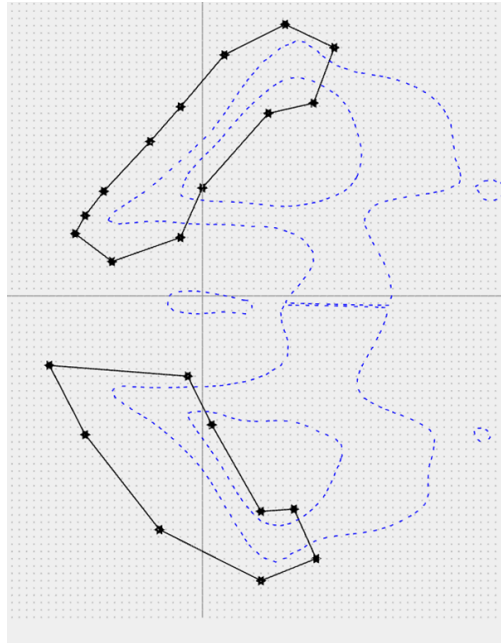


**Figure 4.1:** Symmetric lateral osteotomy

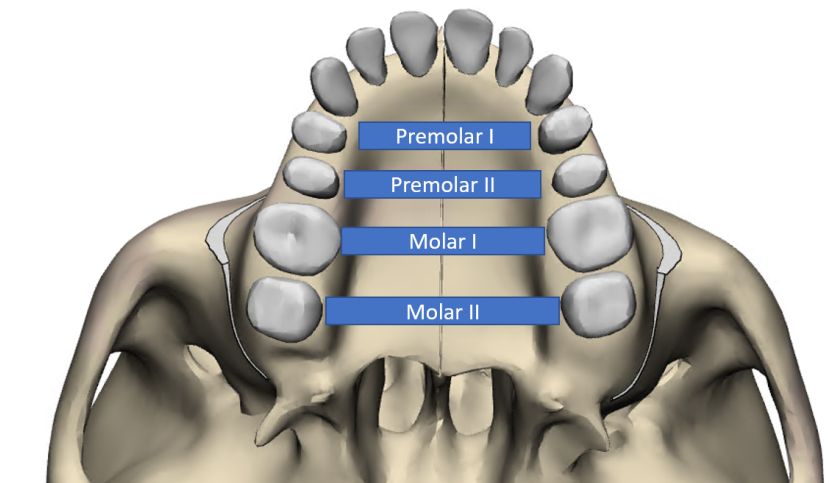


**Figure 4.2:** Four different positions of the palatal expander

## 4.2 Results and discussion

Once the finite element analysis has calculated the stresses, displacements and strains of all the elements, a visual validation is performed. In Figure 4.3, the undeformed and deformed models are shown. Another tool to quickly verify the model is by inspecting the overlay plot. These overlay plots are shown in Figure 4.4. Using these graphical verification methods, a first validation can be performed to see if the model behaves in a realistic way.

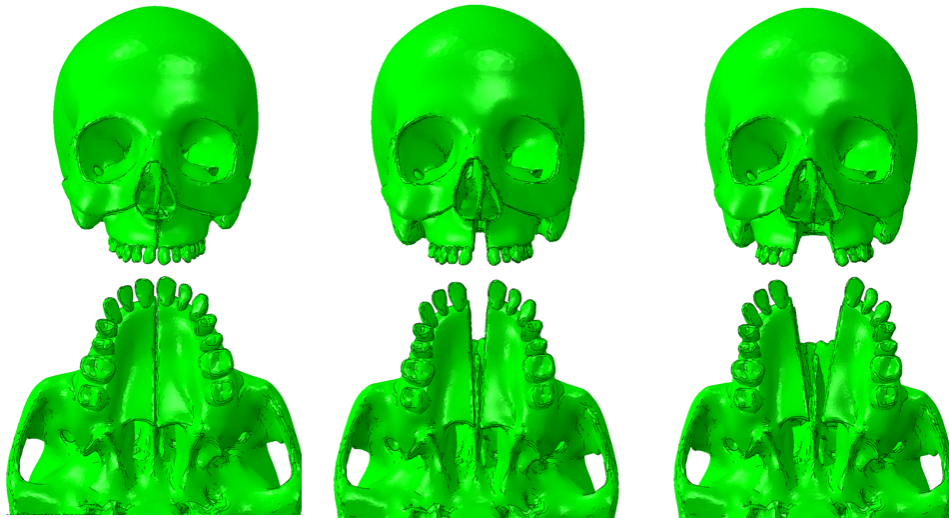


**Figure 4.3:** Graphical result of the expansion: undeformed (left), deformation scale factor 1 (middle) and deformation scale factor 3 (right)

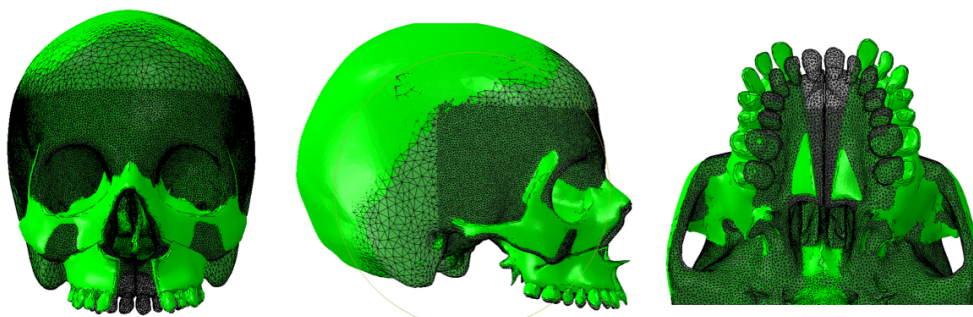


**Figure 4.4:** Overlay plots, where the undeformed model is given in the wireframe, the deformed model in solid green: frontal (left), sagittal (middle) and occlusal (right) view

Next, the contour plots are generated in ABAQUS. Since we are mostly interested in the expansion profile and the resistance to the transversal expansion in the skull, both displacement and Von Mises stresses are plotted. The Von Mises stress is a theoretical value which allows to make a comparison between a multi-axial stress and a uniaxial tensile stress. Multi-axial stresses (normal and shear) applied to a sample are compared to the Von Mises stress  $\sigma_V$  applied to the sample by a tensile test [85]. The equation to calculate the Von Mises stress out of the multi-axial stresses is as follows:

$$\sigma_V = \frac{1}{\sqrt{2}} \sqrt{[(\sigma_{xx} - \sigma_{yy})^2 + (\sigma_{yy} - \sigma_{zz})^2 + (\sigma_{xx} - \sigma_{zz})^2 + 6\sigma_{xy}^2 + 6\sigma_{yz}^2 + 6\sigma_{zx}^2]}$$

In ABAQUS, the Von Mises stress is calculated at the integration points (centroids) of the C3D10 elements. This data then needs to be extrapolated to the element nodes, using averaging methods. For this, first the tensor values of the stress are converted to a single scalar value (Von Mises) using scalar computations. Once the Von Mises stress is calculated at the centroids, an averaging computation converts the values from the centroids to a single nodal value, which can then be seen on these contour plots. The 75% averaging means that the extrapolated nodal values are averaged only if the relative difference between contributions at a node are smaller than the defined threshold (which is 75%). The contour plot of the averaged VM stresses can be seen in Figure 4.5.

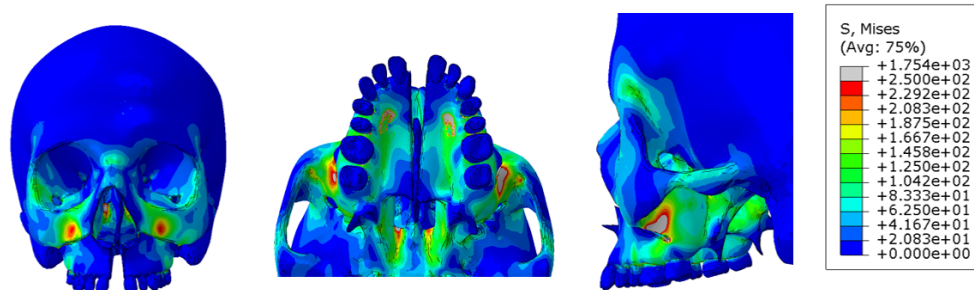
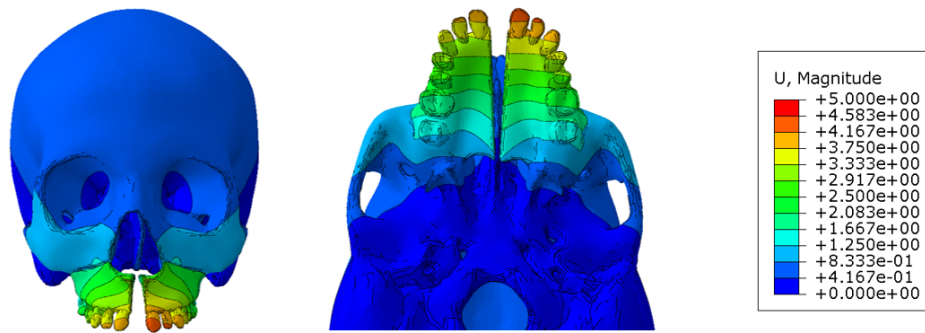


Figure 4.5: Contour plots Von Mises stress (MPa)

The displacement contours can also be requested from ABAQUS, where the displacements are reported in mm. These can be seen in Figure 4.6. In this contour plot, the quantity  $U_{magn}$  is reported. This is the vectorial sum of the displacements in the three axes and can be calculated as follows:

$$U_{magn} = \sqrt{((x_2 - x_1)^2 + (y_2 - y_1)^2 + (z_2 - z_1)^2)}$$



**Figure 4.6:** Contour plots displacement (mm)

Once these contour plots are analyzed and deemed correct, a coordinate system is set up in ABAQUS, which can be seen on Figure 4.7. This coordinate system has an origin at the posterior nasal spine. The x-axis is defined along the midpalatal suture, the y-axis is along the transversal direction and the z-axis is along the superoinferior direction, with positive values for the anterior, lateral and superior direction respectively. Using this newly defined coordinate system, the displacements can be transformed from the general coordinate system to the coordinate system defined at the posterior nasal spine. This is required to compare the different components of the displacement in a standardized way. For measurement, two paths are created: one along the midpalatal suture (from Foramen Incisivum until the posterior nasal spine) and another path to measure the nodal values of the alveolar ridge (inferior of each tooth). These paths are shown in Figure 4.8.a. The measuring points of the maxillofacial complex are indicated in Figure 4.8.

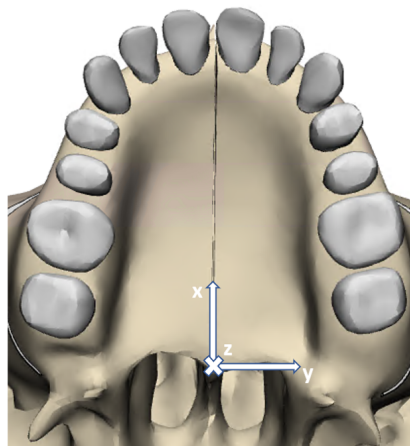
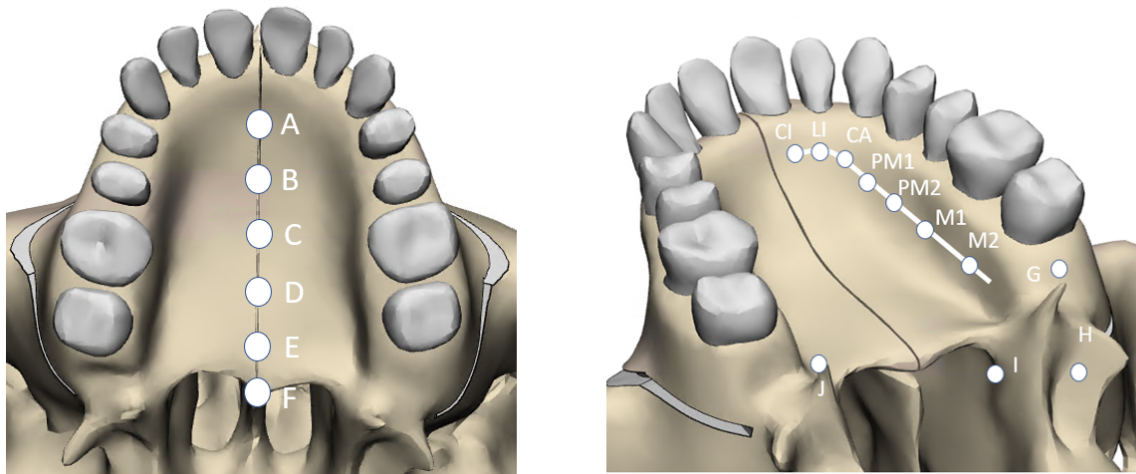
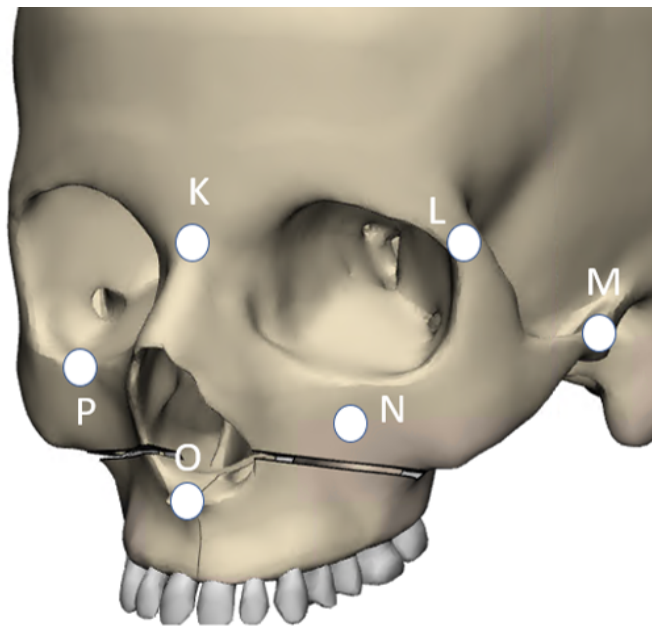


**Figure 4.7:** Local coordinate system



- (a) Evaluated landmarks of the palatum and pterygoid plates: A, point near the incisive Foramen; E, point near the palatine bone; B,C and D, points which divide A-E line in four quarters; F, Posterior Nasal Spine ; CI, Central Incisor; LI, Lateral incisor; Ca, Canine; PM 1/2, Premolar 1/2; M 1/2, Molar 1/2; G, Maxillary tuberosity; I, Medial pterygoid plate; J, Pterygoid Hamulus;



- (b) Evaluated landmarks: K, Frontonasal suture; L, Frontozygomatic suture; M, Zygomatic arch; N, Maxillary body; O, Anterior Nasal Spine; P, Orbital margin

**Figure 4.8:** Evaluated landmarks of the maxillofacial complex

### 4.2.1 Results displacements

Several measurements are made to correctly asses and evaluate the expansion profile. First the symmetric expansion models are analyzed. The displacements in the new coordinate system are reported at both the midpalatal suture and at the alveolar bone, depicted in respectively Figure 4.9 and Figure 4.10. Since this is the first simulation, the general displacement of the maxilla during the expansion will be described. In further results, only the more interesting aspects will be reported and analyzed.

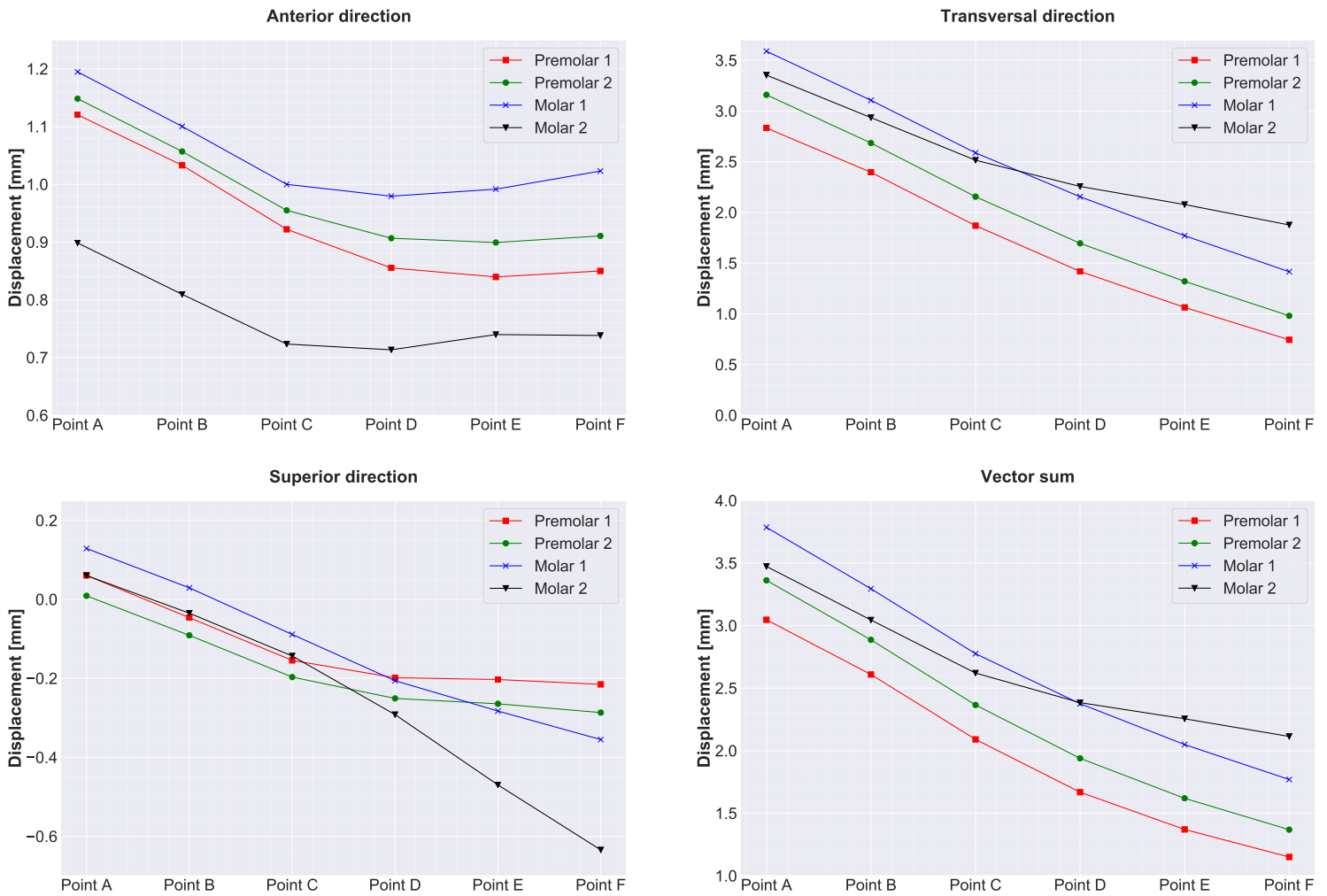


**Figure 4.9:** Displacement at the suture: point A is located around Foramen Incisivum, F at the posterior nasal spine - Palatal expander models

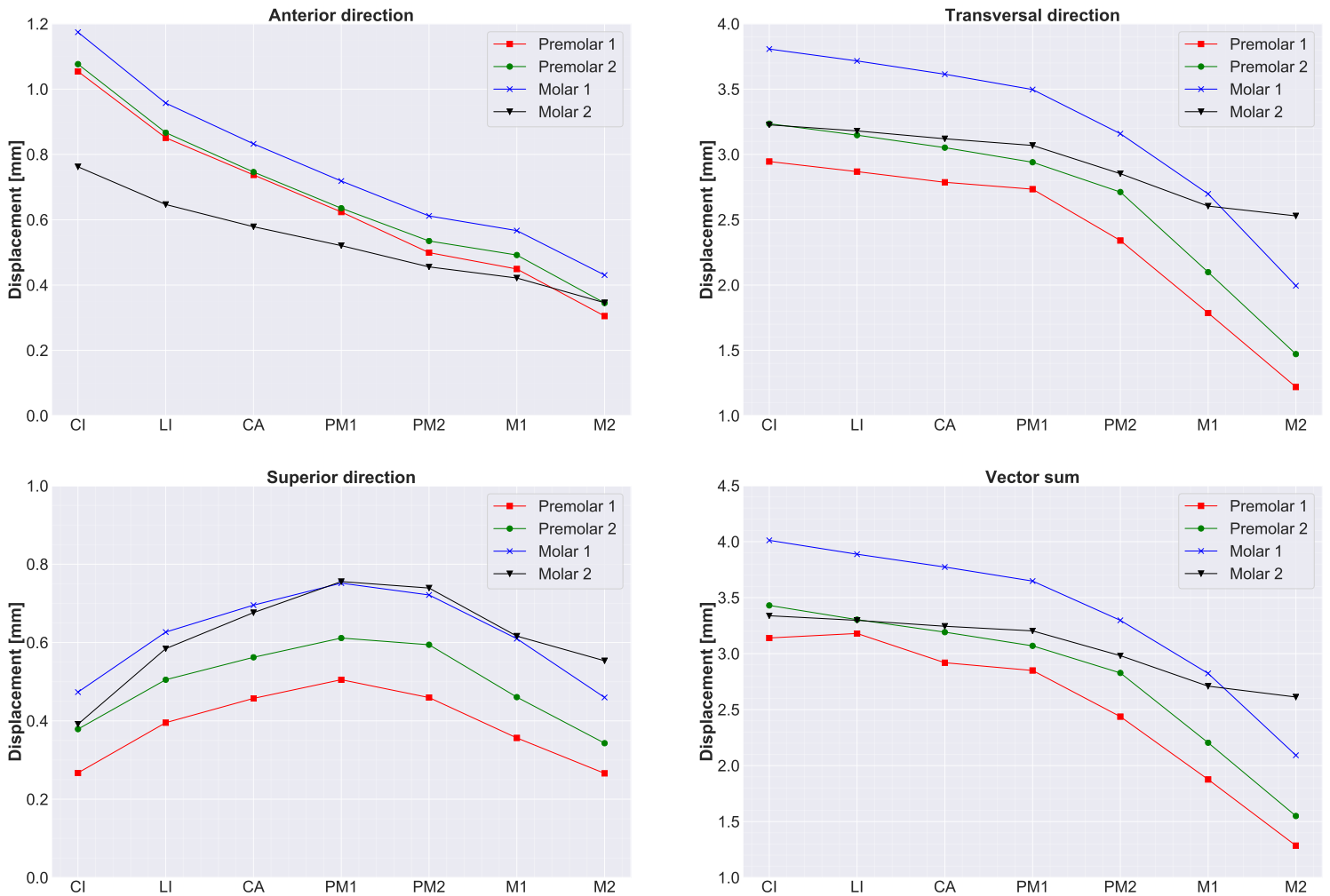


Figure 4.10: Displacement at the alveolar bone - Palatal expander models

In each simulation the expansion is modeled by imposing a 5 mm displacement between two sets of nodes between the alveolar ridge. In this chapter, different locations are chosen, and the same 5 mm displacement was imposed. As can be seen from the results in Figure 4.9 and 4.10, when the expansion is modeled more posteriorly, generally a larger transversal displacement is modeled. As the expansion profile is significantly different, the models can not be compared in an absolute way to each other, as they represent different physical expansion profiles. This is due to the fact that a displacement and not a force is imposed during the modeling. This makes it impossible to directly compare the expansion profiles of the different cases. Still, a comparison between the expansion profile on a relative basis can be made. Following observations are made:

1. **Anterior direction:** In all models, the suture moves anteriorly, with values ranging from minimally 0.74 mm (second molar model, point L) to maximally 1.2 mm (first molar model, point A). This maximal value is around 20% of the imposed transversal expansion. The anterior displacement is the largest in the anterior region for all models. The same behavior is observed at the level of the alveolar bone, albeit with smaller values. The anterior movement of the maxilla can be partly explained by the horizontal tipping, which is further explained in the discussion.
2. **Transversal direction:** The transversal direction is the main direction of the expansion. At the level of the suture, the models 'premolar 1', 'premolar 2' and 'molar 2' show comparable behavior, where a much larger transversal displacement is occurring anteriorly. The largest transversal displacement is obtained for the first molar model at the Foramen Incisivum (point A), with a magnitude of 3.59 mm. From this graph, a large discrepancy between the anterior and posterior values can be noticed. As an example, for the first premolar model a transversal expansion of 2.83 mm is reported in the anterior region, whereas posteriorly, the expansion is only 0.74 mm. This observation shows that tipping in the axial plane is occurring and the maxillary halves are rotating in the occlusal plane. The tipping behavior will be discussed in more detail further in this section. If the palatal expander is positioned at the second molar, the displacement at the suture is much more parallel. Generally, the transversal displacement at the alveolar bone is larger than at the suture, which is trivial as the expander is fixed on the alveolar bone and the displacement loading is placed on this alveolar bone.
3. **Superior direction:** In the superoinferior direction, the suture displacements are almost completely in the inferior direction, meaning the suture moves downwards during the transversal expansion. Values range from maximally 0.129 mm for the first molar model at point A to - 0.63 mm for the second molar model at point F. These values are considerably lower than the displacements in anterior and transversal direction. It can be seen that the alveolar bone moves superiorly during expansion. In all models, the posterior movement is largest at the first and second premolars. Upon further inspection of the model, the complete maxilla will move superiorly, except for the suture. This shows that there is a rotational component in the frontal plane, around an axis parallel to the sagittal direction. This vertical tipping behavior is also discussed in more detail further in this section.
4. **Vector sum:** The vector sum shows the vector sum of the displacement. It can clearly be seen that the largest expansion is obtained when the expander is positioned at the first molar. A V-shaped expansion in both the occlusal and frontal plane is occurring in all the models.

## CHAPTER 4. VARIATIONS IN THE PALATAL EXPANSION DEVICE LOCATION

As was mentioned in the displacement profile analyses, there are unwanted rotational components influencing the expansion profile. The tipping of the maxilla is occurring along two directions: there is vertical tipping, occurring in the frontal plane, and horizontal tipping, occurring in the axial plane. For the horizontal tipping, the opening angle can be calculated by measuring the expansion at the level of the PNS and at the Foramen Incisivum. If the length of the palatum between these points is measured as well, simple goniometrics can calculate the opening angle of the V-shaped expansion. Another measure for this tipping behavior can be obtained by calculating following value:

$$Parallelism = 1 - \frac{\Delta u}{u_{For.Inc.}} \quad (4.1)$$

where  $u_{For.Inc.}$  is the displacement at the Foramen Incisivum and  $\Delta u$  is the difference in displacement at the Foramen Incisivum and the Posterior Nasal Spine. In this way, the different models can be compared to one another in a standardized way. The results for the horizontal tipping behavior can be found in Table 4.1

**Table 4.1:** Horizontal tipping - Palatal expander models

	<b>Premolar 1</b>	<b>Premolar 2</b>	<b>Molar 1</b>	<b>Molar 2</b>
$u_{For.Inc.}$ [mm]	7.9	8.2	8.36	7.03
$u_{PNS}$ [mm]	1.93	1.9	2.91	3.80
$\Delta u$ [mm]	5.97	6.31	5.45	3.23
Opening angle [°]	8.28	8.75	7.57	4.49
Parallelism [%]	0.24	0.23	0.35	0.54

From these results, the observation is made that there is no significant difference between the tipping behavior if the expander is positioned at the first or second premolar. However from this point on, if the device is positioned more posteriorly, the transversal expansion will occur more parallel in the axial plane. Especially the case where the device is positioned at the second molar, a high degree of parallelism is obtained when compared to the other cases. For the second molar model, the difference between the measurement at the Foramen Incisivum and the PNS is 3.23 mm, whereas with the molar 1 model this difference is 5.45 mm. By placing the device slightly more posterior a lot of improvement can be obtained. The opening angles range from 8.28° for the premolar 1 model to 4.49° for the molar 2 model.

Similar measurements and observations can be made for tipping of the maxillary halves in the frontal plane. To analyze the vertical tipping behavior, measurements of the transverse expansion are made at both the Anterior Nasal Spine (ANS) and the Central Incisor (C.I.). The obtained results can be found in Table 4.2.

**Table 4.2:** Vertical tipping - Palatal expander models

	<b>Premolar 1</b>	<b>Premolar 2</b>	<b>Molar 1</b>	<b>Molar 2</b>
$u_{C.I.}$ [mm]	4.28	4.63	5.34	4.45
$u_{ANS}$ [mm]	3.13	3.42	3.91	2.85
$\Delta u$ [mm]	1.15	1.20	1.42	1.60
Opening angle [°]	5.28	5.52	6.52	7.33
Parallelism [%]	0.73	0.74	0.73	0.64

As can be seen in Table 4.2, the amount of tipping of the maxillary halves in the frontal plane is smaller than in the horizontal plane. When the expander is positioned at the first or second premolar or the first molar, similar results are obtained for the parallelism of the expansion. When the palatal expander is positioned at the second molar, the opening angle increases and a more pyramidal shaped expansion in the frontal plane is occurring.

Once the general displacement and parallelism of the expansion is evaluated, the displacement pattern (vector sum) at several maxillofacial landmarks is analyzed. The data is plotted in a line graph and is depicted in Figure 4.11. It can be seen that, as the palatal expander device moves posteriorly, the displacement at the pterygoid plates and the maxillary tuberosity is increased, which can be explained due to the fact that the palatal expander is closer to these anatomical landmarks and hence will impose larger displacements on these structures. No other significant conclusions based on this graph can be made.

Finally, the influence of a two mm deviation in inferior direction on one of the sides of the alveolar bone will be analyzed. For this, the comparison will be made between the symmetric placement at the second premolar and the model with a superior deviation on one side. Bar charts are generated to show the differences between both models, which can be seen on Figure 4.12. As is clear from these graphs, no significant differences are reported between the two cases and a similar expansion profile is obtained. The model with the inferior deviation shows smaller superior displacements when compared to the base symmetric case, however the influence of the slight deviation remains very small.

## CHAPTER 4. VARIATIONS IN THE PALATAL EXPANSION DEVICE LOCATION

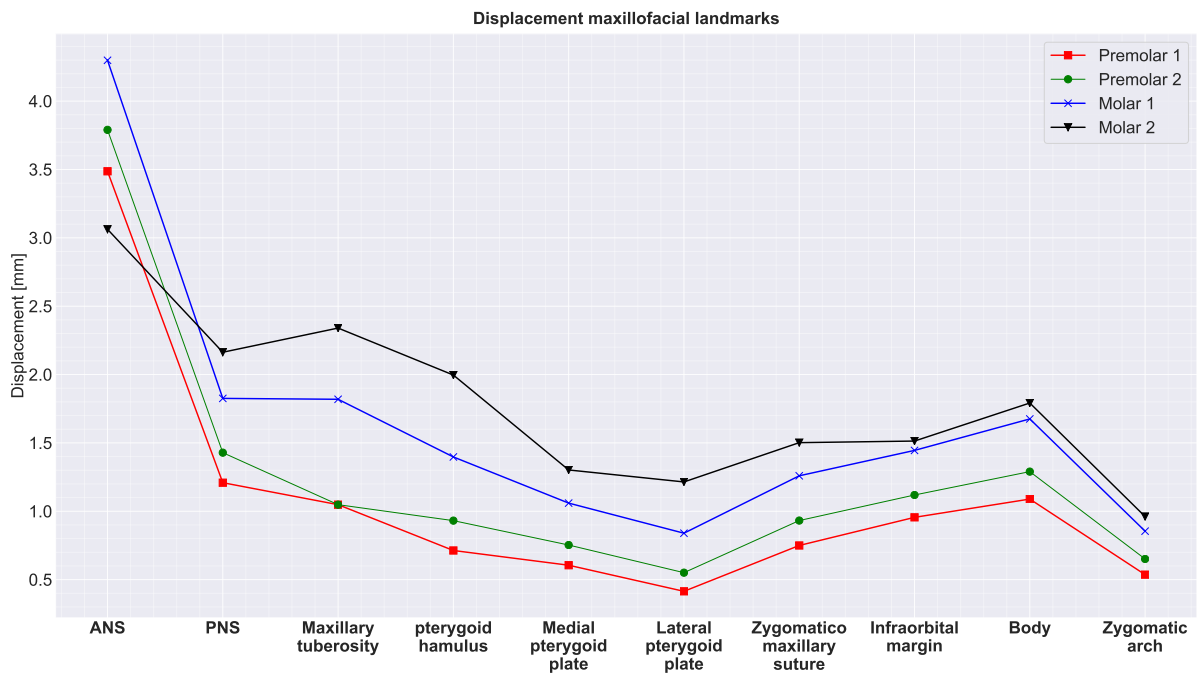


**Figure 4.11:** Displacement (vector sum) at maxillofacial landmarks - Palatal expander models

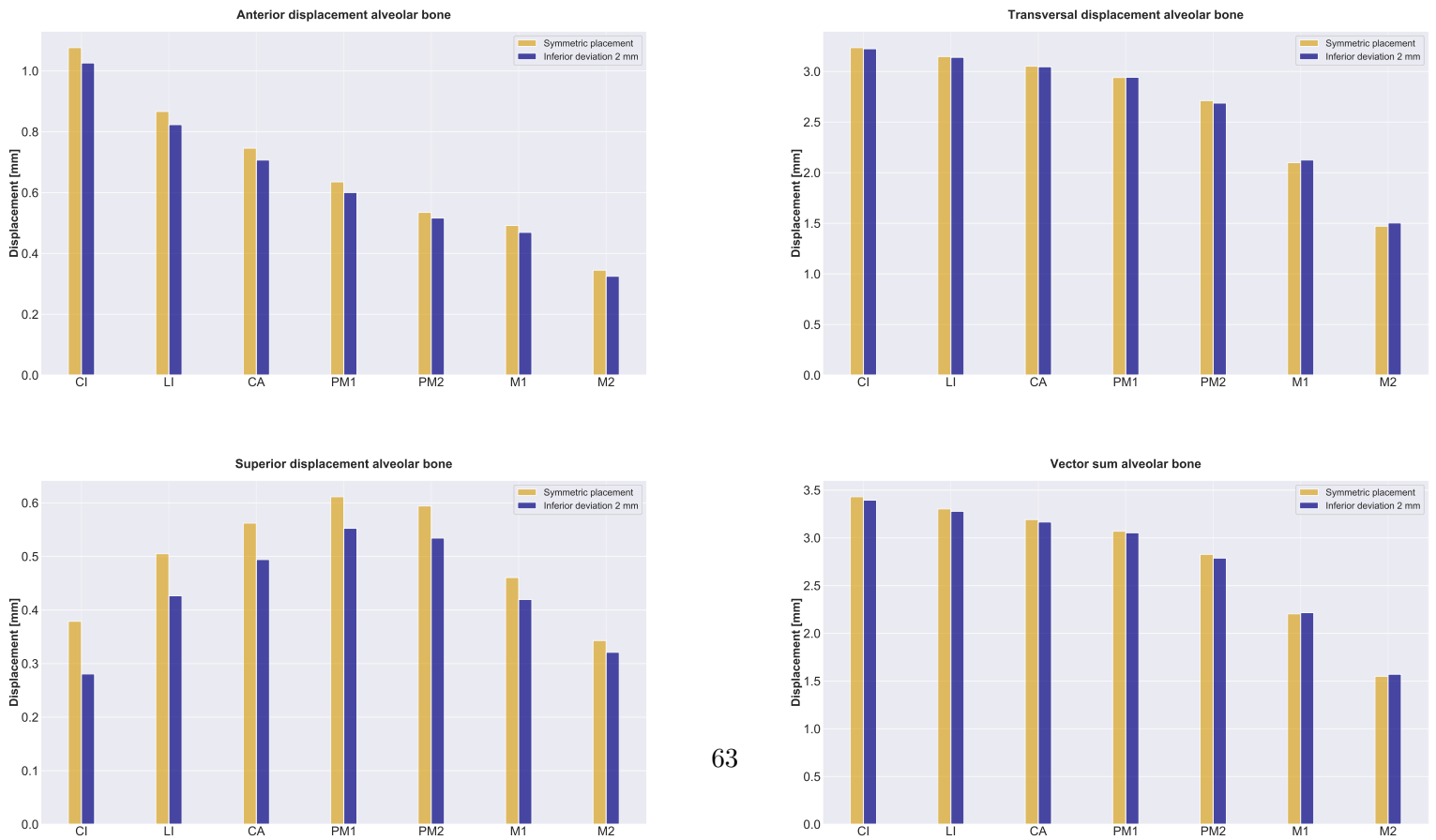


**Figure 4.12:** Displacement at the alveolar bone: symmetric and asymmetric premolar 2 models

### 4.2.2 Discussion displacements

An important note to start the discussion about the displacements is concerning the limitations of this study. Since the actual forces that the expander imposes on the alveolar ridge are unknown, the modeling was performed with a certain displacement imposed between two sets of nodes. When the palatal expander position is changed, the amount of total expansion will also differ, as the expansion is not completely parallel. In this way, when the expander is moved posteriorly and the same 5 mm expansion is imposed on the model, different physical expansions will occur. The displacement profiles can not be compared in an absolute manner as they represent different expansion profiles. The displacement profiles can be considered per case and conclusions about the type of expansion profile can be drawn. In this section the movement of the maxilla will be analyzed and compared to literature and clinical cases to gain more confidence in the model.

#### General displacement maxilla

**Anterior displacement:** In all models, the largest proportion of bone movement was located in the transverse dimension. However, the anterior displacement noticed posteriorly is significant and for some models even comparable to the transverse displacement at these regions. A possible explanation for the anterior displacement of the suture is the rotation of the palatum in the axial plane. The measurements found in Figure 4.10 and Figure 4.9 indicate that tipping of the maxillary halves will occur in the axial plane. Further measurements mentioned in Table 4.1 give more confidence in this theory. A much lower anterior displacement is noticed with the second molar model, which is also an indicator that less horizontal tipping is occurring in this model. The same conclusions are drawn from the calculations and measurements of the parallelism of the expansion in Table 4.1.

According to Biederman and al. [86], the expansion in the occlusal plane occurs in an angular, wedge-shaped displacement, due to the impediment of the posterior articulation and a lowered resistance anteriorly due to the surgical procedure. This behavior was also observed in the results as the horizontal tipping of the maxilla. According to Biederman, two theoretic angular displacements can happen, displayed in Figure 4.13: if the center of rotation is somewhere on the midpalatal suture, point A and the lateral points B and C of the maxilla would move posteriorly and a lot of bone resorption would occur (see shaded area). Another possibility is that the center of rotation is occurring at the points B and C, which would result in an anterior movement of points along the midpalatal suture. Findings of Haas, Davis, Kronman and Biederman support the second theory, and the results obtained in this study comply to this theory as well. All models in this study showed anterior displacements of the maxilla (Figure 4.9 and Figure 4.10). This gives confidence in the correctness of the model [86].

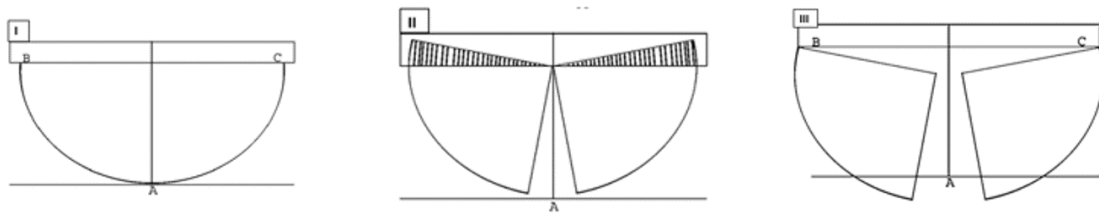


**Figure 4.13:** Possible anteroposterior movements. (I) The semicircle represents the left and right part of the palatum. The rectangle represents the articulation of the bones posteriorly. Point A is the most anterior point of the midpalatal suture. (II) Expansion profile assuming the center of the rotation is somewhere on the midline. (III) Expansion profile assuming the centers of rotation are positioned around point B and C

From the results displayed in Table 4.1, it can clearly be seen that the horizontal tipping effect can be reduced with moving the device more posteriorly, as was suggested by Braun and al. [62]. By moving the palatal expander more posteriorly, the moment-to-force ratio is reduced by decreasing the distance to the center of resistance, resulting in a less rotational movement [62] (see Chapter 2). A significant reduction in this tipping behavior can be seen for the "Molar 2" model, which can explain the reduction in anterior movement of the second molar model when compared to the other models.

Möhlhenrich and al. [84] found that the opening angle decreases with more posteriorly positioned expander devices. However, no significant changes in this angle were reported in his study. An anterior V-shaped pattern resulted at the level of the premolars regardless of the surgical procedure (PMD) or the distractor position, which is in accordance with the results found in this study [84].

Except for the second molar model, the anterior displacement increases with more posterior positioning of the palatal expander device. This may seem contradictory to the results found in Table 4.1. It is important to note that the transverse displacement also increases with more posteriorly positioned palatal expanders, and in this way the effect of the rotation is also magnified. No direct comparison between the cases can be made, as was mentioned in the beginning of this section.

Another important influencing factor in literature seems to be the expander type. Landes and al. [87] reported more parallel expansion along the dental arch when tooth-borne devices are used. Smaller transversal expansions were reported as well.

**Transverse displacements:** Except for the molar 2 model, the transverse expansion increases with increasingly posterior positioning of the TPD. According to Wertz [88], the transverse expansion is larger in the anterior part when compared to the posterior part. This can be explained by the fact that due to the bilateral osteotomy, the resistance against the transverse expansion is lowered anteriorly, resulting in an increased expansion in this region. This also explains the noticed tipping effect in the horizontal plane. The second molar model shows slightly smaller transverse displacements in the anterior region and slightly higher in the posterior region than the molar 1 model. This also shows a more parallel expansion is obtained in the second molar model.

The transversal displacements at the alveolar bone, depicted in Figure 4.10, show that until the level of the first premolar a quite parallel expansion is obtained. The posterior part (PM1 - M2) is nonparallel for all cases, except for the second molar model. This behavior can be explained by the lateral osteotomy, which is only performed posteriorly till the first/second molar. This hypothesis indicates that the lateral osteotomy should run as posteriorly as possible if a parallel expansion is wanted. However, further analyses need to be made to confirm this hypothesis.

**Superior - inferior movement** Haas indicated that in half the cases (found in clinical trials), the most anterior point of the palatum moves inferiorly, meaning the bite tends to close. Koudstaal also reported a slight downward movement of the maxilla, due to the downward direction of the lateral osteotomy. The reasoning of Koudstaal is as follows: the direction of the expansion of the maxillary segments is guided by the oblique osteotomy line (underneath the Zygoma), and this might result in a downward movement of the maxilla [55]. This hypothesis can not be confirmed by the results obtained in this study. In this model, the combination of the lateral osteotomy with an expander located at the alveolar bone seems to move the maxilla superiorly, whereas only the suture moves inferiorly. Another reasoning, opposing to Koudstaal, can be found to explain these results: due to the lateral osteotomy, the resistance against the transversal expansion is lowered. Since the osteotomy is performed superior of the place where the expansion forces are imposed (alveolar ridge), bending of the alveolar bone can occur, resulting in a superior movement of the alveolar bone. In this way, the bite will be opened. An additional non-negligible factor in clinical cases is that there are several thin bones in the midface (nasal bones, walls of the ethmoid...). These bones are more prone to bending due to their low stiffness. With further remodeling of the bone, these thin bones can shorten and in this way further increase the opening of the bite [86]. Another possible

explanation for the inconsistency between literature and this model could be that due to the modeling of the expander device, there is a slightly superior oriented expander force. This is difficult to determine using the current expander model in ABAQUS and hence no definitive conclusion for this posterior displacement behavior can be formulated.

Another intricate displacement is the tipping in the frontal plane. The greatest transversal expansions occur at the level of the teeth with a progressive reduction in transversal expansion towards the nasal floor (superior direction). This is in accordance with literature, where Chamberland and Proffit [52] and Zandi and al. [89] observed similar behavior. As can be seen from Table 4.2, the vertical tipping behavior increases with a more posterior placement of the expander. As was discussed by Pinto and al. [90], the vertical tipping can be decreased by placing the distractor as cranially against the roof of the palatal vault. This advice was followed and the palatal expander is positioned at the most superior position in every model. However, it could be that the palatal expander in the more posterior positions also is placed more inferiorly, increasing the moment lever arm and hence introducing larger tipping behavior. Since no full cephalometric analysis has been performed on the subject, no statements can be reported about this behavior. From the displacement of the other cephalometric landmarks, reported in Figure 4.11, no statements can be made of any clinical significance.

### 4.2.3 Results stresses

The stresses are measured at several maxillofacial landmarks and a comparison is made between the different palatal expander models. The stress distribution is shown in Figure 4.14.

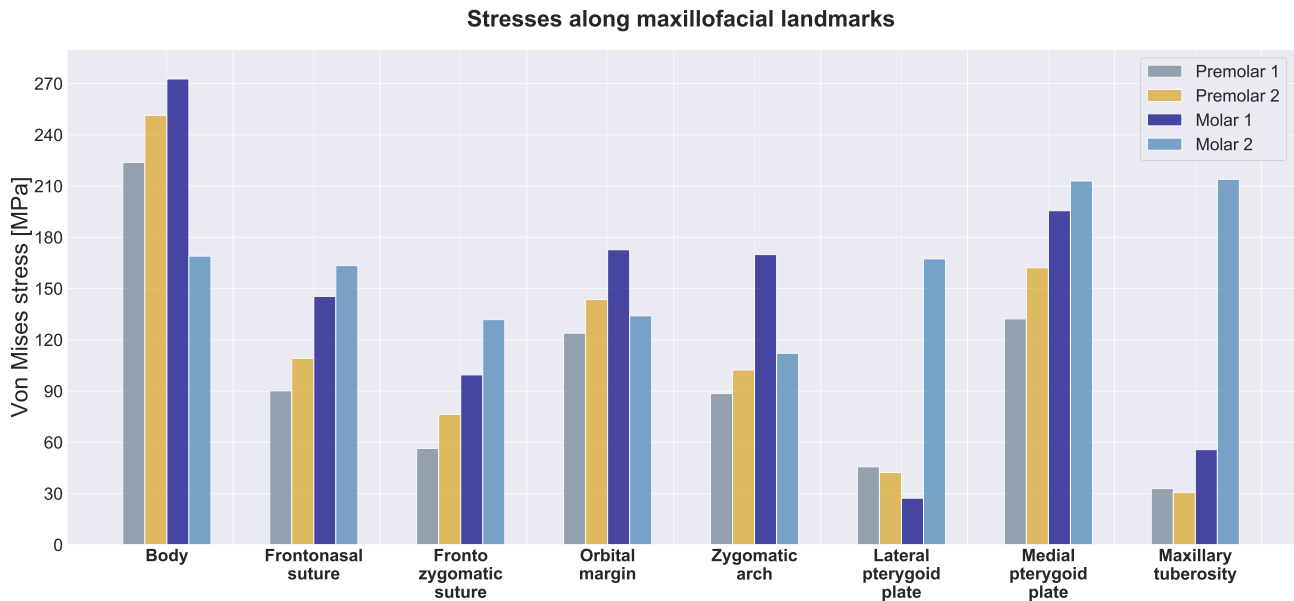


**Figure 4.14:** Stress distribution maxillofacial complex - Palatal expander models

It can be seen that a similar stress pattern is occurring for the premolar 1, premolar 2 and molar 1 model, where the highest stresses are occurring in the body of the maxilla. With the expander located more anteriorly, the maxillary body will be subjected to large forces, and hence the stresses will be quite high at these points. If the expander is positioned at the second molar, the posterior maxillofacial landmarks show higher stresses (lateral pterygoid plate, maxillary tuberosity ...). The stresses in the body of the maxilla are then significantly reduced. The location on the alveolar ridge where the palatal expander is placed also shows very high stresses locally, which is the result of the modeling of the expander device. The model with the small deviation posteriorly showed no significant differences when compared to the model at the second premolar and hence these results are not displayed here.

#### 4.2.4 Discussion stresses

An important side note is that a direct comparison of the stress distribution of the different models is impossible. Due to the fact that other expansion profiles are obtained (since the expander is positioned at different sites, see discussion on displacements), one can not simply compare these results directly to each other, without taking the displacement into account as well. With moving the palatal expander more posteriorly (except for molar 2 model), the absolute displacements (and the expansion in general) also increase. However, stress distributions can be obtained of each of the cases separately and can still lead to interesting conclusions. To make an objective reasoning, the material properties for cortical bone are repeated in Table 4.3 [91].

**Table 4.3:** Material properties cortical bone

Monotonic test	Load case	
	Tension	Compression
Yield stress 0.05%	$71.56 \pm 10.19$ MPa	$115.06 \pm 16.36$ MPa
Yield stress 0.2%	$84.52 \pm 10.47$ MPa	$147.89 \pm 16.36$ MPa
Ultimate stress	$92.95 \pm 10.07$ MPa	$153.59 \pm 21.63$ MPa

It is important to note that some of the stresses in this study are above the yield strength of both cortical and trabecular bone. This reveals a potential limitation of this study.

A first factor which could attribute to the high stress concentrations is that viscoelasticity is not taken into account within this FEA. The human bone consists out of collagen fibers, which show viscoelastic behavior. Since the expansion in real life takes place in steps of 0.5 mm/day and a total expansion of around 5-7 mm, spread out over two-three weeks, the average expansion per day is around 0.35 mm/day. This means that in between consecutive loading steps, there is a large relaxation period, where the stresses are able to dissipate in the cranium. The stresses, measured in real life, will be lower when this relaxation is taken into account. In this FEA, the complete expansion was imposed in one time step. This makes it impossible to make any judgement on an absolute basis concerning the stress components [92].

Several mathematical models exist to express this viscoelasticity. The relaxation time can be best described by using the Maxwell model, which can be represented by a purely viscous damper and elastic spring connected in series. Several other mathematical models exist as well. To find the characteristic relaxation time, stress relaxation tests need to be performed, where a constant strain  $\epsilon_0$  acts as an input to the model, and the expression for the time-dependant stress is sought after, depicted in Figure 4.15 [92].

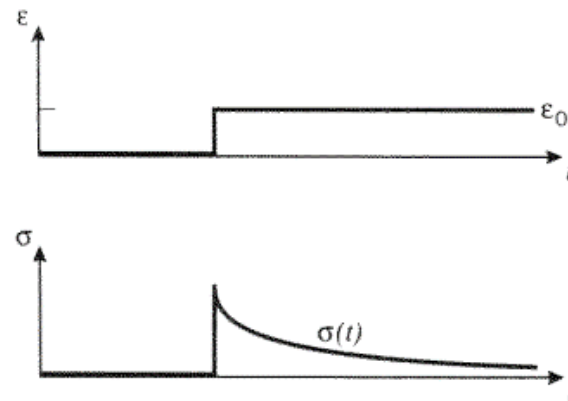


**Figure 4.15:** Stress relaxation test: strain as input, time dependency of the stress as output [92]

The time dependent relation within this stress relaxation test can be written as follows ( $\dot{\epsilon} = 0$ ):

$$\sigma(t) = \sigma_0 \cdot \exp(-t/\tau) \quad (4.2)$$

where  $\tau$  is the characteristic 'relaxation' time. It is physically the time needed for the stresses to fall to  $1/e$  of the initial value.

This shows another problem to properly implement the viscoelastic behavior: the lack of information about the mechanical properties of the maxilla. Every bone in the human has unique material properties due to the loading each bone has (Wolff's law, stating that stronger bone will develop at areas of high loading) and the unique anatomy of each bone. No viscoelastic properties are found in literature for the maxilla and/or cranium and hence, no correct viscoelastic finite element models can be created at this time. Deliggiani and al. [93] showed that the percentage of the remaining stress after relaxation, compared to the maximum stress is around 80%. This study was performed on femoral heads from human cadavers between 55 and 70 year old, which also can have an influence on these results. Based on the dependence of stress relaxation function on the strain level, the viscoelastic behaviour of trabecular bone is considered non-linear [93]. Similar stress reductions due to relaxation (around 20-25 %, independent on the initial preload) are observed in a study by Edgar and al. [94], where the trabecular bone specimens from bovine femoral heads were analyzed. Further research is required to obtain more correct material properties for the maxilla in general. Some other FEA use other values for the elastic moduli of the cortical and trabecular bone as well. No correct values for cortical nor trabecular bone exist and show an important limitation to the accurateness of the performed simulations.

Furthermore, the testing conditions of the bone are of importance for the micromechanical properties of bone. All measurements found in literature are performed in dry conditions (air/in vacuo). In multiple studies, it has been shown that the hydration state of the bone has a severe impact on the micromechanical properties of the bone [95] [96] [97].

The mechanical behavior of cortical bone can be characterised by an initial elastic domain, a post yield domain where irreversible strains and damage are produced and a final fracture zone, where a macrocrack is formed. Unlike in steel, the yielding in bone is rather continuous with a certain transitioning zone. Bone can also be considered as a quasi-brittle material at the tissue level. Many microcracks are developed prior to failure, which do not result immediately in catastrophic failure. For human cortical bone, the ultimate strains depend on the source in literature, where values between 0.7 % and 5.2 % are reported. The maximal strain occurring in the models is around 3 %. There is no clinical knowledge whether yielding is occurring during the SARPE procedure or not [95].

Taking all these modeling inaccuracies into account, the combination of these effects could result in less realistic absolute stresses and a lower accuracy of the simulation. This shows however the need for further research, especially concerning the material properties of the maxilla. The absolute values of the stresses are rendered unusable due to inaccuracy and simplicity of the used material models. As such, the results concerning the stresses can only be used to compare different cases against each other. In these simulations, even a direct comparison can not be made, as the different models represent a different physical expansion. This was discussed in more detail in the previous section.

### 4.3 Conclusions palatal expander location

From the analysis performed in section 4.2, several conclusions can be drawn concerning the optimal placement of the palatal expander, as well as on the influence of small deviations in the frontal plane when installing the transpalatal expander. In this chapter also a verification with literature and clinical cases was performed to gain insight in how the FEA model behaves and if this is in accordance with literature. Following conclusions are drawn from the simulations:

1. The obtained finite element models behave and respond to the expansion as described in literature. This gives confidence the models created in this section give an accurate representation of the displacements. The finite element model can be used to perform research and get correct measurements (concerning the displacement).
2. The general displacement pattern of the maxilla was obtained. All models show a similar displacement pattern, where the maxilla moves superiorly (except at the midpalatal suture), laterally and anteriorly (mostly due to the horizontal tipping).
3. The optimal expander position depends on the required expansion profile. Moving the expander more posteriorly results in a more parallel expansion (less V-shaped). Depending on the type of deficiency another positioning of the palatal expander can be proposed. The tipping of the maxillary halves in the frontal plane increases with increasing posterior position. This effect is however small and could be attributed to a more superior position of the expander in the modeling, as the expander is always positioned as close as possible towards the palatum.
4. Small deviations in the superoinferior direction will only influence the superior displacements. A deviation of 2 mm resulted in 0.1 mm difference in superior displacement at the alveolar bone, which is negligible. Maxillofacial surgeons should try to position the implant as symmetrical as possible, however small deviations do not have a large influence on the general displacement profile.
5. The obtained stresses at some maxillofacial landmarks are larger than the yield strength of cortical bone. The argument was made that due to the modeling of the loading (5 mm in one time step) and the lack of correct (viscoelastic) material properties, no realistic model can be created. This is a limitation of the accuracy of the modeling of the complete surgical procedure. The need for extra experimental and clinical research was demonstrated to obtain more correct material properties.

## CHAPTER 4. VARIATIONS IN THE PALATAL EXPANSION DEVICE LOCATION

It is important to note that in real life conditions, the TPD can not be placed anywhere on the palatum. The TPD is mostly placed either at the second premolar or the first molar, since the device needs to be accessible by the patient to perform the gradual expansion. Sometimes, due to obstruction or a very narrow palatum, the device can only be installed at one certain location. In this way, the clinical relevance of this part of the study is limited, however, the theoretical concepts concerning the tipping behavior and the general displacement of the maxilla were analyzed and more confidence was gained in the correctness of the model. The model behaves as described in clinical cases and experimental research in literature. Also some of the limitations of the FEA model were revealed, indicating already that further research is required, especially concerning the material properties of the maxilla. With further research on these topics, more accurate finite element models can be created and more correct simulations can be performed.

Next to the position of the palatal expander, several other variables can be varied, such as the type of the expander and the surgical procedure. In the next chapter, the influence of several surgical variations will be analyzed. Pterygomaxillary disjunctions (PMD) will be performed, as well as an asymmetric lateral osteotomy. In this way, the influence of the surgical variations can be analyzed. The combined influence, as well as the possible interactions these variables have on each other, is outside of the scope of this research.

CHAPTER 4. VARIATIONS IN THE PALATAL EXPANSION DEVICE LOCATION

# Chapter 5 | Variations in the surgical technique

In this chapter, the influence of surgical variations on the expansion profile and the stress distribution is measured and analyzed. A thorough comparison with literature is made.

The pterygomaxillary disjunction (PMD) may be an important factor which could influence the expansion profile of the skeletal expansion. However, the pterygoid disjunction also remains a controversial subject in literature. The PMD can lead to severe complications: fractures extending to the base of the skull, orbit or pterygopalatine fossa (associated with the PMD) can be the aetiology of blindness [98], trauma of the palatine artery or the cranial nerve can occur, as well as many other complications. The exact influence of the osteotomy on the expansion profile remains unknown: Bays and Greco [69] observed on tooth-borne SARPE more posterior than anterior transversal expansion while Han and al. [99] observed the opposite behavior. This discrepancy in literature shows the necessity for more research on the exact influence of the pterygoid disjunction on both the displacement profile and the stress distribution.

Another important clinical aspect often overlooked in literature is the amount of symmetry during expansion. Clinical asymmetrical expansion was observed in literature, however, the direction, frequency and the magnitude of the asymmetry have not yet been quantified. The presence of asymmetric expansion is mentioned in literature but is mostly out of the scope of the research. Only a few studies in literature explicitly mention the symmetry of the expansion, including studies performed by Ramieri and al. [100], Nada and al. [101] and Huizinga and al. [102].

In a study, performed by Koudstaal [55], a bilateral expansion was required, however the results showed that only the maxilla expanded unilaterally, which is a severe case of an asymmetric expansion. According to Koudstaal, an influencing parameter could be that the surgical mobilization was not performed evenly on both sides [55]. After performing a second surgery to improve the mobilization of the maxilla, the same asymmetric

widening occurred [55]. These findings in literature indicate that a lot of uncertainty is present concerning the symmetry of the expansion and the possible influencing factors. Asymmetric expansions are often present in patients, however no control of this type of behavior is available. Quantifying the direction, magnitude and occurrence of the asymmetric expansion could aid in modifying the surgical procedure and distraction protocol to obtain improved outcome and predictability of the SARPE procedure.

Using the results of the simulations performed in this chapter, new insights will be gained in the expansion of the maxilla when surgical variations are made on the model. The influence of the pterygoid disjunction (PMD) and the (a)symmetric position of the lateral osteotomy on the expansion profile and the symmetry of the expansion is analyzed.

## 5.1 Influence of the pterygoid plate disjunction

### 5.1.1 Models pterygoid disjunction

To simulate the influence of different surgical variations, multiple models had to be created. For a first set of simulations, the influence of the pterygoid plate disjunction was analyzed. In total, three models were created: a standard case, with a symmetrical lateral osteotomy as described in section 3.4, and two models where the pterygoid plates are disjuncted. To measure the precise influence of the pterygoid disjunction, the pterygoid disjunction is performed uni- and bilaterally. The three models are depicted in Figure 5.1. The lateral cuts had to be increased in thickness from 1 mm to 1.5 mm for all models to avoid collision between the superior and inferior part of the maxilla. The models with PMD required osteotomies with a thickness of 2 mm to avoid contact of the alveolar bone with the zygomatic bone during expansion.

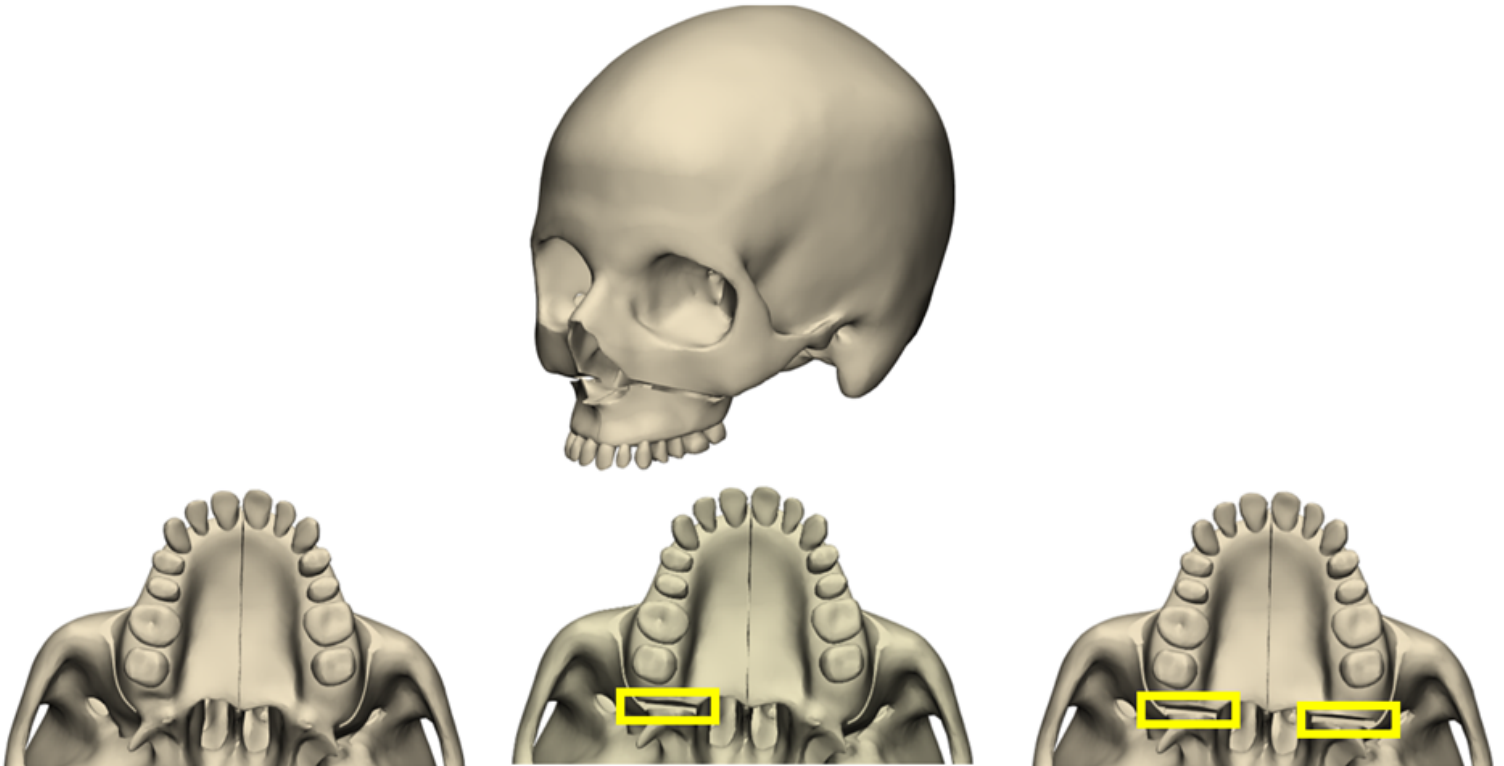


**Figure 5.1:** Pterygoid disjunction models: oblique view, the same for all three models (top), no PMD (left), unilateral PMD (middle) and bilateral PMD (right) models. PMD indicated in yellow

### 5.1.2 Results displacement

In Figure 5.2, the displacements at the level of the suture are shown. The movement in the anterior direction was the largest for the unilateral PMD model. Anteriorly, the lowest anterior displacement was observed for the bilateral PMD, however posteriorly the basic model showed the lowest anterior movement. Similar values for the transversal displacements and vector sum are reported for all cases. The one sided PMD shows the largest inferior displacement of 0.78 mm around point D of the suture. The uni- and bilateral PMD models show the same superoinferior behavior: the inferior movement of the suture is reduced by the presence of the PMD when compared to the model without PMD.

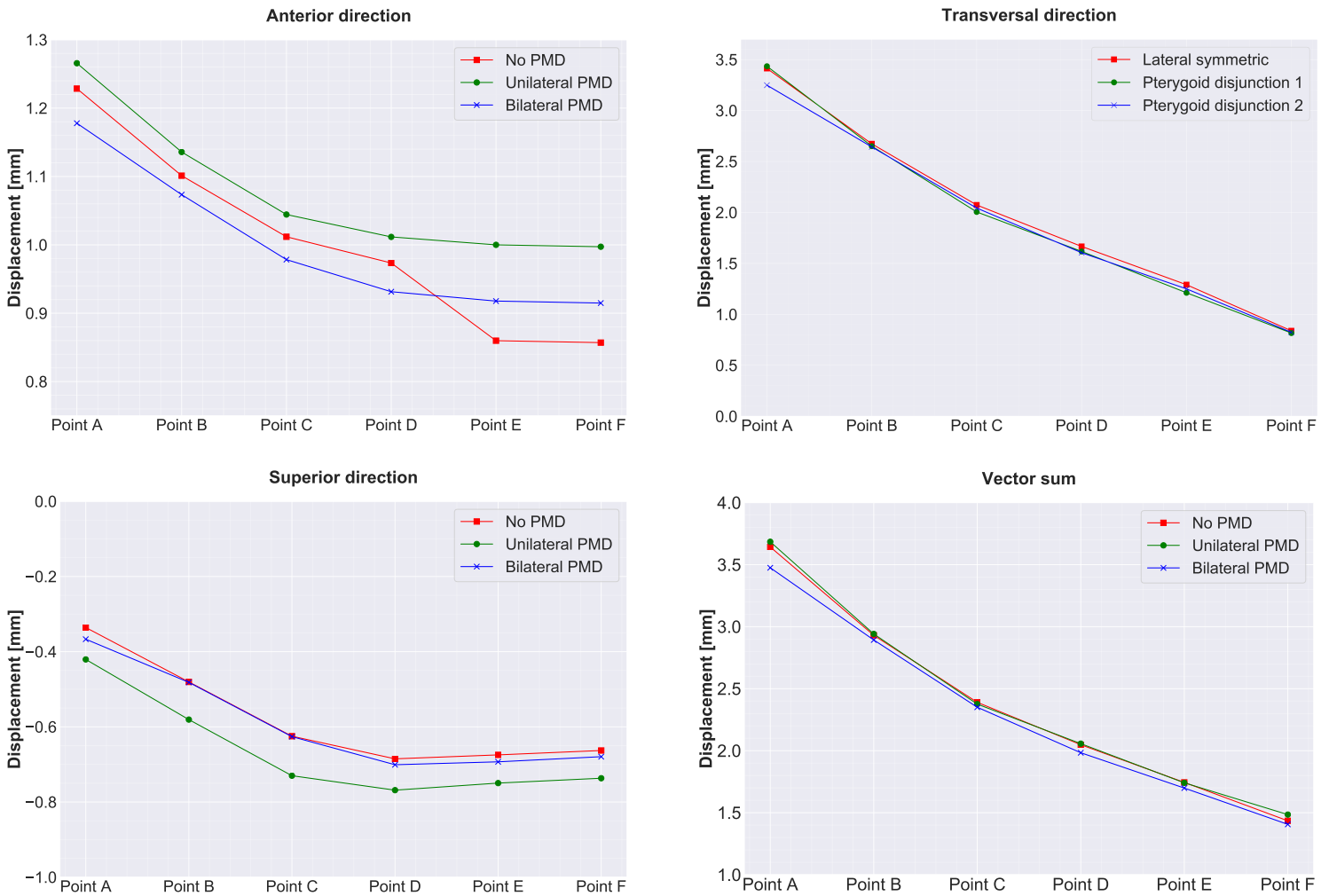


**Figure 5.2:** Displacement at the suture: point A is located around Foramen Incisivum, F at the posterior nasal spine - PMD models

Since asymmetries are introduced in the model (unilateral PMD), the displacements on both the left and on the right side of the model need to be measured. On Figure 5.3, the displacement at the alveolar bone is depicted on the left and right side. The obtained values are also tabulated in Tables 5.1, 5.2 and Table 5.3.

**Table 5.1:** Anterior displacements alveolar bone - PMD models

<b>Anterior displacement</b>	<b>Orientation</b>	<b>T1</b>	<b>T2</b>	<b>T3</b>	<b>T4</b>	<b>T5</b>	<b>T6</b>	<b>T7</b>
No PMD [mm]	Left	1.02	0.84	0.68	0.60	0.53	0.46	0.34
	Right	1.03	0.82	0.66	0.57	0.47	0.44	0.32
Unilateral PMD [mm]	Left	1.06	0.88	0.71	0.63	0.55	0.48	0.37
	Right	1.01	0.81	0.64	0.56	0.46	0.43	0.32
Bilateral PMD [mm]	Left	1.04	0.86	0.65	0.58	0.51	0.44	0.35
	Right	1.1	0.88	0.73	0.61	0.50	0.48	0.37

**Table 5.2:** Transversal displacements alveolar bone - PMD models

<b>Lateral displacement</b>	<b>Orientation</b>	<b>T1</b>	<b>T2</b>	<b>T3</b>	<b>T4</b>	<b>T5</b>	<b>T6</b>	<b>T7</b>
No PMD [mm]	Left	3.16	3.11	2.93	2.74	2.55	1.97	1.39
	Right	3.47	3.38	3.18	3.03	2.73	2.16	1.59
Unilateral PMD [mm]	Left	3.25	3.20	3.00	2.81	2.60	2.00	1.40
	Right	3.42	3.32	3.13	2.98	2.68	2.12	1.57
Bilateral PMD [mm]	Left	3.09	3.01	2.78	2.60	2.41	1.86	1.35
	Right	3.84	3.79	3.64	3.38	3.04	2.53	1.83

**Table 5.3:** Superior displacements alveolar bone - PMD models

<b>Superior displacement</b>	<b>Orientation</b>	<b>T1</b>	<b>T2</b>	<b>T3</b>	<b>T4</b>	<b>T5</b>	<b>T6</b>	<b>T7</b>
No PMD [mm]	Left	-0.16	0.045	0.20	0.23	0.25	0.20	0.13
	Right	-0.05	0.22	0.38	0.44	0.46	0.31	0.27
Unilateral PMD [mm]	Left	-0.23	-0.01	0.16	0.19	0.22	0.16	0.09
	Right	-0.09	0.18	0.33	0.40	0.42	0.31	0.24
Bilateral PMD [mm]	Left	-0.25	-0.03	0.16	0.19	0.22	0.17	1.35
	Right	-0.20	0.15	0.33	0.44	0.49	0.37	0.27

Using this data, the amount of symmetry in the expansion can be obtained. The total displacement (vector sum) is used to quantify the amount of symmetry of the expansion. On average, the expansion on the right side is 52.3%, 51.3% and 56.3% for respectively the symmetric, unilateral and bilateral pterygoid disjunction models. These values are calculated as averages over the seven measurement points of the alveolar bone. More pronounced differences for the unilateral pterygoid disjunction are present for the most posterior measurement point, as can be seen in Figure 5.3.

The model without PMD already shows a slight asymmetry, where 52.3% of the total transversal displacement is on the right side. A more symmetric expansion is obtained by performing the pterygoid disjunction on the left side, however this effect seems quite small. By performing the pterygoid disjunction on both sides, the asymmetry of the expansion increases, with a maximum value of 56.3% of the expansion obtained on the right side. Possible influencing factors of these results are mentioned in the discussion.

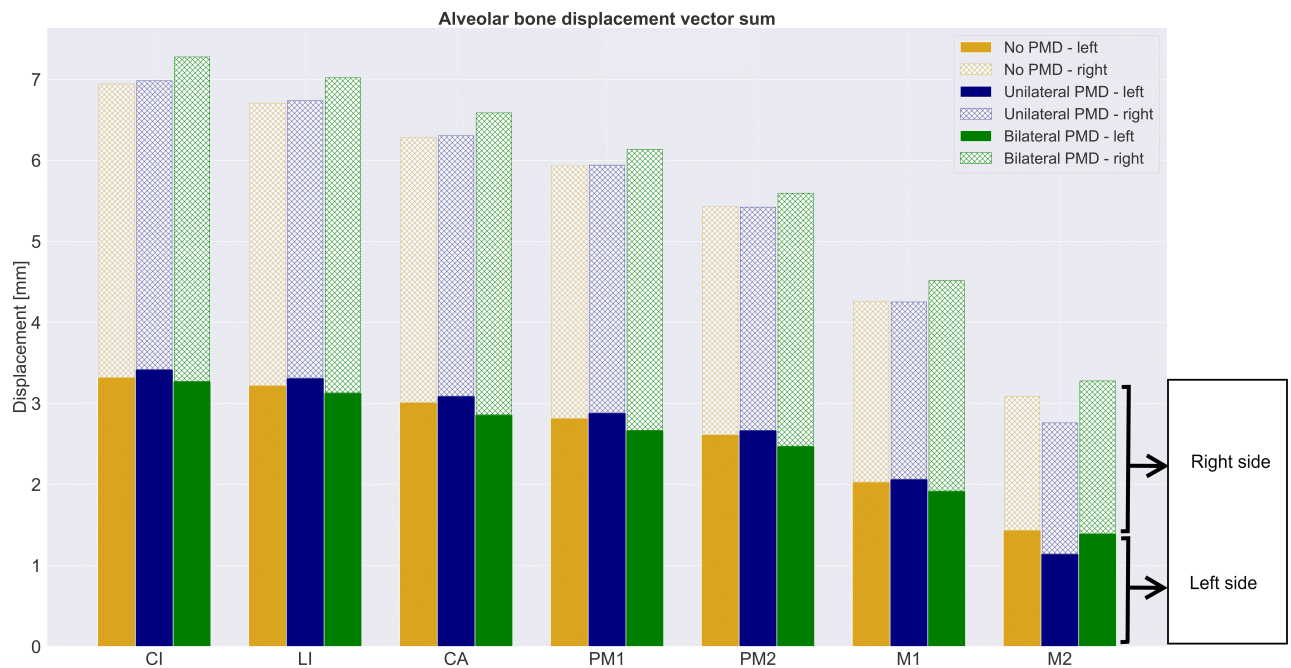


Figure 5.3: Symmetry of the expansion measured at the alveolar bone - PMD models

Next, the influence of the pterygoid disjunction on the tipping behavior is measured as well. In Table 5.4 and in Table 5.5 respectively the horizontal and the vertical tipping measurements are shown. For the horizontal tipping, small opening angles are measured in all models. The lowest opening angle is  $5.82^\circ$ , obtained when the pterygoid disjunction is performed on both sides. The horizontal tipping is the largest when the pterygoid disjunction is only performed on one side, with an opening angle of  $6.71^\circ$ .

In Table 5.5, the vertical tipping behavior is shown. The pterygoid disjunction seems to influence the vertical tipping behavior of the maxilla, where the amount of vertical tipping tends to increase when the PMD is performed. The model without PMD has the lowest opening angle of  $6.13^\circ$ . The maximum opening angle ( $7.42^\circ$ ) was obtained for the bilateral PMD model.

**Table 5.4:** Horizontal tipping - PMD models

	<b>No PMD</b>	<b>Unilateral PMD</b>	<b>Bilateral PMD</b>
$u_{For.Inc.}$ [mm]	6.39	6.97	6.17
$u_{PNS}$ [mm]	2.18	2.14	1.98
$\Delta u$ [mm]	4.21	4.83	4.19
Opening angle [ $^\circ$ ]	5.86	6.71	5.82

**Table 5.5:** Vertical tipping - PMD models

	<b>No PMD</b>	<b>Unilateral PMD</b>	<b>Bilateral PMD</b>
$u_{C.I.}$ [mm]	8.89	8.81	8.97
$u_{ANS}$ [mm]	6.21	6.26	6.13
$\Delta u$ [mm]	2.68	2.56	2.84
Opening angle [ $^\circ$ ]	6.13	6.68	7.42

### 5.1.3 Discussion displacement

Bays & Greco [69] reported that a separation of the pterygoid plates leads to a larger posterior expansion, resulting in a more parallel expansion. Without pterygoid plate disjunction a proportionally less posterior distraction is obtained. However, Han and al. [99] found more posterior widening of the patients where no pterygoid plate disjunction was performed. Vasconcelos [103] found a larger transverse maxillary widening when the PMD was performed. This indicates there is still a lot of uncertainty in literature and that the exact influence of the pterygoid plate disjunction remains unknown. The unique patient anatomy could also play a role in the various effects of the PMD mentioned in literature. Other factors, such as the placement of the expander device, the type of the expander device, age and sex of the patient can also influence the effect of the PMD. In most studies, multiple variables of the SARPE procedure are varied simultaneously. When these results are compared to each other, it is difficult to attribute the differences in displacement profile to a single variable.

Based on the results presented in Figure 5.2, the expansion profile is similar as was discussed in chapter 4. At the level of the suture, no large changes are observed concerning the anterior, transversal and superior direction between the models. Since the vector sum of each of these models is similar, the models can be compared to each other, as they represent the same physical expansion. It is however important to note that the TPD is positioned at the second premolar in these simulations. Moving this TPD more posteriorly can influence the effect of the PMD. This interaction is outside of the scope of this research.

In literature, post-expansion results showed more movement of the posterior part of the palate when pterygoid disjunction was part of the procedure and the distractor was placed at the level of the first molar. Using this procedure, the ratio between increases of intercanine to intermolar width was 1:0.93 (Matteini and Mommaerts [64]) and 1:0.95 (Ramieri et al. [100]). Without pterygoid disjunction and placement of the distractor at the level of the second premolar the ratio was 1:0.71 (Pinto et al. [90]), and 1:0.65 (Ramieri et al. [100]). In the latter three studies, patients had a developmental deformity and a TPD was used [104]. As can be seen from these results in literature, a significantly more parallel expansion is obtained when the pterygoid plate disjunction is performed and the TPD is installed more posteriorly. Verstraaten and al. [104] reported in a systematic review that differences were found for the transverse maxillary changes depending on the associated surgical procedure. Without pterygoid disjunction and with the distractor placed at the level of the second premolar, the expansion profile was V-shaped with more expansion anteriorly than posteriorly. With disjunction of the pterygoid plates and the distractor placed at the level of the first molar, the expansion

was more parallel [104]. Huizinga [102] comes to a similar conclusion. A strong limitation arises in both studies: no separate cases are analyzed where only the presence of the PMD is changed, or the position of the palatal expander. In this way, multiple influencing factors are combined in these results, making it hard to determine the influence of each of the factors separately. This makes it impossible to determine the influence of the PMD on the parallelism of the expansion in these clinical studies.

Next, the tipping behavior in axial and frontal planes is analyzed. Generally speaking, small angles are occurring in the range of  $5.8^\circ$ -  $6.7^\circ$ . These values are lower when compared to the values obtained in chapter 4. In the models considered here, the lateral osteotomies run slightly further in the posterior direction, in this way reducing the transversal expansion resistance and increasing the amount of parallel expansion. The main rationale, mentioned in literature to perform PMD is to increase the parallelism of the expansion profile [11] [52] [64]. As can be seen in Table 5.4, when the pterygoid disjunction is performed in both sides, the smallest opening angle was found ( $5.82^\circ$ ), and the least tipping is observed. when the pterygoid disjunction is performed on one side, the largest angle is obtained ( $6.71^\circ$ ). The obtained results show small differences, which may be clinically irrelevant. These findings are in accordance with Möhlhenrich and al. [105], who reported a more parallel transverse expansion when PMD was performed, however with few statistical differences.

In clinical studies, any form of asymmetric expansion is reported in 55% of the patients [102]. Koudstaal reported that an explanation for the asymmetric expansion might be that an equilibrium exists between the resistance of both maxillary halves. The maxillary halves are connected to the skull in the pterygoid region. Soft tissues, such as muscles and ligaments can affect the resistance on each side. He suggests that when the difference in resistance of both sides is excessive, only the side with the least resistance will expand, leaving the other maxillary half immobilized [55].

The results reported in Tables 5.1, 5.2 and Table 5.3 show the displacement at both sides of the maxilla. In the model without PMD, a small asymmetry is already present between both sides of the alveolar bone. According to the theory of Koudstaal, there should already be an imbalance present in the equilibrium of the resisting forces of the maxillary segments. Several possible reasons for this behavior could exist: unique patient anatomy, small deviations in the palatal expander position or slight differences in the lateral osteotomy on both sides could lead to a difference in resisting forces. These differences in resisting force can occur both in real life (unique anatomy, muscles and soft tissues, during the placement of the expander or due to inaccuracies during the surgical procedure) and due to modeling inaccuracies in ABAQUS.

When the pterygoid disjunction is performed at the left side of the maxilla, extra resistance against the expansion is removed, and therefore the left part of the maxilla can expand more. This results in a slightly more symmetric expansion, as initially the right side expanded more. The effect for the model with one pterygoid disjunction is rather small. When the pterygoid disjunction is performed on both sides of the maxilla, a more asymmetric expansion profile is obtained, and the maxilla expands more to the right side. Using these results, one can see the direct influence of the pterygoid disjunction: by separation of the pterygoid plates, posterior resistance is removed and larger displacements on that side are noticed. Depending on the required expansion profile for a specific patient, the pterygoid disjunction can either be performed on one side or both sides. This shows the importance of a correct diagnosis, where the complete malocclusion needs to be analyzed. If more expansion is required on one of the sides, a pterygoid disjunction can be performed on that side to allow more expansion. However, care should be taken concerning these results, since Koudstaal reported a clinical case where a unilateral expansion occurred due to an excessive difference in resisting force of both sides [55]. Performing a unilateral pterygoid disjunction could also result in an unilateral expansion profile, which is not always preferred. Additional clinical and experimental research should be performed to validate the expansion profile when performing an unilateral pterygoid disjunction to observe if the maxilla still expands bilaterally.

In a study by Laudemann [106] a bigger anterior transverse widening (first premolar region) was found when the pterygoid plates are disjuncted. This behavior was not observed in this study. Due to the transversal expansion, lateral bending of the pterygoid plates occur, which induces stresses and deformations at the sphenoid body. In the study by Laudemann, the age of the patients is of importance, where no pterygoid disjunction is advised for patients younger than 20 years old and pterygoid disjunction is advised for people over 20 years old. This shows that the ossification process of the sutures is of importance, as they influence the behavior of the expansion. In our study, we assume the sutures to be ossified and having the same material properties as the surrounding bone [106]. This study by Laudemann [106] indicates that material properties and assignment can also have a significant influence on the effects of the PMD on the expansion profile.

5.1.4 Results stresses

To compare the different stress distributions, the model without the PMD is compared to the model where the PMD is performed on both sides. For the model with the PMD performed unilaterally, the disjuncted side had similar stresses as the analyzed PMD model, whereas the intact side had a similar stress distribution as the model without PMD. In this way, these results can be omitted from the analysis. The results are shown in Figure 5.4.

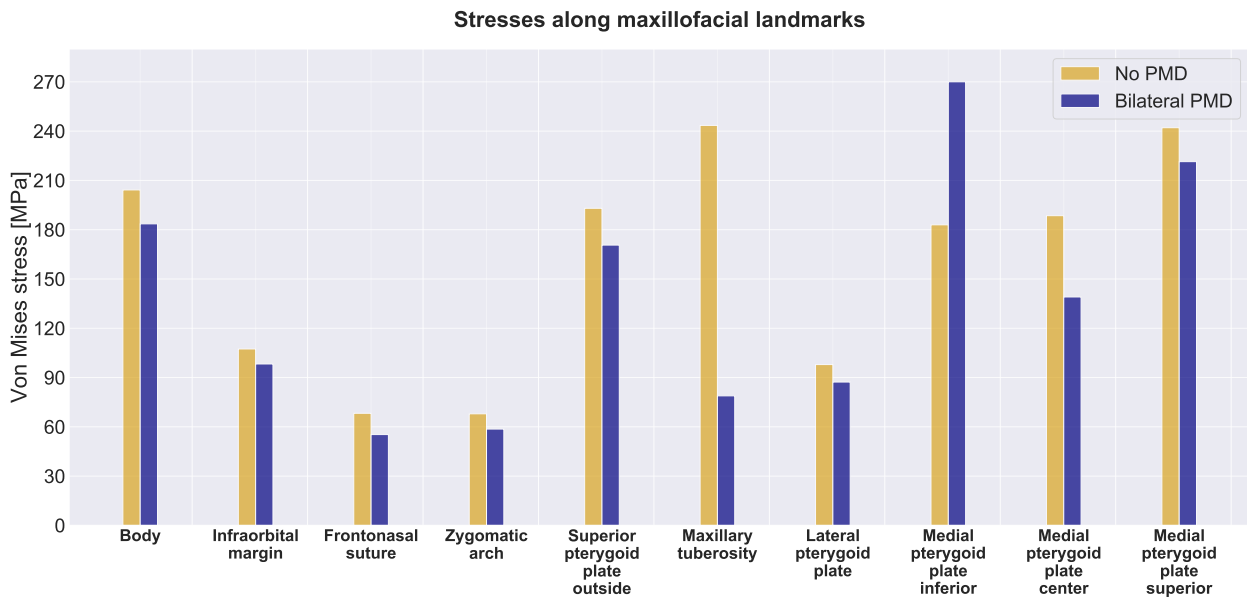


Figure 5.4: Stress distribution in the maxillofacial complex - PMD models

By performing the PMD, a different stress distribution is observed. The anteriorly positioned maxillofacial landmarks, such as the body, infraorbital margin, frontonasal suture and the zygomatic arch all show decreased stresses, with reductions of around 10% to 20%. At the maxillary tuberosity a reduction of around 67% is observed, and an increase of around 47.5 % at the medial pterygoid plate (measured inferiorly). The pterygoid disjunction generally lowers the stresses found in the maxilla, except for the medial pterygoid plate (inferiorly measured). The stresses at the cranial Foramina are also measured, as the pterygoid disjunction tends to lower the stresses around these regions. The obtained results are found in Table 5.6.

**Table 5.6:** Stresses measured at the cranial Foramina - PMD models

	No PMD [MPa]	Bilateral PMD [MPa]	Reduction [%]
<b>Foramen Ovale</b>	51.75	41.71	19.5
<b>Foramen Lacerum</b>	65.65	61.71	6.01
<b>Foramen Optica</b>	83.28	56.54	32.10

As can be seen from the observed results, by performing the pterygoid disjunction the stresses at the cranial Foramina can be reduced, with reductions ranging from 6% to 32%, depending on the specific location of the Foramen.

### 5.1.5 Discussion stresses

A finite element study performed by Holberg and al. [107] showed that the pterygoid disjunction generally reduced stresses at most anatomic structures of the midface. This is confirmed by the simulations performed in this chapter. Generally speaking, the pterygomaxillary separation decreases the stresses. With reduced stresses, the procedure might lead to an increased stability. For the maxillofacial landmarks considered in the study, reductions of around 10% - 20% are observed by Holberg [107]. In the models obtained in this simulation, the pterygoid disjunction led to a decrease of stresses of 15% to 20%, with exceptions at the maxillary tuberosity (67%) and the medial pterygoid plate, measured inferiorly (47%).

In an other study, performed by Dalband et al. [108], the separation of pterygomaxillary plates resulted in a significant increase in the mean displacement in all axes. The pterygoid disjunction led to an increase of displacement of 15% to 20%. In the study conducted in this chapter, as the displacement is kept the same due to the modeling in ABAQUS, the stresses should be different. A general lower stress distribution is observed from these results. From Figure 5.4, one can also see decreases of around generally 10% - 20%. In this way, a similar conclusion as Dalband can be made, where the pterygomaxillary disjunction results in a general decrease of stresses for a certain displacement, or increases the displacement for the same forces applied to the alveolar bone.

The study by Holberg showed significantly reduced stresses at the Foramina of the cranial base, with reductions of up to 75% at the Optic Foramen. When the stresses are reduced at the Foramina of the cranial base, the possibility of (mini)fractures is decreased and severe complications can be avoided. In literature, these fractures are extremely improbable, however, a case report by Lanigan and Mintz [107] showed a fracture of the cranial base after SARPE was performed. There is a close anatomic correlation among the optic canal, the pterygoid, sphenoid and palatine bones. Fractures extending to the base of the skull, orbit or pterygopalatine fossa can also be the aetiology of blindness [98]. A moderate haemorrhage in this area can be devastating, as the retinal tissue and the optic nerve are very pressure sensitive. This is a severe complication since the prognosis is poor once blindness develops [98]. In this way, the stresses around the cranial Foramen should be as low as possible. As can be seen from Table 5.6, similar behavior as the study by Holberg is noticed in this model, albeit with smaller values. A reduction of around 32.1% is observed at the Foramen Optica in this model, whereas Holberg and al. [107] measured reductions up to 75%. Nevertheless, the same conclusion can be drawn: the pterygoid disjunction allows for lower stresses at the cranial Foramen, and in this way reduces the risk of (mini)fractures at these Foramen. It remains important to note that performing the PMD is not risk-free: trauma of the palatine artery or cranial nerve can occur, or an injury of the pterygoid plexus [36] [49]. This can lead to severe complications and hence, the trade off needs to be evaluated by the clinician.

The pterygoid plate disjunction did not reduce the stresses at the alveolar bone/palatum, since the TPD is positioned directly on the alveolar bone. In this way, the PMD will have no influence on alveolar bone-related complications such as gingival recession and root resorption. According to Han et al. [99], this same pterygoid disjunction decreases the stresses at the alveolar bone for tooth-borne devices, successfully reducing the occurrence of gingival recession and root resorption [99]. More models need to be simulated to confirm this study by Han and al. [99], as this study also uses a different expansion device type.

## 5.2 Influence of the lateral osteotomy site

In this section, the results of the model with an asymmetric lateral osteotomy will be reported. A transversal expansion of 5 mm is simulated.

### 5.2.1 Models influence lateral osteotomy

To analyze the influence of the position of the lateral osteotomy, an other model was created. The locations where the lateral osteotomy can be placed are bounded by several limitations. The osteotomy needs to be at least 5 mm superior of the apex of the incisor, to avoid damaging the teeth. Another requirement is that the osteotomy should be at least 5 mm inferior of the Infraorbital Foramen, since this is a weakened location on the skull and fracture patterns can originate from this Foramen. Taking these limitations into account, a model was created where the most inferior location was chosen on one side (left) and on the other side the most superior location (right). This model is shown in Figure 5.5. Surgical cuts of 3 mm thickness were required to avoid collision between the superior and inferior part of the maxilla. Transversal displacements of 5 mm were imposed on all models to simulate the expansion protocol.

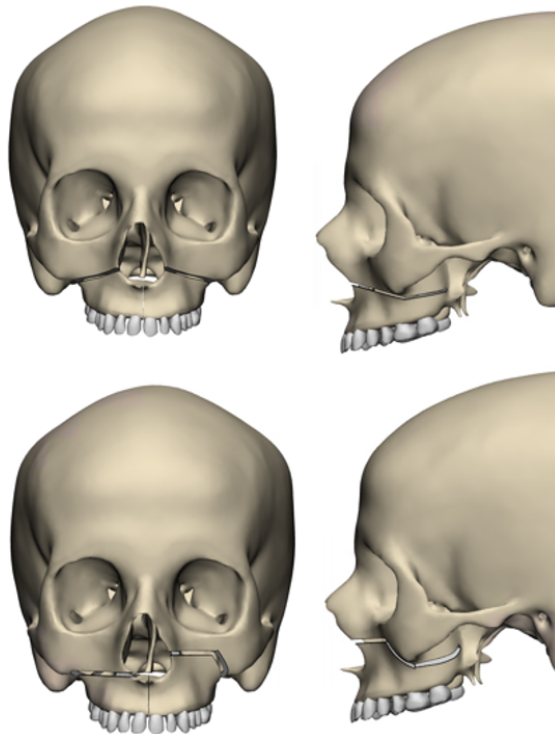


**Figure 5.5:** Symmetric (top) and asymmetric (bottom) lateral osteotomies

### 5.2.2 Results displacement

The results of the alveolar bone at both sides are reported in Tables 5.7, 5.8 and Table 5.9, as well as in Figure 5.6. As can be seen from these results, the overall expansion is quite similar between the two models. However, due to the asymmetry in the lateral osteotomy, an unbalance is created in the amount of expansion on each side. When performing the asymmetric osteotomy, the expansion at the left side is reduced, whereas on the right side it is increased. This is the case at all landmarks of the alveolar bone.

When the asymmetric lateral osteotomy is performed, the anterior and transversal displacement of the alveolar bone show asymmetric behavior. The anterior displacements are generally smaller with the asymmetric model. For the transversal direction, the total amount of displacement is almost equal in two models. The amount of expansion on either side however is in unbalance: the average relative amount of expansion on the right side is around 52% for the symmetric case, whereas it is around 60% for the asymmetric model. This shows a large discrepancy between both models. In the superoinferior direction, both sides of the alveolar bone show a decrease in superior displacements when compared to the asymmetric model.

**Table 5.7:** Anterior displacements alveolar bone - Lateral osteotomy variation models

<b>Anterior displacement</b>	<b>Orientation</b>	<b>T1</b>	<b>T2</b>	<b>T3</b>	<b>T4</b>	<b>T5</b>	<b>T6</b>	<b>T7</b>
Symmetric lateral osteotomy [mm]	Left	1.02	0.84	0.68	0.60	0.53	0.46	0.34
	Right	1.03	0.82	0.66	0.57	0.47	0.44	0.32
Asymmetric lateral osteotomy [mm]	Left	0.83	0.69	0.55	0.49	0.43	0.37	0.29
	Right	1.19	0.94	0.75	0.65	0.53	0.49	0.36

**Table 5.8:** Transversal displacements alveolar bone - Lateral osteotomy variation models

<b>Transversal displacement</b>	<b>Orientation</b>	<b>T1</b>	<b>T2</b>	<b>T3</b>	<b>T4</b>	<b>T5</b>	<b>T6</b>	<b>T7</b>
Symmetric lateral osteotomy [mm]	Left	3.16	3.11	2.93	2.74	2.55	1.97	1.39
	Right	3.47	3.38	3.18	3.03	2.73	2.16	1.59
Asymmetric lateral osteotomy [mm]	Left	2.62	2.59	2.44	2.28	2.13	1.68	1.21
	Right	4.00	3.89	3.67	3.50	3.14	2.51	1.88

**Table 5.9:** Superior displacements alveolar bone - Lateral osteotomy variation models

Superior displacement	Orientation	T1	T2	T3	T4	T5	T6	T7
Symmetric lateral osteotomy [mm]	Left	1.02	0.84	0.68	0.60	0.53	0.46	0.34
	Right	1.03	0.82	0.66	0.57	0.47	0.44	0.32
Asymmetric lateral osteotomy [mm]	Left	-0.16	0.03	0.16	0.19	0.21	0.17	0.11
	Right	0.18	0.40	0.53	0.57	0.56	0.42	0.32

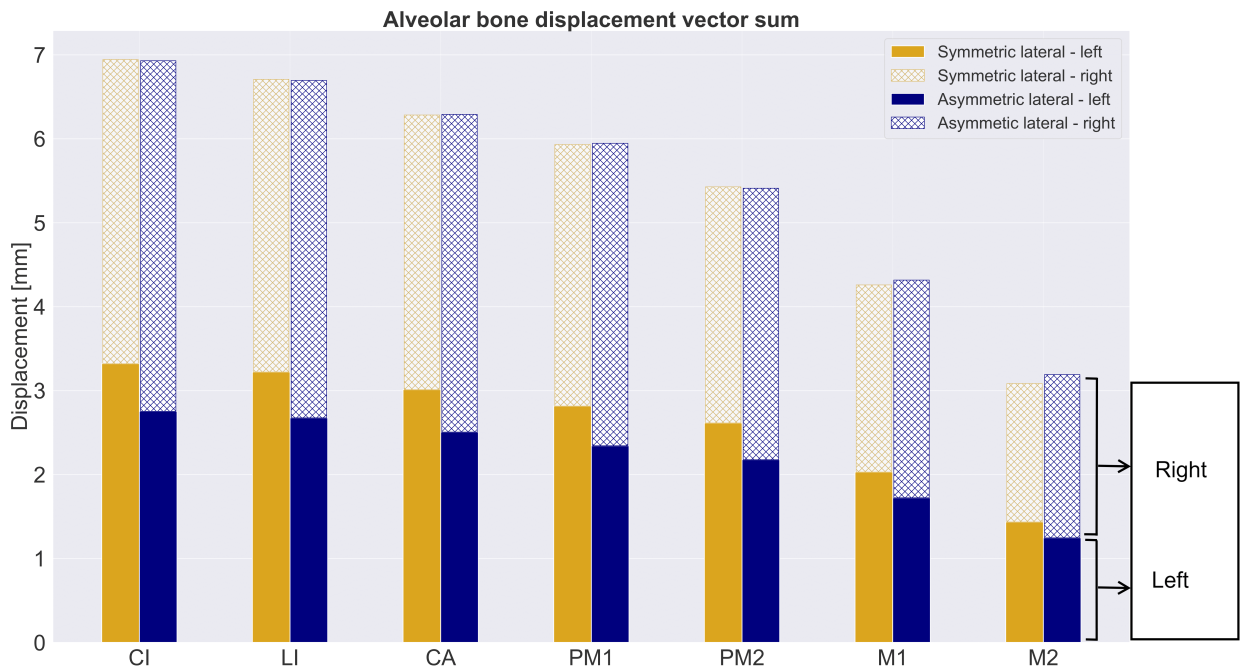


**Figure 5.6:** Comparison displacement alveolar bone - Lateral osteotomy variation models

With the asymmetric model, the lowest vertical tipping was found, with an opening angle of around  $5.4^\circ$ . The symmetric model has an opening angle of around  $6.1^\circ$ . The horizontal tipping showed worse behavior in the asymmetrical model: an opening angle of  $7.3^\circ$  was measured, whereas with the symmetrical model it is an opening angle of  $5.85^\circ$ .

### 5.2.3 Discussion displacement

According to Huizinga and al. [102], clinical relevant asymmetries were found in around 55% of the patients in at least one direction. This study considers asymmetries also to be non-parallel behavior, hence caution is required concerning the terminology used in these reports [102].

Only one study in literature describes the asymmetry between left and right maxillary segments in patients with a bone-borne distractor with PMD [102]. Some factors that could influence the asymmetric behavior are mentioned: there could be differences in the resistance of the surrounding soft tissues and alveolar bone, the placement of distractor on the axial axis could have an influence and the orientation of the distractor in the transversal plane might also play a role. As was discussed in Chapter 4, the symmetric placement of the TPD in the transversal plane is the most difficult for the maxillofacial surgeon, as a narrow and high palatal vault can make it difficult to align the device correctly. According to Huizinga and al. [102], transversal asymmetry may occur when the palatal expander is positioned obliquely in the frontal plane. In Chapter 4, only a small deviation of 2 mm was simulated, however more cases should be simulated to see if a more oblique positioning of the TPD indeed results in a more asymmetric expansion.

No clinical trials or finite element studies have yet been performed on asymmetric lateral osteotomies. Clinical asymmetrical expansions were observed in literature, however the direction, frequency and the magnitude of the asymmetry have not yet been quantified. In this way, no direct comparison with literature can be made.

When the lateral osteotomy is positioned more superiorly, the total amount of expansion remains the same. At the alveolar bone, a larger displacement was obtained at the side with the more posteriorly located lateral osteotomy. Since the maxilla is osteotomized at a more superior location, a larger part of the maxilla is osteotomized, resulting in a lowered resistance against the transversal expansion. As such, the displacement amplitudes will also increase at this side.

Numerous causes for the asymmetric expansion can be considered: the differential bone density at the sutures and their surrounding bones (not in the simulations), the stability of the TPD, the initial asymmetry of the craniofacial skeleton and the initial pattern of the crossbite. By eliminating some of these factors, clinicians and researchers can help in finding an answer to why some patients exhibit asymmetry, and how it can be possibly controlled (surgical procedure, TPD placement, see this research) or how it is influenced by other factors (initial asymmetry, bone density, further clinical research required). In this way, a more predictable procedure can be obtained [109].

### 5.2.4 Results stresses

The stress distribution is shown in Figure 5.7. As can be seen, large differences are observed between both models. A significant reduction of the stresses at the body of the maxilla are measured, where a reduction of 87% is noticed when compared to the symmetric model. For the other maxillofacial landmarks, smaller differences are observed.

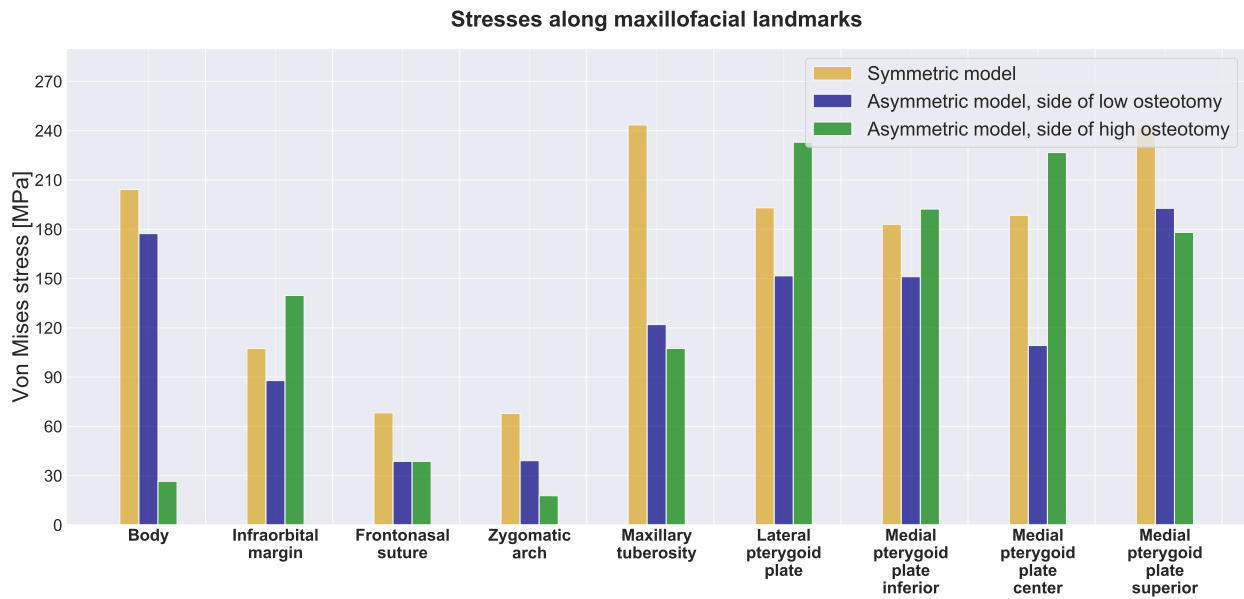


**Figure 5.7:** Stress distribution maxillofacial complex - Lateral asymmetric osteotomy

Slightly higher stress values are observed at the infraorbital margin whereas the zygomatic arch and the frontonasal suture show reduced stresses. The views of the lateral pterygoid plates on both sides are shown in Figure 5.8. Together with the results found in Figure 5.7, following is observed: the stresses at the pterygoid plates of the asymmetric model are generally higher than those observed at the low side osteotomy (and than the symmetric model). Especially at the lateral side of the pterygoid plates, high stress concentrations are observed for the asymmetric model with the most superior lateral osteotomy.

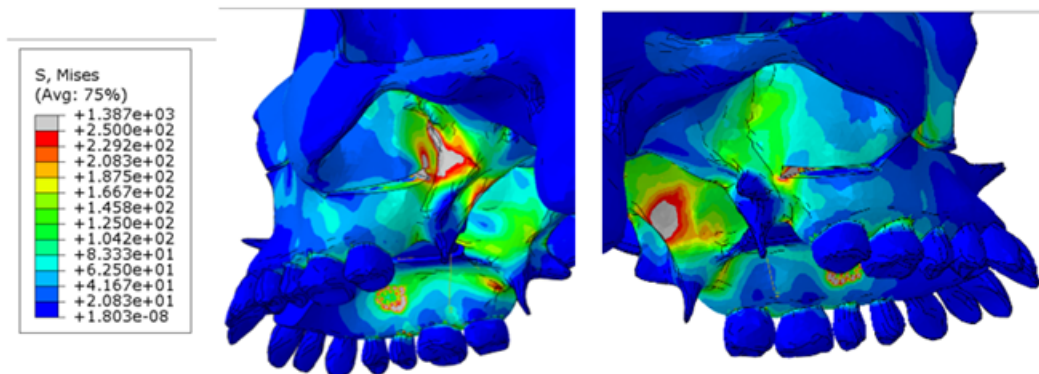


**Figure 5.8:** Stresses at the lateral pterygoid plates, left (superior lateral osteotomy) and right (inferior lateral osteotomy) side of the model

### 5.2.5 Discussion stresses

According to Möhlhenrich and al. [84], who investigated the influence of several osteotomies, the largest stress reduction is found when performing the lateral osteotomy. This indicates that the anterior piriform aperture pillars and the lateral zygomatic buttresses show the largest resistance against the transversal expansion. Hence, the lateral osteotomy is the most important to reduce stresses in the maxillofacial complex. One could argue that variations in this lateral osteotomy could also lead to significant changes in the stress distribution. The results obtained in the previous section also confirm this theory. The stresses found at the body of the maxilla were significantly reduced for the asymmetric model at the side of the superior osteotomy. As a larger part of the maxilla is disjuncted, the complete maxilla is mobilized more and hence lower stresses will occur at these landmarks. Due to the high mobility of the maxilla, the stresses are transferred to deeper anatomical regions, such as the pterygoid plates. This is also noticed in the results, where high stress concentrations are observed at most of the pterygoid plates. A recommendation is made to also separate the pterygoid plates if it is opted to perform a more superiorly lateral osteotomy. In this way the stresses at the pterygoid plates and the cranial Foramina are reduced, and possible fractures at the pterygoid plates are avoided. If the plate fracture is handled inappropriately, there is a risk of massive bleeding. When the pterygoid plate is damaged, an edema can be developed due to hemorrhage, which can lead to an airway obstruction. Damage to the cranial nerves can also occur. As the pterygoid plates provide the insertions for the lateral pterygoid muscles, limitations in mouth opening could occur as well [110]. This trade off should always be taken into account by the clinician. The interaction of the pterygoid plate disjunction together with the superior located lateral osteotomy is outside of the scope of this master dissertation and requires further research.

### 5.3 Conclusions

In this chapter, surgical variations of the SARPE procedure were analyzed, and the corresponding displacement profile and stress distributions were measured. Two possible factors that could influence the expansion profile were included in this research. First a uni- or bilaterally pterygoid disjunction was performed onto the models. Following conclusions are drawn concerning the presence of the PMD:

1. The general expansion profile remains unaltered by the presence of the pterygoid disjunction. No significant changes are observed when the PMD is performed: a similar expansion profile was obtained as in Chapter 4.
2. By performing the pterygoid disjunction, (posterior) resistance against the transversal expansion is removed. For an unilateral pterygoid disjunction, the transversal expansion at that side will increase. This effect is more noticeable in posterior regions of the alveolar bone. The effect of the unilateral pterygoid disjunction remains quite small, and may be clinically irrelevant. The amount of horizontal tipping is increased with the presence of the unilateral PMD.
3. By performing the pterygoid disjunction bilaterally, the amount of expansion is increased at the alveolar bone level. More resistance against the transversal expansion is removed and hence larger expansions are obtained for the same input. In accordance with several authors in literature, the amount of horizontal tipping was decreased by the disjunction of both the pterygoid plates. The measured values are small, and these differences may be clinically irrelevant. The vertical tipping was increased by the presence of the pterygoid disjunctions.
4. The PMD allows generally for a stress reduction in the maxillofacial complex of around 10% to 20%, depending on the exact location of the measurement. Similar stresses are measured at the alveolar bone for bone-borne devices. Hence, the PMD does not reduce the occurrence of gingival recession and root resorption. At other anatomical landmarks, the stresses are increased by the PMD, such as at the medial pterygoid plate, where the measurement was taken inferiorly. For any other measurement on the pterygoid plates, the stresses are also reduced.
5. Holberg and al. [107] showed that the PMD allows for significantly reduced stresses at the Foramina of the cranial base. As the possibility of fractures needs to be diminished as much as possible around these Foramina (as they guide nerves and important arteries), the PMD is advised by Holberg to lower the stresses in these areas. Similar results as Holberg were found in this study, albeit with smaller values when compared to Holberg [107].

6. In literature, mostly the combined effect of placing the TPD at the first molar and the presence of the PMD is compared to cases where no PMD is performed and the TPD is installed at the second premolar. The effects are not measured separately in these studies, making it difficult to draw clear conclusions about the effect of each factor separately. This complicates the validation of the obtained results, making further clinical research necessary.

For the simulations regarding the variations in superoinferior location of the lateral osteotomy, following conclusions are drawn:

1. The more superiorly located osteotomy allows for a larger displacement on that side, but the total transversal expansion remains the same. For the symmetric case, around 52% of the transversal expansion was measured on the right alveolar bone side, whereas around 60% was observed for the asymmetrical model. Lower vertical tipping was observed, but higher horizontal tipping of the maxillary halves.
2. With the more superior osteotomy, the stresses at the lateral pterygoid plates and the medial pterygoid plates (centrally measured) increased. The stresses in the body of the maxilla, zygomatic arch and frontonasal suture decreased. As more of the maxillary body is mobilized, these anatomical regions will not be able to resist the transversal motion and hence lower stresses are occurring.
3. The superoinferior placement of the lateral osteotomy has a significant influence on the stress distribution. Care should be taken for the pterygoid plates, as an increased stress distribution is observed at the lateral pterygoid plates. An additional PMD is suggested based on these results, to locally reduce the stress concentrations. This interaction however was not investigated and hence, this remains a hypothesis which still needs to be verified with other simulations.
4. Clinical relevant asymmetries are found in a lot of patients, but not a lot of research has been conducted yet on this topic. As the influence of these higher positioned lateral osteotomies has not yet been evaluated in clinical trials or experimental research, no verification with literature can be made. Further research is required.

Based on the results presented in this chapter, several conclusions can be drawn. More importantly, the need for more research is shown as well, indicating there are still a lot of unknown influencing factors or interactions between multiple variables of the SARPE procedure. These interactions are outside of the scope of this research.



# Chapter 6 | General conclusion and future work

As was indicated in the literature review of this dissertation, there is a lot of uncertainty among clinicians and researchers concerning the optimal surgical procedure, the expansion profile, the influence of the expander type and the optimal location of the device of the SARPE procedure. Due to the complexity of the stomatognathic system and the inability to perform in vivo research, the medical world has embraced the use of finite element analyses. In this master thesis, specific parameters of the SARPE procedure were varied and the influence it has on the expansion profile and stress distribution was analyzed. The influence of the palatal expander location and variations in the surgical procedure were measured on a finite element model of the cranium.

In a first set of simulations, the influence of the palatal expander location was measured, as was discussed in Chapter 4. In this chapter, the finite element model was compared to clinical studies and contemporary literature. Extensive verification and validation of the finite element model was performed, and a lot of confidence was gained in the model. In this way, the model can be used to perform further research with. Independent of the palatal expander position, the general displacement profile indicates a superiorly, laterally and anteriorly movement of the maxilla. The palatal expander position influences the expansion profile, as with more posteriorly positioned expanders, a lower degree of horizontal tipping is observed. Depending on the patient specific malocclusion or transverse deficiency, the optimal expander location will also change. Moving the expander more posteriorly results in a more parallel expansion (less V-shaped), indicating lower horizontal tipping. The vertical tipping behavior is increased with this more posterior positioning, however only small differences are occurring. The effect is rather small and could be attributed to other effects, such as the potentially more superior positioning of the expander. The simulations also revealed that small deviations during the positioning of the expander in the superoinferior direction did not significantly change the expansion profile. With a more inferior positioning on one side of the alveolar bone, only the superoinferior displacements change. This difference is rather small (with a

2 mm deviation, only 0.1 mm difference in superior deviation is observed) and hence it is clinically irrelevant. Maxillofacial surgeons should try to position the implant as symmetrical as possible, however small deviations do not have a large influence on the displacement profile.

In a second set of simulations, variations in the surgical procedure are analyzed. The results and discussion can be found in Chapter 5. As was indicated in the literature review, the pterygomaxillary disjunction remains a controversial topic in literature. Performing the disjunction can result in fractures at the base of the skull, resulting in blindness or trauma. The exact influence of the osteotomy also remains unknown. The results in this chapter showed that the PMD did not significantly alter the general expansion profile of the maxilla. The PMD removes posterior resistance against the transversal expansion, and with a similar input (5 mm displacement at the level of the second premolar) larger displacements are occurring at the side where the PMD is performed. The main rationale to perform the PMD is to increase the parallelism of the expansion in the axial plane. This study also indicated that with the presence of the PMD, lower horizontal tipping values are occurring. However, the vertical tipping behavior is increased by the PMD. Generally speaking, the PMD allows for reduced stresses of around 15%. At the cranial Foramina, the reductions are slightly larger, with reductions of around 35% at the Optical Foramen. This decreases the risk of fractures at these Foramina and increases the stability of the procedure.

Furthermore, the influence of an asymmetrical positioned lateral osteotomy was analyzed. Asymmetric expansions are often present in patients, however no control of this type of behavior is available. Quantifying the direction, magnitude and occurrence of this asymmetric expansion behavior could aid in modifying certain aspects of the surgical procedure to obtain improved outcome and stability. By performing simulations on a model with on the one side the most superior, on the other side the most inferior placement of the lateral osteotomy, active control of this asymmetric expansion was observed. By moving the lateral osteotomy more superiorly, the displacements at that side are increased (but the same overall expansion was observed). For the symmetric case (lateral osteotomies at same superoinferior level), around 52% of the expansion was measured on the right side of the alveolar bone. When the osteotomy was moved more superiorly, the relative amount of expansion on this side increased to around 60%. The stress distribution changes significantly by moving the osteotomy superiorly: the stresses at the body of the maxilla, the zygomatic arch and frontonasal suture decreased. The stresses at the lateral pterygoid plates increased, and a PMD is advised based on these results. Possible interacting factors are not considered, and further research is required to correctly evaluate the interaction of these parameters.

Next to these conclusions, several opportunities to improve this finite element model were also revealed. A first recommendation is to perform more experimental research on the (mechanical) material properties of the maxilla. With more accurate material properties, a higher accuracy of the simulations can be obtained. Viscoelasticity could also be added to the model. This would allow to perform time dependent simulations. In this way, the ideal consolidation period, the ideal amount of expansion per day and the relaxation of the stresses throughout the cranium could be simulated. The procedure could be simulated more in detail and more realistic results could be obtained. Inclusion of the soft tissues could also allow for more realistic results, as these soft tissues influence the resistance against the transversal expansion, which could significantly alter the (a)symmetry of the expansion. These opportunities could be expanded upon in further research to increase the accuracy of the simulation.

The current finite element model could also be used to perform further research on: the possible interactions between the variations in palatal expander location and surgical variations could be analyzed. In further research, the influence of the expander type on the expansion could be evaluated as well. As multiple parameters are varied simultaneously, different interactions between parameters could amplify or reduce the effect of certain parameters.

As a lot of uncertainty remains, more research is required and still a lot of improvements are possible. In this research, a focus was put on the expansion profile of the maxilla, however, the SARPE procedure has multiple facets. The amount of complications, the stability and invasiveness of the procedure are not investigated in much detail during this research. This shows the complexity of the procedure, and the need for more research on these other aspects as well.



# Bibliography

- [1] R. Nowak, A. Strzałkowska, and E. Zawisłak, “Treatment options and limitations in transverse maxillary deficiency,” *Dental and Medical Problems*, vol. 52, no. 4, p. 389–400, 2015.
- [2] *Innovative perspectives in oral and maxillofacial surgery*. Springer Nature, 2021.
- [3] M. C. D. Andrucioi and M. A. N. Matsumoto, “Transverse maxillary deficiency: treatment alternatives in face of early skeletal maturation,” *Dental Press Journal of Orthodontics*, vol. 25, no. 1, p. 70–79, 2020.
- [4] K. Jha and M. Adhikari, “Surgically assisted rapid palatal expansion for transverse maxillary discrepancy in adults - case report,” *International Journal of Surgery Case Reports*, vol. 90, p. 106687, 2022.
- [5] K. Manzella, L. Franchi, and T. Al-Jewair, “Correction of maxillary transverse deficiency in growing patients with permanent dentitions,” *Journal of clinical orthodontics : JCO*, vol. 52, pp. 148–156, 03 2018.
- [6] Philippe, “Palatal expansion (rapid maxillary expansion): Bücco,” Sep 2019. [Online]. Available: <https://www.orthodontisteenligne.com/en/palatal-expansion-rapid-maxillary-expansion/>
- [7] “Medical definition of suture,” Mar 2021. [Online]. Available: <https://www.medicinenet.com/suture/definition.htm>
- [8] “Bones of the skull.” [Online]. Available: <https://teachmeanatomy.info/head/osteology/skull/>
- [9] “What is rapid maxillary expansion treatment?” Aug 2021. [Online]. Available: <https://orthodonticsaustralia.org.au/rapid-maxillary-expansion-treatment/>
- [10] A. Agarwal, “Maxillary expansion,” *International Journal of Clinical Pediatric Dentistry*, vol. 3, no. 3, p. 139–146, 2010.

- 
- [11] V. Shetty, J. Caridad, A. A. Caputo, and S. J. Chaconas, "Biomechanical rationale for surgical-orthodontic expansion of the adult maxilla," *Journal of Oral and Maxillofacial Surgery*, vol. 52, no. 7, p. 742–749, 1994.
- [12] M. Koudstaal, L. Poort, K. V. D. Wal, E. Wolvius, B. Prahl-Andersen, and A. Schulten, "Surgically assisted rapid maxillary expansion (sarme): a review of the literature," *International Journal of Oral and Maxillofacial Surgery*, vol. 34, no. 7, p. 709–714, 2005.
- [13] S. Bartlett, M. Ehrenfeld, G. Mast, and A. Sugar, "Surgically assisted rapid palatal expansion." [Online]. Available: <https://surgeryreference.aofoundation.org/cmef/orthognathic/maxilla/maxilla-transverse-hypoplasia-of-maxilla/surgically-assisted-rapid-palatal-expansion#osteotomy>
- [14] S. Shyam Sundar, B. Nandlal, D. Saikrishna, and G. Mallesh, "Finite element analysis: A maxillofacial surgeon's perspective," *Journal of Maxillofacial and Oral Surgery*, vol. 11, no. 2, p. 206–211, 2011.
- [15] D. Bignotti, A. Gracco, G. Bruno, and A. D. Stefani, "Fem in orthodontics: a review of the palatal expander clinical investigation," *ORAL amp; Implantology*, p. 161–167, Feb 2019.
- [16] "1.4d: Body planes and sections," Aug 2020. [Online]. Available: <https://med.libretexts.org/>
- [17] R. Bailey, "Anatomical directional terms and body planes," Aug 2020. [Online]. Available: <https://www.thoughtco.com/anatomical-directional-terms-and-body-planes-373204>
- [18] H. Gray, *Gray's anatomy*, 41st ed. Medina University Press International, 2020.
- [19] N. S. Norton and F. H. Netter, *Netters head and neck anatomy for dentistry*. Elsevier., 2017.
- [20] D. A. Samra and R. Hadad, "Midpalatal suture: evaluation of the morphological maturation stages via bone density," *Progress in Orthodontics*, vol. 19, no. 1, 2018.
- [21] B. S. Knapp, By:., and S. Knapp, "Sphenoid bone - the definitive guide," Aug 2020. [Online]. Available: <https://biologydictionary.net/sphenoid-bone/#body-of-the-sphenoid-bone>
- [22] "The sphenoid bone." [Online]. Available: <https://teachmeanatomy.info/head/osteology/sphenoid-bone/>
- [23] *Atlas of operative oral and maxillofacial surgery*. WILEY-BLACKWELL, 2015.

- 
- [24] K. F. Linnau, R. B. Stanley, D. K. Hallam, J. A. Gross, and F. Mann, "Imaging of high-energy midfacial trauma: What the surgeon needs to know," *European Journal of Radiology*, vol. 48, no. 1, p. 17–32, 2003.
- [25] S. Celin, *Fractures of the upper facial and midfacial skeleton*, ser. Myers EN ed., Operative Otolaryngology Head and Neck Surgery. WB Saunders Company, 1997.
- [26] "Tooth." [Online]. Available: <https://www.britannica.com/science/tooth-anatomy>
- [27] T. W. Oates and D. L. Cochran, "Dental applications of bone biology," *Topics in Bone Biology*, p. 129–140.
- [28] O. Team, "Bone matrix." [Online]. Available: <https://www.orthobullets.com/basic-science/9003/bone-matrix>
- [29] W. Murphy, J. Black, and G. W. Hastings, *Handbook of Biomaterial Properties*. Springer, 2016.
- [30] "Bone morphology." [Online]. Available: <https://www.britannica.com/science/bone-anatomy/Bone-morphology>
- [31] G. Osterhoff, E. F. Morgan, S. J. Shefelbine, L. Karim, L. M. McNamara, and P. Augat, "Bone mechanical properties and changes with osteoporosis," *Injury*, vol. 47, 2016.
- [32] J. Peterson, Q. Wang, and P. C. Dechow, "Material properties of the dentate maxilla," *The Anatomical Record Part A: Discoveries in Molecular, Cellular, and Evolutionary Biology*, vol. 288A, no. 9, p. 962–972, 2006.
- [33] B. Melsen, "Palatal growth studied on human autopsy material," *American Journal of Orthodontics*, vol. 68, no. 1, p. 42–54, 1975.
- [34] F. Angelieri, L. H. Cevidanes, L. Franchi, J. R. Gonçalves, E. Benavides, and J. A. M. Jr, "Midpalatal suture maturation: Classification method for individual assessment before rapid maxillary expansion," *American Journal of Orthodontics and Dentofacial Orthopedics*, vol. 144, no. 5, p. 759–769, 2013.
- [35] F. Angelieri, L. Franchi, L. Cevidanes, J. Gonçalves, M. Nieri, L. Wolford, and J. McNamara, "Cone beam computed tomography evaluation of midpalatal suture maturation in adults," *International Journal of Oral and Maxillofacial Surgery*, vol. 46, no. 12, p. 1557–1561, 2017.

- 
- [36] L. Suri and P. Taneja, "Surgically assisted rapid palatal expansion: A literature review," *American Journal of Orthodontics and Dentofacial Orthopedics*, vol. 133, no. 2, p. 290–302, 2008.
- [37] H. Korbmacher, A. Schilling, K. Püschel, M. Amling, and B. Kahl-Nieke, "Age-dependent three-dimensional microcomputed tomography analysis of the human midpalatal suture\*," *Journal of Orofacial Orthopedics / Fortschritte der Kieferorthopädie*, vol. 68, no. 5, p. 364–376, 2007.
- [38] M. C. Andrucoli and M. A. Matsumoto, "Transverse maxillary deficiency: Treatment alternatives in face of early skeletal maturation," *Dental Press Journal of Orthodontics*, vol. 25, no. 1, p. 70–79, 2020.
- [39] D. S. F. R. D. Assis, T. A. Xavier, P. Y. Noritomi, and E. S. Gonçalves, "Finite element analysis of bone stress after sarpe," *Journal of Oral and Maxillofacial Surgery*, vol. 72, no. 1, 2014.
- [40] S. Menon, R. Manerikar, and R. Sinha, "Surgical management of transverse maxillary deficiency in adults," *Journal of Maxillofacial and Oral Surgery*, vol. 9, no. 3, p. 241–246, 2010.
- [41] A. Kapetanović, C. I. Theodorou, S. J. Bergé, J. G. Schols, and T. Xi, "Efficacy of miniscrew-assisted rapid palatal expansion (marpe) in late adolescents and adults: A systematic review and meta-analysis," *European Journal of Orthodontics*, vol. 43, no. 3, p. 313–323, 2021.
- [42] J. Y. Jeon, S.-H. Choi, C. J. Chung, and K.-J. Lee, "The success and effectiveness of miniscrew-assisted rapid palatal expansion are age- and sex-dependent," *Clinical Oral Investigations*, 2021.
- [43] C. Marchetti, M. Pironi, A. Bianchi, and A. Musci, "Surgically assisted rapid palatal expansion vs. segmental le fort i osteotomy: Transverse stability over a 2-year period," *Journal of Cranio-Maxillofacial Surgery*, vol. 37, no. 2, p. 74–78, 2009.
- [44] A. Y. Saga, O. M. Antelo, C. M. de Araujo, I. T. Maruo, and O. M. Tanaka, "Sarpe treatment of a class iii malocclusion with maxillary transverse deficiency, short roots, gingival recession, and alveolar bone loss: Long-term stability," *AJO-DO Clinical Companion*, 2022.
- [45] S. Brody-Camp and R. Winters, *Craniofacial Distraction Osteogenesis*. StatPearls Publishing, 2022.

- [46] T. Starch-Jensen and T. L. Blæhr, “Transverse expansion and stability after segmental le fort i osteotomy versus surgically assisted rapid maxillary expansion: A systematic review,” *Journal of Oral and Maxillofacial Research*, vol. 7, no. 4, 2016.
- [47] S. Bartlett, M. Ehrenfeld, G. Mast, and A. Sugar, “Planning of orthognathic surgery.” [Online]. Available: <https://surgeryreference.aofoundation.org/cmf/orthognathic/further-reading/planning-of-orthognathic-surgery#3d-virtual-planning>
- [48] “Chapter 9 - orthognathic surgery,” in *Clinical Review of Oral and Maxillofacial Surgery (Second Edition)*, second edition ed., S. C. Bagheri, Ed. St. Louis (MO): Mosby, 2014, pp. 293–332. [Online]. Available: <https://www.sciencedirect.com/science/article/pii/B9780323171267000091>
- [49] A. Sygouros, M. Motro, F. Ugurlu, and A. Acar, “Surgically assisted rapid maxillary expansion: Cone-beam computed tomography evaluation of different surgical techniques and their effects on the maxillary dentoskeletal complex,” *American Journal of Orthodontics and Dentofacial Orthopedics*, vol. 146, no. 6, p. 748–757, 2014.
- [50] S. Chamberland and W. R. Proffit, “Closer look at the stability of surgically assisted rapid palatal expansion,” *Journal of Oral and Maxillofacial Surgery*, vol. 66, no. 9, p. 1895–1900, 2008.
- [51] M. Muñoz-Pereira, O. Haas-Junior, L. Da Silva Meirelles, A. Machado-Fernández, R. Guijarro-Martínez, F. Hernández-Alfaro, R. de Oliveira, and R. Pagnoncelli, “Stability and surgical complications of tooth-borne and bone-borne appliances in surgical assisted rapid maxillary expansion: A systematic review,” *British Journal of Oral and Maxillofacial Surgery*, vol. 59, no. 2, 2021.
- [52] S. Chamberland and W. R. Proffit, “Short-term and long-term stability of surgically assisted rapid palatal expansion revisited,” *American Journal of Orthodontics and Dentofacial Orthopedics*, vol. 139, no. 6, 2011.
- [53] “transpalatal distractor. a bone-borne modular distraction device for surgically assisted, rapid, palatal expansion.”
- [54] “Hyrax,” Mar 2018. [Online]. Available: <https://www.johnsdental.com/lateral-expansion/hyrax/>
- [55] M. Koudstaal, E. Wolvius, A. Schulten, W. Hop, and K. van der Wal, “Stability, tipping and relapse of bone-borne versus tooth-borne surgically assisted rapid maxillary expansion; a prospective randomized patient trial,” *International Journal of Oral and Maxillofacial Surgery*, vol. 38, no. 4, p. 308–315, 2009.

- 
- [56] M. Krüsi, T. Eliades, and S. N. Papageorgiou, “Are there benefits from using bone-borne maxillary expansion instead of tooth-borne maxillary expansion? a systematic review with meta-analysis,” *Progress in Orthodontics*, vol. 20, no. 1, 2019.
- [57] M. Mommaerts, “Transpalatal distraction as a method of maxillary expansion,” *British Journal of Oral and Maxillofacial Surgery*, vol. 37, no. 4, p. 268–272, 1999.
- [58] V. P. Curvêllo, F. P. Valarelli, L. N. Pegoraro, R. H. Cançado, and T. M. Oliveira, “The use of bone-borne distractor for correcting the maxillary transverse discrepancy in an adult patient,” *Iranian Journal of Orthodontics*, vol. In Press, no. In Press, 2016.
- [59] F. Kunz, C. Linz, G. Baunach, H. Böhm, and P. Meyer-Marcotty, “Expansion patterns in surgically assisted rapid maxillary expansion,” *Journal of Orofacial Orthopedics / Fortschritte der Kieferorthopädie*, vol. 77, no. 5, p. 357–365, 2016.
- [60] M. Smeets, O. Da Costa Senior, S. Eman, and C. Politis, “A retrospective analysis of the complication rate after sarpe in 111 cases, and its relationship to patient age at surgery,” *Journal of Cranio-Maxillofacial Surgery*, vol. 48, no. 5, p. 467–471, 2020.
- [61] G. Dergin, S. Aktop, A. Varol, F. Ugurlu, and H. Garip, “Complications related to surgically assisted rapid palatal expansion,” *Oral Surgery, Oral Medicine, Oral Pathology and Oral Radiology*, vol. 119, no. 6, p. 601–607, 2015.
- [62] S. Braun, J. Bottrel, K.-G. Lee, J. J. Lunazzi, and H. L. Legan, “The biomechanics of rapid maxillary sutural expansion,” *American Journal of Orthodontics and Dentofacial Orthopedics*, vol. 118, no. 3, p. 257–261, 2000.
- [63] F. Jiang, K. Kula, and J. Chen, “Estimating the location of the center of resistance of canines,” *The Angle Orthodontist*, vol. 86, no. 3, p. 365–371, 2015.
- [64] C. Matteini and M. Y. Mommaerts, “Posterior transpalatal distraction with pterygoid disjunction: A short-term model study,” *American Journal of Orthodontics and Dentofacial Orthopedics*, vol. 120, no. 5, p. 498–502, 2001.
- [65] C.-H. Chung, “Dental tipping and rotation immediately after surgically assisted rapid palatal expansion,” *The European Journal of Orthodontics*, vol. 25, no. 4, p. 353–358, 2003.
- [66] F. K. Byloff, “Skeletal and dental changes following surgically assisted rapid palatal expansion,” *The European Journal of Orthodontics*, vol. 26, no. 4, p. 403–409, 2004.

- [67] A. Anttila, “Feasibility and long-term stability of surgically assisted rapid maxillary expansion with lateral osteotomy,” *The European Journal of Orthodontics*, vol. 26, no. 4, p. 391–395, 2004.
- [68] J. L. Berger, V. Pangrazio-Kulbersh, T. Borgula, and R. Kaczynski, “Stability of orthopedic and surgically assisted rapid palatal expansion over time,” *American Journal of Orthodontics and Dentofacial Orthopedics*, vol. 114, no. 6, p. 638–645, 1998.
- [69] R. A. Bays and J. M. Greco, “Surgically assisted rapid palatal expansion: An outpatient technique with long-term stability,” *Journal of Oral and Maxillofacial Surgery*, vol. 50, no. 2, p. 110–113, 1992.
- [70] C.-H. Chung, “Dental tipping and rotation immediately after surgically assisted rapid palatal expansion,” *The European Journal of Orthodontics*, vol. 25, no. 4, p. 353–358, 2003.
- [71] N. Sharma, A. Ray, K. Shukla, S. Sharma, S. Pradhan, A. Srivastva, and L. Aggarwal, “Automated medical image segmentation techniques,” *Journal of Medical Physics*, vol. 35, no. 1, p. 3, 2010.
- [72] Unknown, “Cone-beam ct.” [Online]. Available: <https://www.azsintjan.be/nl/diensten/radiologie/campus-sint-jan/onderzoeken/cone-beam-ct>
- [73] J. Li, M. Erdt, F. Janoos, T.-c. Chang, and J. Egger, “Medical image segmentation in oral-maxillofacial surgery,” *Computer-Aided Oral and Maxillofacial Surgery*, p. 1–27, 2021.
- [74] “What are hounsfield units (hu)?” [Online]. Available: <https://www.materialise.com/>
- [75] G. Swennen, *3D virtual treatment planning of orthognathic surgery a step-by-step approach for orthodontists and surgeons*. Springer Berlin, 2018.
- [76] J. J.-C. Kuo, “Validating the 3d and 2d mandibular plane to the frankfort plane for craniofacial measurement,” *Taiwanese Journal of Orthodontics*, vol. 31, no. 3, p. 142–152, 2019.
- [77] “A three-dimensional cephalometric analysis.”
- [78] E. Zawiślak, A. Olejnik, R. Fraczak, and R. Nowak, “Impact of osteotomy in surgically assisted rapid maxillary expansion using tooth-borne appliance on the formation of stresses and displacement patterns in the facial skeleton—a study using finite element analysis (fea),” *Applied Sciences*, vol. 10, no. 22, p. 8261, 2020.

- [79] R. Nowak, A. Olejnik, H. Gerber, R. Fratzczak, and E. Zawisłak, “Comparison of tooth- and bone-borne appliances on the stress distributions and displacement patterns in the facial skeleton in surgically assisted rapid maxillary expansion—a finite element analysis (fea) study,” *Materials*, vol. 14, no. 5, p. 1152, 2021.
- [80] S. C. Lee, J. H. Park, M. Bayome, K. B. Kim, E. A. Araujo, and Y.-A. Kook, “Effect of bone-borne rapid maxillary expanders with and without surgical assistance on the craniofacial structures using finite element analysis,” *American Journal of Orthodontics and Dentofacial Orthopedics*, vol. 145, no. 5, p. 638–648, 2014.
- [81] Y.-R. Zhang, W. Du, X.-D. Zhou, and H.-Y. Yu, “Review of research on the mechanical properties of the human tooth,” *International Journal of Oral Science*, vol. 6, no. 2, p. 61–69, 2014.
- [82] P. Gautam, A. Valiathan, and R. Adhikari, “Stress and displacement patterns in the craniofacial skeleton with rapid maxillary expansion: A finite element method study,” *American Journal of Orthodontics and Dentofacial Orthopedics*, vol. 132, no. 1, 2007.
- [83] K. Srinivas, “Abaqus - tips and tricks vol 1 - finite element analysis fea consulting services: Hyperelastic thermoplastics rubber composite material fatigue testing laboratory,” Dec 2017. [Online]. Available: <https://advances.com/abaqus-tips-and-tricks-vol-1/>
- [84] S. Möhlhenrich, A. Modabber, K. Kniha, F. Peters, T. Steiner, F. Hölzle, U. Fritz, and S. Raith, “Simulation of three surgical techniques combined with two different bone-borne forces for surgically assisted rapid palatal expansion of the maxillofacial complex: A finite element analysis,” *International Journal of Oral and Maxillofacial Surgery*, vol. 46, no. 10, p. 1306–1314, 2017.
- [85] “What is von mises stress in fea?: Simwiki,” Sep 2021. [Online]. Available: <https://www.simscale.com/docs/simwiki/fea-finite-element-analysis/what-is-von-mises-stress/>
- [86] W. Biederman, “Rapid correction of class iii malocclusion by midpalatal expansion,” *American Journal of Orthodontics*, vol. 63, no. 1, p. 47–55, 1973.
- [87] C. A. Landes, K. Laudemann, F. Schübel, O. Petruchin, M. Mack, S. Kopp, and R. A. Sader, “Comparison of tooth- and bone-borne devices in surgically assisted rapid maxillary expansion by three-dimensional computed tomography monitoring,” *Journal of Craniofacial Surgery*, vol. 20, no. 4, p. 1132–1141, 2009.
- [88] R. A. Wertz, “Skeletal and dental changes accompanying rapid midpalatal suture opening,” *American Journal of Orthodontics*, vol. 58, no. 1, p. 41–66, 1970.

- 
- [89] M. Zandi, A. Miresmaeili, and A. Heidari, “Short-term skeletal and dental changes following bone-borne versus tooth-borne surgically assisted rapid maxillary expansion: A randomized clinical trial study,” *Journal of Cranio-Maxillofacial Surgery*, vol. 42, no. 7, p. 1190–1195, 2014.
- [90] P. X. Pinto, M. Y. Mommaerts, G. Wreakes, and W. V. Jacobs, “Immediate postexpansion changes following the use of the transpalatal distractor,” *Journal of Oral and Maxillofacial Surgery*, vol. 59, no. 9, p. 994–1000, 2001.
- [91] M. J. Mirzaali, J. J. Schwiedrzik, S. Thaiwichai, J. P. Best, J. Michler, P. K. Zysset, and U. Wolfram, “Mechanical properties of cortical bone and their relationships with age, gender, composition and microindentation properties in the elderly,” *Bone*, vol. 93, p. 196–211, 2016.
- [92] D. Roylance, *Engineering Viscoelasticity*. MIT, 2001.
- [93] D. Deligianni, A. Maris, and Y. Missirlis, “Stress relaxation behaviour of trabecular bone specimens,” *Journal of Biomechanics*, vol. 27, no. 12, p. 1469–1476, 1994.
- [94] R. D. Edgar I., A. H. José J., R. C. Osvaldo, J. A. Victor H., and O. P. Armando, “Viscoelastic characterization of bovine trabecular bone samples,” *International Journal of Mechanical and Mechatronics Engineering*, vol. 9, no. 5, 2015.
- [95] U. Wolfram and J. Schwiedrzik, “Post-yield and failure properties of cortical bone,” *BoneKEy Reports*, vol. 5, 2016.
- [96] J. Schwiedrzik, R. Raghavan, A. Bürki, V. LeNader, U. Wolfram, J. Michler, and P. Zysset, “In situ micropillar compression reveals superior strength and ductility but an absence of damage in lamellar bone,” *Nature Materials*, vol. 13, no. 7, p. 740–747, 2014.
- [97] N. Rodriguez-Florez, M. L. Oyen, and S. J. Shefelbine, “Insight into differences in nanoindentation properties of bone,” *Journal of the Mechanical Behavior of Biomedical Materials*, vol. 18, p. 90–99, 2013.
- [98] Rodríguez-Navarro and F. Gonzalez-Valverde, “Unilateral blindness after orthognathic surgery: Hypotensive anaesthesia is not the primary cause,” *International Journal of Oral and Maxillofacial Surgery*, vol. 47, no. 1, p. 79–82, 2018.
- [99] U. A. Han, Y. Kim, and J. U. Park, “Three-dimensional finite element analysis of stress distribution and displacement of the maxilla following surgically assisted rapid maxillary expansion,” *Journal of Cranio-Maxillofacial Surgery*, vol. 37, no. 3, p. 145–154, 2009.

- 
- [100] G. Ramieri, M. Spada, M. Austa, S. Bianchi, and S. Berrone, "Transverse maxillary distraction with a bone-anchored appliance: Dento-periodontal effects and clinical and radiological results," *International Journal of Oral and Maxillofacial Surgery*, vol. 34, no. 4, p. 357–363, 2005.
- [101] R. M. Nada, P. S. Fudalej, T. J. Maal, S. J. Bergé, Y. A. Mostafa, and A. M. Kuijpers-Jagtman, "Three-dimensional prospective evaluation of tooth-borne and bone-borne surgically assisted rapid maxillary expansion," *Journal of Cranio-Maxillofacial Surgery*, vol. 40, no. 8, p. 757–762, 2012.
- [102] M. P. Huizinga, J. W. Meulstee, P. U. Dijkstra, R. H. Schepers, and J. Jansma, "Bone-borne surgically assisted rapid maxillary expansion: A retrospective three-dimensional evaluation of the asymmetry in expansion," *Journal of Cranio-Maxillofacial Surgery*, vol. 46, no. 8, p. 1329–1335, 2018.
- [103] B. C. do Egito Vasconcelos, A. F. Caubi, E. Dias, C. A. Lago, and G. G. Porto, "Surgically assisted rapid maxillary expansion: A preliminary study," *Brazilian Journal of Otorhinolaryngology*, vol. 72, no. 4, p. 457–461, 2006.
- [104] J. Verstraaten, A. M. Kuijpers-Jagtman, M. Y. Mommaerts, S. J. Bergé, R. M. Nada, and J. G. Schols, "A systematic review of the effects of bone-borne surgical assisted rapid maxillary expansion," *Journal of Cranio-Maxillofacial Surgery*, vol. 38, no. 3, p. 166–174, 2010.
- [105] S. Möhlhenrich, K. Ernst, F. Peters, K. Kniha, S. Chhatwani, A. Prescher, G. Danesh, F. Hölzle, and A. Modabber, "Immediate dental and skeletal influence of distractor position on surgically assisted rapid palatal expansion with or without pterygomaxillary disjunction," *International Journal of Oral and Maxillofacial Surgery*, vol. 50, no. 5, p. 649–656, 2021.
- [106] K. Laudemann, O. Petrushin, M. G. Mack, S. Kopp, R. Sader, and C. A. Landes, "Evaluation of surgically assisted rapid maxillary expansion with or without pterygomaxillary disjunction based upon preoperative and post-expansion 3d computed tomography data," *Oral and Maxillofacial Surgery*, vol. 13, no. 3, p. 159–169, 2009.
- [107] C. Holberg, S. Steinhäuser, and I. Rudzki, "Surgically assisted rapid maxillary expansion: Midfacial and cranial stress distribution," *American Journal of Orthodontics and Dentofacial Orthopedics*, vol. 132, no. 6, p. 776–782, 2007.
- [108] M. Dalband, J. Kashani, and H. Hashemzahi, "Three-dimensional finite element analysis of stress distribution and displacement of the maxilla following surgically assisted rapid maxillary expansion with tooth- and bone-borne devices," *Journal of Dentistry, Tehran University of Medical Sciences*, vol. 12, no. 4, Apr 2015.

- [109] I. Elkenawy, L. Fijany, O. Colak, N. A. Paredes, A. Gargoum, S. Abedini, D. Cantarella, R. Dominguez-Mompell, L. Sfogliano, W. Moon, and et al., “An assessment of the magnitude, parallelism, and asymmetry of micro-implant-assisted rapid maxillary expansion in non-growing patients,” *Progress in Orthodontics*, vol. 21, no. 1, 2020.
- [110] N.-R. Choi, S.-H. Shin, S.-S. Kim, G. Sandor, and Y.-D. Kim, “Healing pattern of intentional pterygoid plate fracture after posterior movement of maxilla through le fort i osteotomy,” *Journal of Cranio-Maxillofacial Surgery*, vol. 46, no. 10, p. 1828–1833, 2018.



# Numerical study of the impact of osteotomies and expander location in surgically assisted rapid palatal expansion for transverse maxillary deficiency

Tomas Verplanken

Student number: 01708012

Supervisors: Prof. dr. ir. Wim Van Paepegem, Renaat Coopman

Counsellor: Dr. Manuel Da Silva Pinheiro (Former postdoctoral researcher at UGent, now enrolled for MBA program in Portugal)

Master's dissertation submitted in order to obtain the academic degree of  
Master of Science in Electromechanical Engineering

Academic year 2021-2022